

Perilipins: Protectors of lipid reservoirs

Regulation of lipid droplets and lipid flux by Plin2 and Plin5

Yuchuan Li



Dissertation for the degree of Doctor Philosophiae

Department of Nutrition
Institute of Basic Medical Sciences
Faculty of Medicine

University of Oslo

2020

© Yuchuan Li, 2020

*Series of dissertations submitted to the
Faculty of Medicine, University of Oslo*

ISBN 978-82-8377-659-1

All rights reserved. No part of this publication may be
reproduced or transmitted, in any form or by any means, without permission.

Cover: Hanne Baadsgaard Utigard.
Print production: Reprintsentralen, University of Oslo.

TABLE OF CONTENTS

TABLE OF CONTENTS	2
ACKNOWLEDGEMENTS	4
ABBREVIATIONS	6
1 INTRODUCTION	10
1.1 Lipids and diseases	10
1.2 Traffic and metabolism of fatty acids and cholesterol	11
1.2.1 Traffic and metabolism of fatty acids	11
1.2.2 Traffic and metabolism of cholesterol.....	15
1.3 Lipid droplets	19
1.3.1 Basic structure of lipid droplets.....	19
1.3.2 Biogenesis and regulation of lipid droplets	23
1.3.2.1 Biogenesis of lipid droplets.....	23
1.3.2.2 Regulation of lipid droplets.....	24
1.3.3 Lipid droplets and lipid flux	27
1.3.3.1 Lipid flux and lipid droplet turnover	27
1.3.3.2 Lipid droplets are lipid reservoirs to buffer lipid flux.....	28
1.4 Perilipins (Plins)	31
1.4.1 Basic structures of perilipins in mice	31
1.4.2 Tissue distribution and transcriptional regulation of perilipins.....	33
1.4.3 LD targeting and post-translational regulation of perilipins.....	34
1.4.4 Perilipins regulate lipolysis and lipid droplets: The classic barrier theory and beyond ...	36
1.4.4.1 Perilipin 1: The classic barrier interacts with lipases	36
1.4.4.2 Perilipin 2: A flexible barrier links lipolysis and lipophagy	38
1.4.4.3 Perilipin 5: A bridge connects lipid droplets and mitochondria.....	39
2 AIMS OF THE STUDY	41
3 SUMMARY OF PAPERS	42
4 METHODOLOGICAL CONSIDERATIONS	45
4.1 Ethical considerations	45
4.2 Studies of perilipins and lipid droplets in mice	45
4.3 Studies of perilipins and lipid droplets in cell culture models	48
4.4 Histology and quantification of lipid droplets	52
4.5 Radioactive traced fatty acid and glucose metabolic flux assays	55
4.6 Analysis of genes, proteins and lipids	57
4.7 Statistics	58
5 GENERAL DISCUSSION	60
5.1 Perilipins, lipolysis and lipid droplets	60
5.1.1 Plin2 and TAG-LDs in skeletal muscle cells	60
5.1.2 Plin2 and CE-LDs in adrenal cortex	61
5.1.3 Plin5 and TAG-LDs in cardiomyocytes	63
5.1.4 LD morphology and direction of lipid flux	64

5.2	Perilipins regulate lipid flux	65
5.2.1	Plin2 and fatty acid flux in skeletal muscle cells.....	65
5.2.2	Plin2 and cholesterol flux in adrenal cortical cells.....	66
5.2.3	Plin5 and fatty acid flux in cardiomyocytes	68
5.3	Perilipins and energy homeostasis	70
5.3.1	Plin2 and energy metabolism in skeletal muscle.....	70
5.3.2	Plin5 in energy metabolism of cardiomyocytes and myocardial ischemia	73
6	CONCLUSION	76
7	REFERENCES	78

ACKNOWLEDGEMENTS

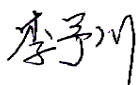
The work included in this thesis was performed from 2014 to 2019, in the laboratory of Associate Professor Knut Tomas Dalen at Department of Nutrition, and laboratory of Professor Kåre-Olav Stensløykken at Department of Molecular Medicine, Institute of Basic Medical Science, University of Oslo.

I am grateful to my supervisor Knut Tomas Dalen for giving me the opportunity to start in the field of lipid droplet research. Your wide knowledge, open mind, careful planning and great patience during the supervision have made this study a joyful and fruitful journey. At the same time, I would also thank my co-supervisors Ingvar Jarle Vaage, Kåre-Olav Stensløykken and Arkady Rutkovskiy for their supervision in cardiac research and contribution to this work. I appreciate all of you for letting me be a member of heart physiology family and I really enjoy the open-minded discussion on every topic during lunchtime.

After the join of Prabhat Khanal, Frode Norheim and Marit Hjorth into the lipid droplets group, I seldom facing challenges alone. We used to collaborate in lab work, discuss papers and exchange ideas on every project. In heart physiology group, I got many helps from May-Kristin Torp and Christina Mathisen Heiestad in heart experiment. Thank all of you for the support and contribution to this work. I thank Ingunn Musum Jermstad, Shaista Khan, Anne Randi Enget and Torun Flatebø for your helps in lab assistance, you are always very kind and supportive. I also thank Christian A. Drevon, Torgeir Holen and Niels Christian Danbolt for their support and guidance in the early period of my scientific career.

Finally, I would like to thank all my colleagues, family members and friends for their support to my work and life. I specially thank my parents and my wife Xiaochan, for always being with me and your endless love.

Oslo, February 2020



Yuchuan Li

LIST OF PUBLICATIONS AND MANUSCRIPTS

I. Feng, Y. Z., J. Lund, Y. Li, I. K. Knabenes, S. S. Bakke, E. T. Kase, Y. K. Lee, A. R. Kimmel, G. H. Thoresen, A. C. Rustan and K. T. Dalen (2017). "Loss of perilipin 2 in cultured myotubes enhances lipolysis and redirects the metabolic energy balance from glucose oxidation towards fatty acid oxidation." *J Lipid Res* 58(11): 2147-2161.

II. Yuchuan Li, Prabhat Khanal, Frode Norheim, Marit Hjorth, Thomas Bjellaas, Christian Drevon, Ingvar Jarle Vaage, Alan Kimmel and Knut Tomas Dalen (2019). "Absence of Plin2 causes adrenal enlargement with increased accumulation of cholesteryl ester-containing lipid droplets." Manuscript.

III. Yuchuan Li, May-Kristin Torp, Frode Norheim, Prabhat Khanal, Alan Kimmel, Kåre-Olav Stensløykken, Jarle Vaage and Knut Tomas Dalen (2019). "Plin5 deficient cardiomyocytes have reduced lipid droplet storage but increased tolerance to hypoxia after fatty acid stimulation." Manuscript.

Related publications/manuscripts not included in this thesis

IV. Prabhat Khanal, Yuchuan Li, Frode Norheim, Atefeh Ranjbar, Alan Kimmel and Knut Tomas Dalen (2019). "Whole-body energy metabolism is increased in sedentary but not exercised *Plin5*^{-/-} mice fed a high-fat diet." Manuscript.

V. Li, Y., S. Lee, T. Langleite, F. Norheim, S. Pourteymour, J. Jensen, H. K. Stadheim, T. H. Storås, S. Davanger, H. L. Gulseth, K. I. Birkeland, C. A. Drevon and T. Holen (2014). "Subsarcolemmal lipid droplet responses to a combined endurance and strength exercise intervention." *Physiol Rep* 2(11).

VI. Lund, J., S. A. Helle, Y. Li, N. G. Lovsletten, H. K. Stadheim, J. Jensen, E. T. Kase, G. H. Thoresen and A. C. Rustan (2018). "Higher lipid turnover and oxidation in cultured human myotubes from athletic versus sedentary young male subjects." *Sci Rep* 8(1): 17549.

ABBREVIATIONS

ABCA	ATP-binding cassette, sub-family A
ABCG	ATP-binding cassette, sub-family G
ACAT	Acetyl-Coenzyme A acetyltransferase 1
ACC	Acetyl-CoA carboxylase
ACL	ATP citrate-lyase
ACSL3	Acyl-CoA synthetase, long chain family member 3
ACTH	Adrenocorticotropic hormone
ADRP	Adipose-differentiation related protein (Perilipin 2)
AGPAT3	1-acylglycerol-3-phosphate O-acyltransferase 3
Akt	AKT Serine/Threonine Kinase (Protein kinase B)
AMPK	5' AMP-activated protein kinase
ANOVA	Analysis of variance
ApoB	Apolipoprotein B
ApoE	Apolipoprotein E
ARE	Sterol acyltransferase (yeast)
ASM	Acid soluble metabolites
ATGL	Adipose triglyceride lipase
ATP	Adenosine triphosphate
BDM	2,3-Butanedione monoxime
BSA	Bovine serum albumin
BSCL2	Berardinelli-Seip congenital lipodystrophy 2 (seipin)
CCT	CTP: phosphocholine cytidyltransferase
CE	Cholesteryl ester
CE-LDs	Cholesteryl ester containing lipid droplets
CEL	Carboxyl ester lipase
CETP	Cholesteryl ester transfer protein
CGI-58	Comparative gene identification-58 (ABHD5)
CIDEA/C	Cell death-inducing DFFA-like effector a/c
CMA	Chaperone-mediated autophagy
CoA	Coenzyme A
CPT	Carnitine palmitoyltransferase
DAG	Diacylglycerol
DGAT	Diacylglycerol O-acyltransferase
DMSO	Dimethyl sulfoxide
ELISA	Enzyme-linked immunosorbent assay
ER	Endoplasmic reticulum
FA	Fatty acid
FADH ₂	Dihydroflavine-adenine dinucleotide
FBS	Fetal bovine serum

FFA	Free fatty acid
FIT	Fat storage-inducing transmembrane protein
G0S2	G0/G1 switch gene 2
G3P	Glyceraldehyde 3-phosphate
Gapdh	Glyceraldehyde 3-phosphate dehydrogenase
GPAT	Glycerol-3-phosphate acyltransferase
HCV	Hepatitis C virus
HDL	High-density lipoproteins
HMGCR	3-Hydroxy-3-Methylglutaryl-CoA Reductase
HPLC	High Performance Liquid Chromatography
HR	Heart rate
Hsc70	Heat shock cognate 71 kDa protein
HSL	Hormone-sensitive lipase
LAL	Lysosomal acid lipase
Lamp-2A	Lysosome-associated membrane protein 2A
LC3	Microtubule-associated protein 1A/1B-light chain 3
LD	Lipid droplet
LDH	Lactate dehydrogenase
LDL	Low-density lipoproteins
LDLR	Low-density lipoprotein receptor
LPA	Lysophosphatidic acid
LPL	Lipoprotein lipase
LVdevP	Left ventricular developed pressure
LVEDP	Left ventricular end diastolic pressure
LVSP	Left ventricular systolic pressure
LXR	Liver X receptor
MAG	Monoacylglycerol
MGL	Monoacylglycerol lipase
Myh6/7	Myosin heavy chain 6/7
NAD ⁺ /NADH	Nicotinamide adenine dinucleotide
NASH	Nonalcoholic steatohepatitis
NPC1/2	NPC intracellular cholesterol transporter 1/2
Nppa/b	Natriuretic peptide A/B
OA	Oleic acid
OCT	Optimal cutting temperature compound
PA	Phosphatidic acid
PAP	Phosphatidic acid phosphatase
PAT	Perilipin/ADRP/TIP47
PBS	Phosphate-buffered saline
PC	Phosphatidylcholine

PDH	Pyruvate dehydrogenase
Pdha1	Pyruvate dehydrogenase E1 component subunit alpha 1
Pdk4	Pyruvate dehydrogenase kinase 4
PE	Phosphatidylethanolamine
PFA	Paraformaldehyde
PG	Phosphatidylglycerol
PGC-1 α	Peroxisome proliferator-activated receptor gamma coactivator 1-alpha
PIIn	Phosphatidylinositol
PKA	Protein kinase A
Pkm	Pyruvate kinase muscle isozyme
PL	Phospholipids
Plin	Perilipin
PPAR	Peroxisome proliferator-activated receptor
PS	Phosphatidylserine
PUFA	Polyunsaturated fatty acid
Pygm	Glycogen phosphorylase, muscle associated
qPCR	Quantitative polymerase chain reaction
RER	Respiratory exchange ratio
ROS	Reactive oxygen species
Rplp0	Ribosomal protein lateral stalk subunit P0
RPP	Rate Pressure Product
SD	Standard deviation
SEM	Standard error of the mean
SIRT1	Sirtuin 1
Slc2a1/4	Solute carrier family 2 member 1/4 (Glucose transporter 1/4)
SOAT1	Sterol O-acyltransferase 1
SPA	Scintillation proximity assay
SR-B1	Scavenger receptor class B type 1
SREBP	Sterol regulatory element-binding protein
StAR	Steroidogenic acute regulatory protein
T2DM	Type 2 diabetes mellitus
TAG	Triacylglycerol
TAG-LDs	Triacylglycerol containing lipid droplet
Tbp	TATA-Box Binding Protein
TCA cycle	Tricarboxylic acid cycle
TEM	Transmission electron microscopy
TIP47	Tail-interacting protein of 47 kD (Perilipin 3)
TLC	Thin-layer chromatography
TOF-MS	Time of flight-mass spectrometry
TTC	Triphenyl tetrazolium chloride

UCP2/3 Mitochondrial uncoupling protein 2/3
VLDL Very low-density lipoproteins

1 INTRODUCTION

1.1 Lipids and diseases

The four major classes of macromolecules that constitute living organisms are proteins, lipids, carbohydrates and nucleic acids. Lipids are central in this thesis. They provide energy and function as building blocks in cells. They contribute to numerous important physiological and pathological processes, such as immune response, cell signaling and transcriptional regulation. According to the classification system by LIPID MAPS (1), lipids can be grouped into eight major classes and even more subclasses. Most types of cells are able to esterify fatty acids with glycerol to generate triacylglycerol (TAG) or with cholesterol to generate cholesterol esters (CE). These neutral lipids are stored intracellularly in lipid droplets (LDs). Among them, changes in the metabolisms of fatty acids (fatty acyls) and cholesterol (sterol lipids) are directly associated with human metabolic disorders frequently occurring in the modern society.

One common pathological feature of metabolic diseases is abnormal accumulation of LDs in the implicated tissues/cells, which underpin the close relationships between LDs, lipid metabolism and metabolic diseases (2-5). Adipose tissue is the main site for TAG storage. Excess accumulation of LDs in adipose tissue is a hallmark of obesity, while defects in adipose LD storage leads to lipodystrophy. Interestingly, both these conditions disturb whole body lipid balance and result in ectopic lipid deposition (accumulation of neutral lipids in non-adipose tissues), such as in liver, skeletal muscle and myocardium - in the LDs (3, 6). Liver redistributes lipids through lipoprotein particles and is a hub to regulate whole body lipid balance. Liver is highly sensitive to ectopic lipid deposition. Excessive accumulation of hepatic LDs results in nonalcoholic fatty liver disease (NAFLD), which can progress to nonalcoholic steatohepatitis (NASH) if accompanied with inflammation and cell damage (7). Skeletal muscle constitutes the largest organ in the body by mass and is another site prone to have ectopic lipid accumulation. Contraction of skeletal muscle consumes large amount of ATP, which is mainly produced by mitochondria through the oxidation of both fatty acids and glucose. The changed lipid balance induced by mismatched energy substrate supply and muscle ATP consumption disturbs insulin signaling in skeletal muscle, and is a well-known risk factor for development of T2DM (8). Accordingly, exercise increases muscle contraction and energy consumption, which improves muscular and whole body insulin sensitivity. Exercise is therefore effective

as a supportive therapy in pre-diabetic and type 2 diabetic patients. The ATP used for heart contraction is mainly produced from oxidation of fatty acid, and to a less extent glucose (9). Myocardium normally stores very little LDs with a very rapid lipid turnover. Many metabolic related diseases (such as obesity and T2DM) increase ectopic lipid accumulation in cardiac muscle, which can alter energy metabolism of cardiomyocytes and eventually impair heart function (10). Ectopic lipid accumulation in the coronary artery wall is strongly linked to the development of ischemic heart disease. Adrenal glands have two functional endocrine parts: the external cortex and internal medulla. The adrenal medulla secretes catecholamines that mainly regulate the cardiovascular system. The adrenal cortex secretes corticosteroids that have multiple functions, including metabolic regulation. All corticosteroids share the same precursor - cholesterol, which is stored in CE containing LDs in adrenal cortical cells (11). Dysregulation of LDs in the adrenal cortex may therefore disturb adrenal cholesterol balance and steroid hormone synthesis, and cause metabolic disturbances.

In this thesis, the role of LDs in metabolism of fatty acids and cholesterol have been investigated in skeletal muscle, heart, and the adrenal cortex, with focus put on a family of LD-associated proteins - the perilipins.

1.2 Traffic and metabolism of fatty acids and cholesterol

1.2.1 Traffic and metabolism of fatty acids

Fatty acids are a primary energy substrate for most cells and constitute the main building block in the unpolar segment of cellular membranes. Cells acquire fatty acids from different sources: **1)** In the postprandial state, cells mainly take up dietary fatty acids carried by plasma lipoprotein particles (mostly chylomicrons and VLDLs). Fatty acids are enzymatically released from these circulating lipoprotein particles either by lipoprotein lipase (LPL, localized on the surface of capillary endothelial cells) catalysis (12), or via endocytosis of lipoprotein particles followed by their lysosomal degradation. **2)** During starvation (pre-prandial state), mobilization of triglycerides stored in adipocytes is the major source of fatty acids for non-adipose tissues. The released free fatty acids are bound to albumin (13) in the circulation and transported to peripheral tissues (e.g., cardiac and skeletal muscle). **3)** Some cells, especially adipocytes and hepatocytes (14), are able to synthesize fatty acids *de novo* from acetyl-CoA. This mechanism is important to preserve extra energy provided from non-lipid substrates

by converting it to acetyl-CoA that can be stored in adipose tissue in the form of TAG. Lastly, **4)** Fatty acids can be provided from lipolytic or lipophagic degradation of intracellularly stored LDs (15).

The fate and disposal of fatty acids depend on metabolic status and differ between organs. Fatty acids are utilized in several ways: **1)** Energy production via β -oxidation and the tricarboxylic acid cycle (TCA cycle); **2)** Synthesis of complex lipids (such as phospholipids and glycolipids); **3)** Incorporated into membranes; or **4)** Mediating cell signaling. Fatty acids can also be stored in LDs when the supply exceeds the cellular demand. The movements of fatty acids between main organs (systemic fatty acid flux) are summarized in Figure 1. After ingestion of a lipid-containing meal, fatty acids are taken up by the intestine and packed into chylomicrons and released into the circulation via the lymph. Excess fatty acids will be incorporated into LDs in white adipose tissue for long-term storage. When energy demand increases or during fasting, fatty acids will be released from white adipose tissue and used as fuel in non-adipose tissue (16). In liver, fatty acids can be used for β -oxidation and produce ATP, be temporarily stored in hepatic LDs, or incorporated into VLDL and secreted to the circulation for a 'second round' re-distribution to be consumed by other tissues (17). Alternatively, fatty acids can be used for ketogenesis by hepatocytes during fasting. As a form of 'pre-digested' fatty acids, the ketone bodies are efficient energy substrates for tissues that are unable to utilize fatty acids (such as brain) when glucose levels are low (18, 19). In adult myocardium and skeletal muscle, fatty acids are mainly oxidized to produce energy for contraction, and only a small portion is stored in LDs.

The facts above point out the well-organized, and tissue-to-tissue integrated communicating network involved to regulate the flux and metabolism of fatty acids in the whole body: **1)** White adipose tissue act as a major fatty acid and energy reservoir. Here, fatty acids can be stored for long term when nutrients are abundant, and release when needed. **2)** Liver act as a re-distributor. Fatty acids that are not utilized by other tissues can be temporarily stored in liver and re-distributed to circulation as VLDL. During starvation, a portion of fatty acids released by adipose tissue will be 'pre-digested' into ketone bodies by the liver and partly compensate for the energy requirements when glucose is in shortage. **3)** Tissues such as heart and skeletal muscles are main consumers of fatty acids, where fatty acids are mainly utilized for

energy production. Under extreme conditions such as prolonged fasting, chronic exposure to high fat-containing diets, or developed insulin resistance, fatty acids are abundant in circulation. When circulating fatty acid levels rise, nonadipose cells will increase their ability to store and buffer fatty acids intracellularly by expanding the pool of LDs (20-22). Dysregulation in any of these steps will disturb whole body fatty acid balance and may potentially lead to metabolic disorders.

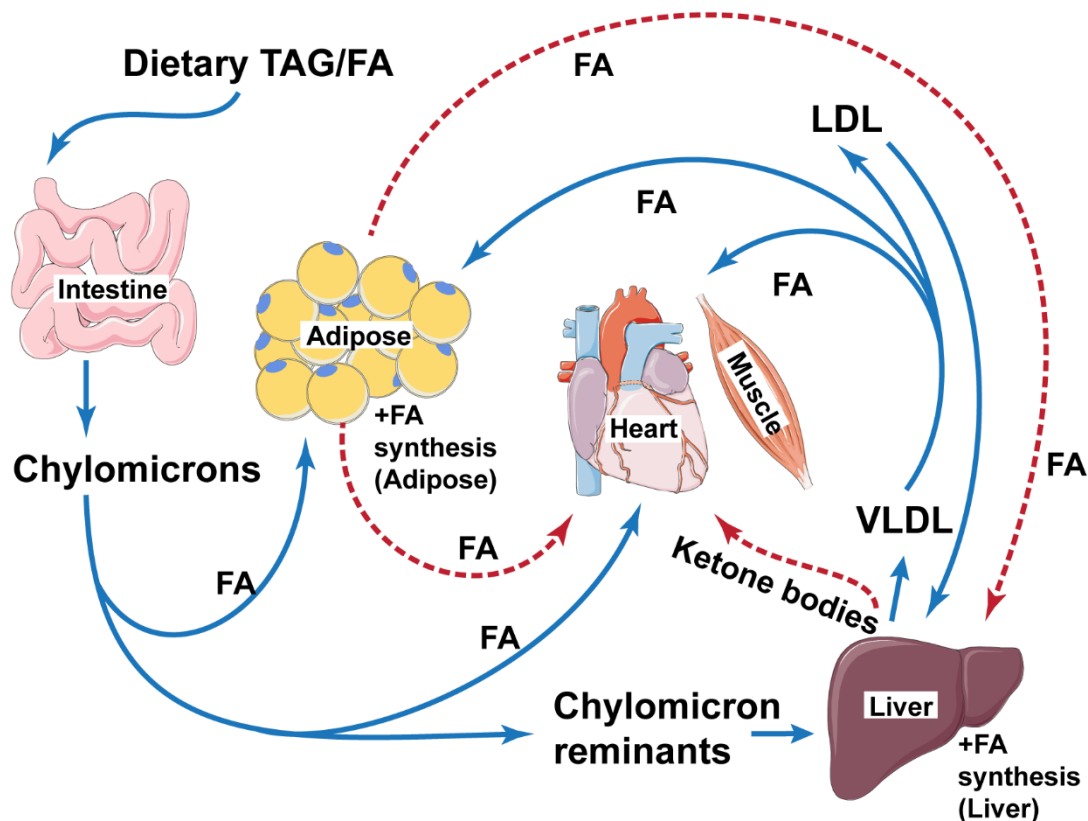


Figure 1. Systemic fatty acid flux. In the fed state (blue solid lines), dietary TAG is digested into fatty acids and monoacylglycerol in small intestine and subsequently taken up by the enterocytes and packed into chylomicrons. Chylomicrons are then released to the lymph and enter the blood circulation at the thoracic duct. Chylomicrons therefore bypass the liver and the majority of dietary fatty acids are delivered to other tissues. The chylomicron remnants, with the majority of fatty acid cleaved off, are taken up by endocytosis in the liver. When energy is in excess, liver (and to some extent adipose tissue) are able to convert other substrates (e.g. glucose, amino acids and acetyl-CoA) into fatty acids to conserve the energy. Excessive lipids in the liver may be repacked into VLDL-particles and secreted back to the circulation. Fatty acids taken up by peripheral tissues can be used to produce energy (mostly in heart and skeletal muscle) or be stored in adipose tissue in the form of TAG. Fasting (red dotted lines) triggers TAG mobilization in adipose tissue. Fatty acids released from adipocytes bind to albumin and are transported in the circulation to other tissues. Liver can convert fatty acids to ketone bodies, which are secreted to the circulation as easily accessible ‘pre-digested’ fatty acids to other tissues.

All forms of fatty acid utilization start with activation of the free fatty acid by synthesis of acyl-CoA (23). Catabolism of the acyl-CoA to produce energy is usually routed through β -oxidation, although alternative pathways such as α -oxidation and ω -oxidation also exist. The reaction steps in mitochondrial β -oxidation are catalyzed by a set of enzymes located in the mitochondria matrix in eukaryotes. However, acyl-CoAs longer than six carbons ($C>6$) cannot freely pass the inner membrane of mitochondria. Two key enzymes, carnitine palmitoyltransferase I and II (CPT1 and CPT2) in the 'carnitine shuttle' facilitate the entry of fatty acids into mitochondria (24). Once inside the matrix, the acyl-CoA is shortened with two carbon units for each round of β -oxidation, which generates one acetyl-CoA, one shortened acyl-CoA, one NADH and one $FADH_2$. The shortened acyl-CoA then enters a new cycle of β -oxidation until the whole acyl-CoA has been converted into two-carbon acetyl-CoAs and NADH and $FADH_2$. The generated acetyl-CoAs enter the TCA cycle where they are completely oxidized into CO_2 and H_2O , with more NADH and $FADH_2$ generated. The transfer of electrons from NADH and $FADH_2$ to oxidative phosphorylation builds up a proton gradient across mitochondrial inner membrane. The backflow of protons through ATP synthase generates ATP. If ATP generated through the oxidation of NADH (2.5 ATP) and $FADH_2$ (1.5 ATP) are considered, each round of β -oxidation and oxidation of one acetyl-CoA in the TCA cycle result in the net production of 14 ATP (25).

Except of mitochondria, peroxisome is another place where β -oxidation can take place. The reaction steps in peroxisomal β -oxidation are more or less similar to mitochondrial β -oxidation, albeit some peroxisomal specific enzymes are catalyzing the reactions and less ATP being produced (26). In mammalian cells, peroxisomal β -oxidation normally contributes less to overall energy production. However, it is critical to degrade very long chain fatty acids and branch chain fatty acids (27). Defective peroxisomal β -oxidation results in chronic accumulation of these lipids and causes tissue damage, as seen in certain congenital peroxisomal disorders (28).

Oxidation of fatty acids also interacts with metabolism of the other primary energy substrate - the glucose. The interplay between the metabolic pathways for oxidation of fatty acids and glucose, and evidence for fuel selection in mammalian cells, were first described in 1963 known as Randal cycle (29). Later studies have revealed details about the interplays of these and other energy substrates, including ketone

bodies, lactate and amino acids. The interaction between metabolic pathways of different energy substrates applies to almost all types of cells. For additional details, see the latest review by Hue L and Taegtmeyer H (30). In brief, increased fatty acid oxidation elevates mitochondrial acetyl-CoA and NAD^+ , which saturates the TCA cycle and feedback to inhibit multiple enzymatic steps in glucose utilization. The sites of inhibition vary between tissues, but include inhibition of glucose uptake and glycolysis, mostly at the step of conversion of pyruvate to acyl-CoA catalyzed by pyruvate dehydrogenase (PDH). Oppositely, high ratio of glucose oxidation leads to accumulation of cytosolic malonyl-CoA. In this situation, increased oxidation of pyruvate (the final product of glycolysis from glucose) in mitochondria generates more acetyl-CoA. Acetyl-CoA cannot pass mitochondrial inner membrane, but its downstream product in TCA cycle - citrate, can leak out to cytoplasm and be converted back to acetyl-CoA by ATP citrate lyase (ACL). Acetyl-CoA in cytoplasm can then be used to synthesize malonyl-CoA by Acetyl-CoA carboxylase (ACC), which is the initial and rate-limiting step of fatty acid *de novo* synthesis. Malonyl-CoA is a strong inhibitor of CPT1 and prevents the entry of fatty acids into mitochondria, thereby repressing fatty acid oxidation but favoring fatty acid synthesis. In addition, increased glycolysis generates more glyceraldehyde 3-phosphate (G3P), which stimulates reesterification of fatty acids into TAG for storage in LDs, rather than directing them to β -oxidation.

Levels of fatty acids and lipoproteins in circulation fluctuate with nutritional conditions. Moreover, the cellular demand for fatty acids change with physiology/pathology status. Therefore, the ability to store fatty acids intracellularly is essential for cells that rely on fatty acid oxidation. Fatty acids are mainly stored esterified in lipid droplets (LDs), either temporarily (hours to days) or long term (months to years. e.g., in adipocytes). The importance of LDs for fatty acid flux is discussed in section 1.3.3.

1.2.2 Traffic and metabolism of cholesterol

Cholesterol is essential for cellular functions and involved in multiple biological processes, such as regulation of membrane fluidity, cell signaling, steroid hormone synthesis, Vitamin D and bile acid production. Cholesterol is synthesized endogenously or acquired from exogenous sources. The transport of cholesterol

between liver, intestine, steroidogenic organs and other tissues is illustrated in Figure 2.

Diet is an important source of cholesterol, especially when it includes animal products (31). Dietary cholesterol consists of both unesterified cholesterol and cholesteryl esters (CE). CE is degraded into free cholesterol and fatty acids in the intestine by carboxyl ester lipase (CEL) before absorption (32). Intestinal enterocytes take up cholesterol through a mechanism mediated by Niemann-Pick C1-like 1 (NPC1L1) protein (33). Absorbed cholesterol is reesterified into CE by acyl-CoA: cholesterol acyltransferases (ACAT) in enterocytes, packed in chylomicron particles and released to the lymph before entering the blood stream (34). The main function of chylomicrons is to transport dietary fatty acids (in form of TAG) to peripheral tissues, but a low level of CE is added in addition to TAG. When entering the blood stream, chylomicrons are rapidly depleted of TAG and converted into chylomicron remnants. These cholesterol-rich particles are taken up and recycled by liver, where CE and the remaining TAG are re-packed into VLDL and secreted (35). When TAG is removed from the VLDL, the particle is transformed into IDL (Intermediate-density lipoprotein) and finally LDL. LDL in plasma is the main cholesterol donor to cells (36). Cells may take up LDL particles via LDL receptor-mediated endocytosis and cycle the cargo to lysosomes. There, CE is hydrolyzed by lysosomal acid lipase (LAL) and cholesterol is released to the cytoplasm by NPC 1 and NPC 2 proteins.

Another lipoprotein particle important for cholesterol transport is HDL which originates from liver and small intestine. In most non-haptic tissues, HDL mainly removes extra cholesterol and retrogradely transports it back to liver (37). Some cells, such as steroidogenic adrenal cortical cells, have high demand of cholesterol for the synthesis of steroid hormones. In such cells, HDL function as an important source of cholesterol through SR-BI-mediated cholesteryl ester selective uptake (38, 39). Recent studies revealed that Aster proteins are involved in nonvesicular transport of HDL cholesterol from the plasma membrane to ER (40). This mechanism is the dominant pathway for cholesterol uptake in steroidogenic cells of rodents (41).

As an alternative to take up exogenous cholesterol, all cells are equipped with enzymes for *de novo* synthesis of cholesterol from acetyl-CoA. Biosynthesis of cholesterol involves more than 30 reaction steps. The rate-limiting step is the

conversion of 3-hydroxy-3-methyl-glutaryl-CoA to mevalonic acid, catalyzed by 3-Hydroxy-3-Methylglutaryl-CoA reductase (coded by the *Hmgcr* gene) (42). The majority of the endogenous cholesterol in the body is produced by liver and intestine, with a minor contribution from adrenals and gonadal glands (43).

Excess of cholesterol is detrimental, especially if accumulated in its unesterified form. Most mammalian cells are unable to degrade cholesterol *in situ* due to its stable four-ring structure. Hepatocytes are able to convert cholesterol into water-soluble bile acids and excrete them into the intestine. Other cells remove excessive cholesterol by transferring it to HDL, a process termed as reverse cholesterol transport (RCT). Several proteins, including ABCAs, ABCGs and ApoE are involved in reverse cholesterol transport. Several of these proteins are regulated by transcription factors such as liver X receptors (LXRs) and sterol regulatory element-binding proteins (SREBPs) (44). Excess cholesterol delivered to HDL-particles in the plasma is converted into CE by lecithin-cholesterol acyltransferase (LCAT) in HDL. CE in HDL is taken up by liver via SR-BI mediated selective transport (45). Alternatively, CE in HDL can be transferred to LDL and VLDL via cholesteryl ester transfer protein (CETP) mediated CE-TAG exchange (46), which can be taken up both by liver and other tissues via LDL receptor-mediated endocytosis. Cholesterol transported to liver may be metabolized into bile acids or reused in other processes. A considerable amount of cholesterol in the bile is reabsorbed in the small intestine, at levels that can exceed the dietary cholesterol uptake (47). Hence, cholesterol levels in the whole body are balanced by dietary intake, *de novo* biosynthesis, bile acid secretion and bile reabsorption (48).

Cholesterol is a precursor for synthesis of steroid hormones. Most endocrine cells, such as insulin producing pancreatic β -cells, can pre-synthesize and store large amounts of matured hormones in vesicles for rapid release. In contrast, steroid hormone producing cells such as adrenal cortical cells lack the ability to store steroid hormones, but releases these as they are synthesized (49). Steroid hormone secretion is therefore directly dependent on storage and availability of the precursor molecule - cholesterol. The cholesterol content in membranes affects membrane fluidity and charge, influences membrane protein functions and lipid dynamics (50). Therefore, membrane structures have quite stable cholesterol levels with limited ability to buffer cellular cholesterol. Cholesterol content above ~5 mol% in ER will inhibit activation of

SREBP-2 and reduce transcription of genes involved in cholesterol uptake and synthesis in an attempt to restore cellular cholesterol balance (51). Instead, the main intracellular storage of cholesterol in steroidogenic cells are CE deposited in LDs. Storage and mobilization of CE containing LDs are linked to cholesterol balance and production of steroid hormones in these cells. The next chapter is devoted to these organelles and their role in metabolism.

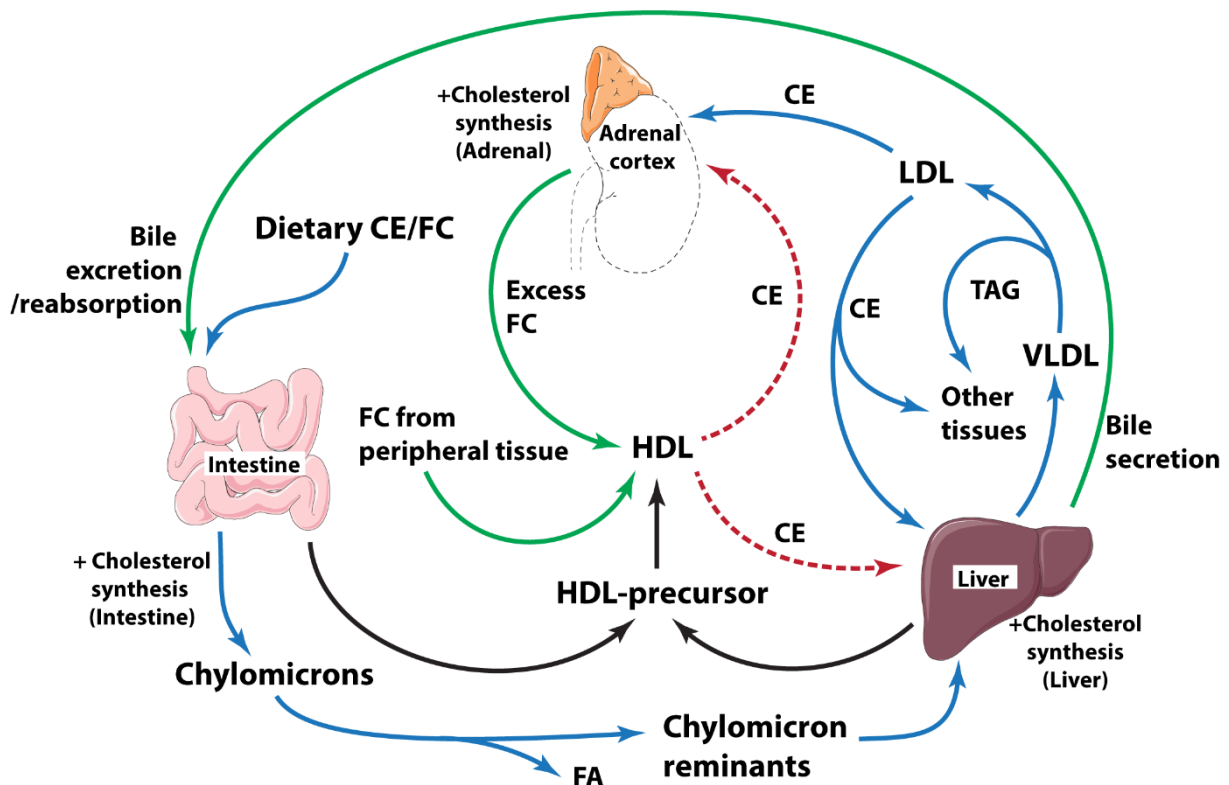


Figure 2. Systemic cholesterol flux. Dietary cholesterol is absorbed in the small intestine and packed into chylomicrons. Chylomicrons rapidly release the majority of fatty acids to peripheral tissues and the remaining chylomicron remnant carries the absorbed dietary cholesterol to the liver. Liver may metabolize cholesterol into bile acids, or alternatively, pack cholesteryl esters in VLDL for redistribution to the circulation. Bile acids are only partly reabsorbed in the intestine, which enables excretion of excessive cholesterol from the body. VLDL become LDL when TAG is delivered to peripheral tissues, which can be taken up by steroidogenic tissues or liver. Most cells depend on reverse cholesterol transport to HDL-particles to remove extra cholesterol. The HDL-particle is mainly taken up by liver, but it is also an important cholesterol donor for steroidogenic tissue such as adrenal cortex (especially in rodents). In addition to the described cholesterol transport, tissues can synthesis cholesterol *de novo* whenever needed. Still, the majority of the endogenous cholesterol is produced in liver, intestine and steroidogenic tissue. Transport of dietary cholesterol is shown as solid blue arrows; HDL-mediated cholesterol uptake is illustrated as dashed red arrows; reverse cholesterol transport, cholesterol conversion into bile acids and excretion to the intestine is indicated as solid green arrows.

1.3 Lipid droplets

Lipid droplets (LDs) are intracellular organelles present in most types of cells that are highly conserved in a variety of species, from bacteria, fungi, insects to higher mammals. These spherical structures were first discovered by the introduction of light microscopes but were for a long time neglected by scientists and regarded as 'passive' lipid storage particles. After identification of the first mammalian LD-binding protein in the early 1990s (52), this view changed gradually, and LDs are now looked upon as *bona fide* organelles that are highly active and of vital importance for regulation of cellular lipid flux (53). Moreover, LDs are involved in many biological processes that are not directly linked with lipid metabolism and energy storage (54). Depending on the cell type, metabolic state, nutrition availability and cell signaling, the morphology (e.g. size, number and localization/distribution) of LDs may change dramatically, which demonstrates the significance of LD biology and dynamics for cell physiology.

1.3.1 Basic structure of lipid droplets

LD organelles consist of a core of neutral lipids surrounded by a monolayer of phospholipids and decorated proteins (55), an organization that resembles lipoprotein particles in the circulation (Figure 3). However, unlike lipoprotein particles, LDs are found intracellularly and coated with distinct sets of proteins. Further, the range of LD size is much broader than for lipoprotein particles, with the reported LD diameters ranging from under 1 μm to over 100 μm (56). The complexity of the three principal components of LDs will be described in the following sections.

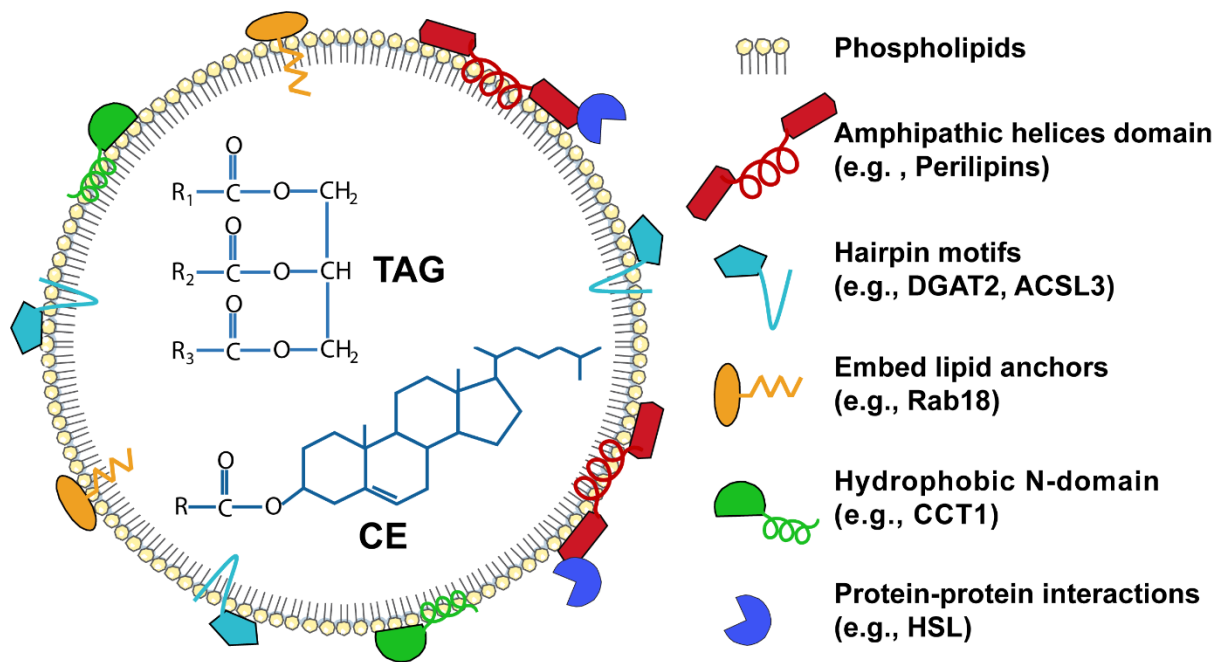


Figure 3. Basic structure of lipid droplets and the mechanisms for protein targeting. Lipid droplets consist of a phospholipid monolayer (and some free cholesterol), a hydrophobic neutral lipid core (mostly TAG and CE), and cell-specifically expressed LD-associated proteins. Identified mechanisms for targeting of proteins to the LD surfaces are illustrated.

The neutral lipid core – Nonpolar hydrophobic neutral lipids constitute the core of LDs. Triacylglycerols (TAG) and cholesterol esters (CE) are the most common core lipids in LDs of mammalian cells (57), whereas other lipids such as retinyl esters, neutral ether lipids and free cholesterol are rarely present. The types of core lipids are cell type dependent to meet cell-specific functions. The dominant core lipid in most cell types is TAG, found in cells such as adipocytes, hepatocytes, skeletal and cardiac myocytes. In these cells, a major function of TAG-containing LDs is to store fatty acids for utilization as energy substrate. In steroidogenic cells, the dominant component of core lipids is CE. CE is the main core lipid in adrenal cortical cells, ovary granule cells and testicular Leydig cells, as well as macrophage derived foam cells (58). In these cells, LDs function as a cholesterol reservoir for steroidogenesis or a place to sequester excessive cellular free cholesterol. In hepatic stellate cells, the main site of vitamin A storage in the body (59), and retinal pigment epithelium cells, involved in visual phototransduction (60), core lipids are mainly retinyl esters. Different core lipids may segregate in separate LDs, but may also coexist within the same LD (61). The biological significance of segregated storage is unclear.

Monolayer phospholipids – To store hydrophobic neutral core lipids in the aqueous hydrophilic cytosol, amphipathic polar phospholipids (PLs) are needed to emulsify the interfaces between the core lipids and the cytoplasm. Due to differences in size between their polar head groups and the two unpolar acyl chains, the various PL species used to generate the single-layered LD membrane will form various curvatures, which are likely to influence the stability, dynamics and morphology of the LD organelle (62). In CHO cells, lipidomics studies suggest that more than 160 different PL species are present on LDs (57). The PL composition of the monolayer LD membrane is unique compared to other bilayer membrane structures: it mainly consisted of phosphatidylcholine (PC), followed by phosphatidylethanolamine (PE) and phosphatidylinositol (PI), rich in lysophosphatidylcholine (lysoPC) and lysophosphatidylethanolamine (lysoPE), but less in sphingomyelin, phosphatidic acid (PA) and phosphatidylserine (PS) (57). The unique PL components may be important to maintain the monolayer structures and regulate specific docking and binding of LD-associated proteins.

LD-associated proteins – A unique characteristic that distinguishes lipid droplets from other organelles, is the LD-associated proteomes. Based on proteomic studies of LDs isolated from different cell types, hundreds of proteins are found associated with LD surfaces (63, 64). Similar to the variability among core lipids, LD-associated proteins differ among cell types, cellular states and even between individual LDs within the same cell. Some are integral scaffold proteins that reside on LDs stabilizing the structure, while others bind transiently and translocate between the LD surfaces and the cytosol or other organelles. Influenced by metabolic status of the cell, LD-associated proteins regulate the formation, growth, degradation, cellular distribution of LDs and interactions between LDs and other organelles.

The molecular mechanisms involved for targeting of proteins to the LD surfaces remains largely unclear. Compared to bilayer membrane structures, the unique biophysical properties of monolayer-phospholipids and the underneath hydrophobic core imply that distinct mechanisms are involved for targeting of proteins to the LD surface. So far, several binding mechanisms have been proposed (illustrated in Figure 3), including: **1)** amphipathic helices domains; **2)** short hydrophobic N-terminal domains; **3)** embedded hairpin loops; **4)** embedded lipid anchors, **5)** and protein-protein interactions (65). In addition, the surface tension of monolayer-PL membranes

(high surface tension = low PL density) can also influence protein targeting. One example is the CTP: phosphocholine cytidyltransferase α (CCT α) catalyzing PC synthesis, which contains a helical domain that binds more efficiently to PL-poor LD surfaces (high surface tension) and activates the enzyme upon binding. This mechanism is believed to stabilize LD structures by providing more PLs to the surface and reduce the surface tension of LDs (66, 67).

Based on the relationship with other membrane structures and the source of recruitment, LD-associated proteins are divided into two major classes: membrane associated proteins that diffuse from ER to LDs (class I), and proteins recruited from the cytosol to LD surfaces (class II) (68). By function, identified LD-associated proteins can be grouped into several classes: **1**) LD scaffold proteins (e.g. perilipins); **2**) core lipid synthetic enzymes (e.g. DGAT2); **3**) lipolytic enzymes (e.g. ATGL and HSL) and enzymatic co-factors (e.g. Cgi-58 and G0s2); **4**) signaling proteins (e.g. ubiquitination factors, Ras related proteins); **5**) LD fusion proteins (e.g. Cide a and Cide c), and **6**) sterol synthetizing enzymes (69, 70). Due to the complex interactions between LDs and other cellular membranes, including ER, mitochondria, peroxisomes and endosomes, residual organelle-contamination of isolated LD fractions are likely to have overestimated the true number of 'LD-associate proteins' identified by proteomic analysis (70). On the other side, some proteins have dual localization properties and bind to LD surfaces and other structures. Their LD regulatory function may have been overlooked due to their well-known alternative function and cellular localization. Therefore, interactions with LDs must be thoroughly examined using various molecular methods before a protein can be looked upon as a true LD binding protein. Co-localization studies with high-resolution fluorescence microscopy are often used to identify LD-associated proteins, where a characteristic ring-structure indicates localization of the protein to the LD surface (71). Importantly, some proteins may under certain conditions target LD-associated structures rather than phospholipid-monolayer of LDs. In such cases, ultra-structural studies via electron microscopy, as well as in vitro binding experiment on isolated or artificial LDs may be necessary to confirm whether these proteins are truly LD-localized (72). One of the dominant LD-associated protein families: the perilipins, is the focus of this thesis. Two of the perilipin family members, Plin2 and Plin5 have been investigated in skeletal muscle (**paper I**), adrenal

glands (**paper II**) and myocardium (**paper III**). The perilipin family will be introduced in details later (chapter 1.4).

1.3.2 Biogenesis and regulation of lipid droplets

1.3.2.1 Biogenesis of lipid droplets

LDs can be assembled *de novo* or self-replicate by dividing large LDs into daughter LDs (73). Newly formed LDs are reported to associate with ER at contact sites, as revealed by high resolution microscopy imaging (74). The majority of enzymes catalyzing synthesis of core lipids, including DGATs for the synthesis of TAG, as well as ACATs for the synthesis of CE are localized in the ER membrane (75-77). Such experimental evidence suggests that *de novo* synthesis of LDs most likely occurs in ER. However, molecular mechanism by which how the mono-membrane encircled LDs can arise from the double-layered ER membrane remains unclear. A widely accepted 'budding' model proposes that neutral lipids are initially synthesized in specialized domains of ER and aggregate like a 'lens' between the two leaflets of the ER double-membrane, followed by budding off as a nascent LDs from the cytosolic side of the ER membrane (78). In this budding-hypothesis, it is not understood why ER synthesized core lipids aggregate instead of diffusing laterally between the two ER membranes, why the LD budding sites seems to be restricted to certain ER domains, or what controls the direction of budding to the cytosolic side and not into the ER lumen. Assembly and release of LDs from the ER is likely controlled by key proteins facilitating LD formation, such as ER located Berardinelli-Seip congenital lipodystrophy 2 (Bsc12, also known as seipin). Loss of function mutations of Bsc12 in humans causes lipodystrophy (79), whereas yeast fails to assemble LDs in its absence (80). Molecular analyses suggest that BSCL2 stabilizes ER-LD contact sites and facilitates budding and/or LD diffusion from ER (81, 82). Another protein believed to be involved in LD formation is fat storage-inducing transmembrane protein (FIT). The FIT protein has high affinity to TAG. The lack off or overexpression of the FIT protein reduce or enhance TAG-LD storage in 3T3-L1 adipocytes, respectively (83), possibly by affecting LD budding from ER (74). In addition, perilipin family members (Perilipin 1, 2 and 3) have been suggested to stabilize the LD surface when nascent LDs are released from ER (84, 85).

1.3.2.2 Regulation of lipid droplets

Once formed, the size, number, localization as well as composition of LDs change with the metabolic status of the cell. LD growth and LD degradation balance cellular lipid storage versus utilization. These processes are under dynamic control by various LD-associated proteins.

Growth of lipid droplets - LDs are able to grow after their initial budding from ER. Two basic components must expand in parallel during growth of LDs: the neutral lipids in the core and the surface phospholipids. LDs are likely to acquire these components via three mechanisms: 1) local synthesis on LDs, 2) cargo delivery from other organelles, mostly from ER and 3) LD-LD fusion. Both the biophysical properties of the LD phospholipid surface and the various LD-associated proteins are important for the regulation of these processes.

Protein analysis and immunohistochemistry studies suggest that when cells are exposed to elevated levels of fatty acids, a subset of ER resident TAG synthesizing enzymes are temporarily translocated to LDs. This has been observed for GPAT4, the enzyme converts G3P to LPA during the first step of TAG synthesis; AGPAT3, the enzyme converts LPA to PA; PAP (lipin), the one catalyzes the reaction from PA to DAG; as well as DGAT2, the enzyme catalyzes the final step synthesis of TAG from DAG (86, 87). In addition, ACSL3 have been found on expanding LDs, which may help to provide acyl-CoA for lipid synthesis (88, 89). CCT, the rate-limiting enzyme for PC synthesis, is retargeted to the LD surface and activated when more PC are needed to coat the growing core of neutral lipids during LD expansion (90). Whether CE-containing LDs are able to self-grow is still unclear. Enzymes esterifying cholesterol to CE in mammals (ACATs or SOATs) and their related analogues in yeast (AREs) seem to reside in the ER, only (91, 92). Expansion of nascent LDs may acquire lipids or lipid precursors from ER. Additionally, LDs pitched off from ER may temporarily dock back to ER. They may also remain connected with ER membranes after their formation for transport of proteins and lipids. Observations of cargo transport between LDs and ER supports such alternative ways to ensure functional connection of these two organelles (81, 93, 94).

From a biophysical point of view, few and large LDs results in less surface tension and lower free energy in the PL-membrane compared to the same volume of

numerous and small LDs. Improper coating of LDs will therefore favor coalescence of small LDs into larger LDs to release free energy and achieve a stable state. However, LDs are usually small and numerous in most cell types, while unilocular large LDs are rare and exist mainly in matured white adipocytes. Thus, LDs fusion is unlikely to occur spontaneously, but are under strict control. Phospholipids (as the surfactants) and LD-associated proteins influence separation or fusion of LDs. Under unbalanced conditions, such as PC deficiency or PA accumulation, fusion of LDs increases and may result in the formation of giant LDs in cells that normally contains many small LDs (90, 95). In addition, LD fusion can be experimentally induced by pharmacological stimulation, e.g. by propranolol (96). Physiologically, LD fusion occurs during maturation of white adipocytes, which is mediated by cell death-inducing DFFA-like effectors (CIDEs) (97).

Degradation of lipid droplets – A main function of LDs is to store lipids intracellularly and release them to meet cellular needs. Released lipid components can be utilized to generate energy, to build membrane structures, to synthesize special lipids and to serve as cell signaling molecules. Stored lipids can be mobilized stepwise via the lipolytic degradation in cytosol, or by autophagy pathway in lysosomes.

Lipolytic enzymes catalyze hydrolysis of ester bonds of complex neutral lipids (such as TAG and CE) and release free carboxylic acids (fatty acids) and their alcoholic group containing backbones (mainly glycerol or cholesterol). Cytosolic lipolysis is believed to take place on the surface of LDs and includes several reaction steps catalyzed by a set of neutral lipases. In mammals, adipose triglyceride lipase (ATGL), hormone-sensitive lipase (HSL) and monoacylglycerol lipase (MGL) are the three main neutral lipases that mediate degradation of TAG in LDs. The first and rate-limiting step of TAG hydrolyzation is catalyzed by ATGL (98, 99). ATGL has high catalytic activity for TAG, but with low activity for DAG and MAG. The main action of this lipase is to hydrolyze the sn-2 ester bond in TAG, releasing one free fatty acid and 1,3-DAG. Following the action of ATGL that produces DAG, HSL cleaves off one more fatty acid from DAG and yields MAG. HSL is less specific with enzymatic activity towards a broader selection of substrates, and may hydrolyze ester bonds in DAG, CE and retinyl esters (100). The downstream reaction from MAG is hydrolyzed by MGL with release of the last free fatty acid and the glycerol. Compared to hydrolysis of the three ester bonds in TAG, hydrolysis of CE is much simpler and involves only one ester bond. In

steroidogenic cells, this step is mainly catalyzed by HSL (101). In addition to the best characterized lipase triplet: ATGL, HSL and MGL, other proteins with lipase activity may exist, while yet to be identified. Additional investigations are needed to get a full overview of enzymes catalyzing lipolysis of LDs in various mammalian cell types. The activity of ATGL and HSL is regulated by perilipins and lipase co-factors. The complex interplay between lipases, perilipins and co-factors for regulation of LD degradation will be addressed later (section 2.3).

Autophagy is an evolutionarily conserved self-degradation process that degrades organelles and cell components. This process also serve as an alternative pathway to degrade LDs in bulk. When referred selectively to autophagic degradation of LDs, the process is termed as 'lipophagy'. Two forms of lipophagy, macrolipophagy and microlipophagy, have been identified (102). In macrolipophagy, whole LDs (occasionally partial) are surrounded by an autophagosome membrane. The cargo (LDs) is subsequently fused with lysosomes where the whole LD is degraded by various lysosomal acid lipases (LAL). In microlipophagy, lysosomes directly interact with LDs and 'pinch off' segments of the LD organelle without formation of autophagosomes. Compared to the stepwise and easily reversible lipolytic reaction, degradation of LDs via lipophagy represent an 'all or none' reaction. The latter process is more efficient when activated, but also less controllable. It is poorly understood how the autophagy machinery targets LDs. ATGL bound to the LD surface may interact directly with the autophagosome marker LC3 (103) and promote lipophagy via SIRT1 signaling (104). These observations suggest that ATGL may act as a regulator of lipophagy and promotes LD degradation independent of its lipase activity. In addition to directly degrade core lipids via lipophagy, recent studies in hepatocytes reported that chaperone-mediated autophagy (CMA), a third form of autophagy, also facilitates mobilization of LDs. CMA targets proteins, not lipid components itself. However, removal of LD-associated proteins (e.g., Plin2 and Plin3) by CMA facilitates subsequent cytosolic lipolysis and lipophagy (105). Activation of CMA seems to depend on AMPK activated phosphorylation of target proteins, at least for removal of Plin2 from LDs (106).

1.3.3 Lipid droplets and lipid flux

An important function of LDs is to store lipid components for later use. Their function was for a long time considered mainly (if not only) to store fatty acids as energy substrates. Recent investigations on LD biology in the last decades have revealed many functions of LDs beyond energy storage (54). They can store lipid molecules (e.g. Vitamin A, Vitamin E, arachidonic acid) that participate in cell signaling and inflammation (107). They are involved in management of cell stress (such as ER stress and oxidative stress) (108). They serve as platforms for storage and turnover of certain proteins (e.g. histones and ApoB) (109), and participate in the assembly of viruses (e.g. HCV, dengue virus and rotaviruses) (110). The most studied function of LDs related to human health, is their impact on cellular lipid flux and lipid metabolism.

1.3.3.1 Lipid flux and lipid droplet turnover

The term '*lipid flux*' used in this thesis refers to trafficking of lipids, mainly fatty acids and cholesterol, in esterified and unesterified forms. In this thesis, lipid trafficking between different tissues, such as intestine, white adipose tissue, liver, skeletal muscle, myocardium and adrenals will be referred to as *systemic lipid flux*. Lipid trafficking between different intracellular compartments, mostly between ER, LDs, mitochondria, autolysosomes and nuclei will be referred to as *intracellular lipid flux*. Excessive intracellular accumulation of free fatty acids, cholesterol and some of their intermediate metabolites are detrimental. They may alter membrane fluidity and charge, disturb signaling pathways, impair cell metabolism, and eventually cause cell/tissue damage and organ dysfunction - collectively referred to as 'lipotoxicity' (111). To prevent these detrimental effects from occurring, most cells express enzymes and LD-structural proteins needed to store fatty acids and cholesterol as their esterified form in LDs. These stored lipids can be mobilized and released from LDs when needed. In this thesis, the whole process starting from incorporation of these lipids into LDs via esterification to their release from the LDs via lipolysis is termed *LD turnover*. A widely accepted concept is that lipolysis and reesterification occurs simultaneously on LD surfaces (at least in TAG-LDs) (112, 113). Accordingly, the amount of lipid molecules that are incorporated versus released from LDs reflects the contribution of LDs to overall intracellular lipid flux. Lipid flux dynamics will differ between cell types, lipid species [e.g., palmitic acid vs. oleic acid, (114)], nutrient availability, hormone milieu, the LD-pool size and possibly for LD expansion. Hence, the dynamic balance between

LD synthesis and LD degradation affects not only LD morphology, but more importantly, the net lipid flux toward either storage or utilization. In human skeletal muscle (115) and hearts of *Atgl*^{-/-} mice (116, 117), a large fraction of newly internalized fatty acids are incorporated into LDs before being directed to mitochondria for oxidation. Changes of LD turnover in animal models and cell studies affect metabolism of fatty acids (118-121), which emphasize the importance of LD turnover for regulation of lipid flux and energy metabolism.

1.3.3.2 Lipid droplets are lipid reservoirs to buffer lipid flux

Adipose LDs process considerable amounts of dietary lipids (122, 123) and serve as the major site to store TAG and preserve energy substrates for the organism. Metabolic complications associated with whole-body lipid imbalance and lipotoxicity, such as hepatic steatosis and FFA-mediated impaired insulin sensitivity, occur in obese individuals where adipose LDs are saturated (124), and in lipodystrophic individuals where adipose LDs are unable to store lipids efficiently (125). These two seemingly opposite abnormalities of adipose LDs have the same consequence in whole-body metabolism, suggesting that impaired expandability of adipose LDs, rather than the size of LDs *per se*, is the main cause of dysregulated systemic lipid balance (126). Additionally, abnormal LD turnover and disrupted lipid flux in white adipocytes may alter adipose microenvironment and lead to chronic inflammation *in situ*. Numerous cytokines and inflammatory factors released by unhealthy adipose tissue may further exacerbate metabolic disorders both in adipose tissue and in the whole body (127). Overall, LDs of white adipose tissue function as the 'primary' lipid reservoir to buffer lipid flux and maintain whole-body lipid balance.

Compared to the large and relatively long-lived adipose LDs (128, 129), LDs in most non-adipose tissues are usually small and transient. Except for some specialized cells such as adrenal cortical cells and hepatic stellate cells, most non-adipose cell types contain few LDs at basal state. However, in response to an increased lipid influx such as during fasting (induces fat mobilization from adipose tissue) or high-fat diet feeding, these LDs may expand dramatically in size and numbers. Recent studies show that LDs in non-adipose tissue are also active in lipid turnover (130). Excessive accumulation of these LDs in non-adipose tissues is often referred to as ectopic lipid deposition, which is associated with local and systemic metabolic disorders such as

fatty liver diseases, cardiomyopathy and heart failure, obesity, as well as type II diabetes (131). The downregulation of lipogenic genes in adipose tissue of obese individuals suggests that the expansion and buffering capacity of this 'primary' lipid reservoir are limited (132). On the other side, increased ectopic LD accumulation in non-adipose tissue such as liver, heart and skeletal muscle following dysregulations of adipose function and plasma lipids suggests that non-adipose LDs may function as 'secondary' lipid reservoirs and regulate lipid flux locally. The role of non-adipose LDs for buffering of excessive fatty acids has been studied in different tissues, including skeletal muscle (133), myocardium (134) and liver (135). In addition, non-adipose LDs may regulate local cholesterol balance (11, 136). However, how these TAG- or CE-containing LDs participate in lipid flux regulation and their significance in many physiological and pathological conditions remain less understood. In this thesis, we focused on the role of these non-adipose LDs for regulation of fatty acid flux in skeletal muscle and myocardium (Figure 4), and for regulation of cholesterol flux in adrenal cortex (Figure 5). The regulation of these LDs and lipid flux by a family of proteins: the perilipins, will be discussed in following chapters.

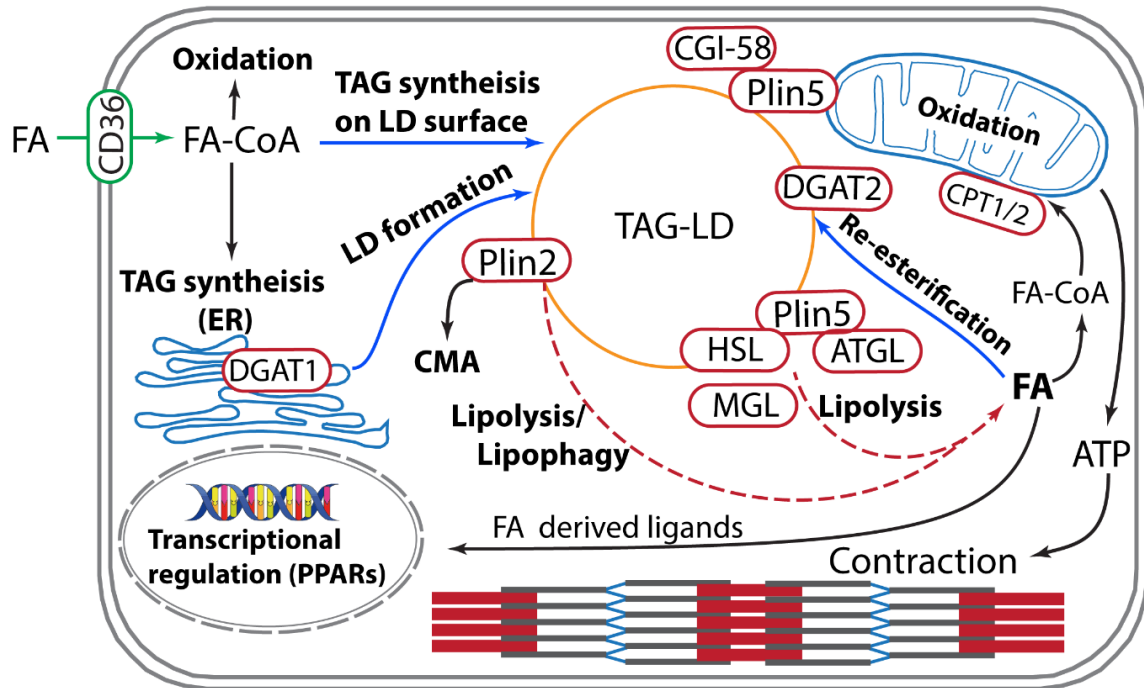


Figure 4. Intracellular fatty acid flux in muscle cells. Fatty acids taken up by muscle cells are activated into acyl-CoA. A majority of generated FA-CoA are directed against TAG-LDs, either by *de novo* synthesis of TAG-LDs from ER (by DGAT1), or incorporated into existing LDs (by DGAT2). Under the regulation by Plins and lipolytic enzymes, FA stored in TAG-LDs can remain as TAG or be mobilized for oxidation in mitochondria to produce ATP required for muscle contraction. A fraction of the released FA will be reesterified to TAG-LDs to balance intracellular FA levels. Released FA and FA derived molecules can affect transcription of genes important for fatty acid metabolism by activating e.g. PPARs.

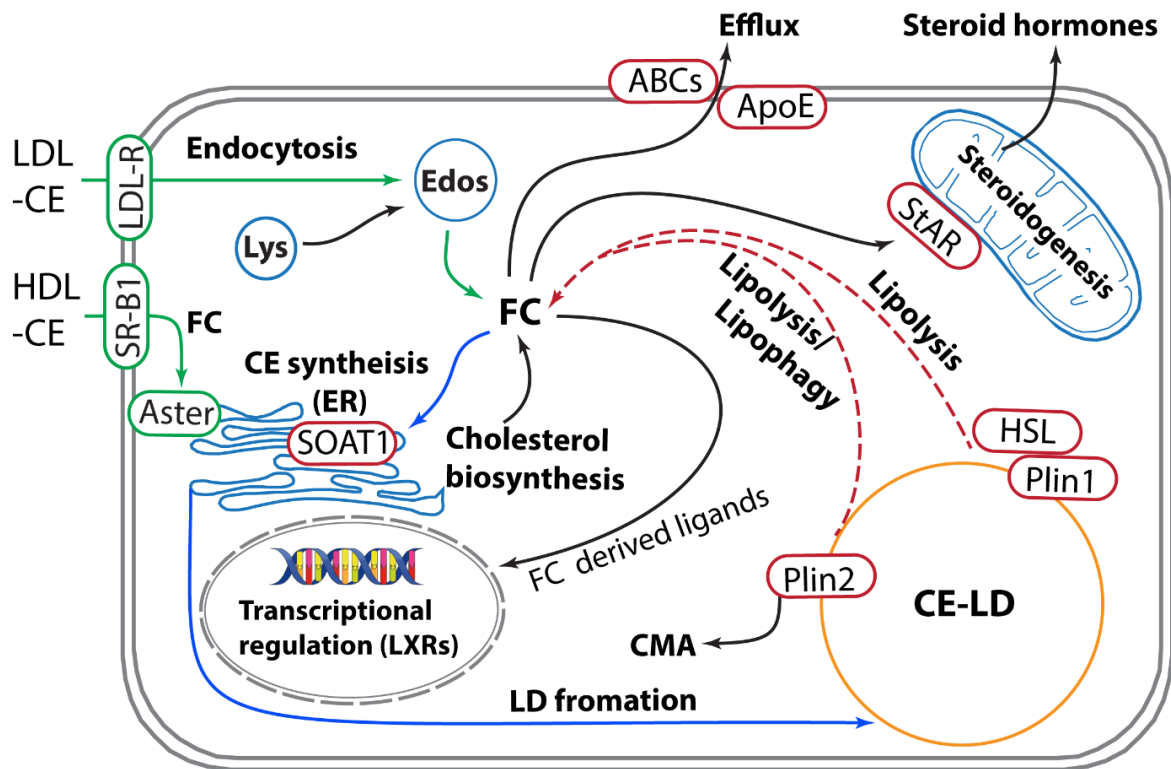


Figure 5. Intracellular cholesterol flux in adrenal cortical cells. Adrenal cortical cells acquire exogenous cholesterol by endocytosis of LDL followed by lysosomal degradation of the particle, or from HDL via SR-B1/Aster mediated selective cholesterol uptake routed to ER. Adrenal cortical cells may additionally synthesize cholesterol from acetyl-CoA. Cytosolic free cholesterol can be used as substrate for production of steroid hormones (in mitochondria), esterified to CE and stored in CE-LDs, or removed from the cell by reverse cholesterol transport. Cholesterol derived intermediates are ligands for transcription factors (LXRs) that control expression of enzymes and transporters involved in cholesterol balance. (Lys, lysosomes; Edos, endosomes.)

1.4 Perilipins (Plins)

Perilipins are a family of proteins that bind to the surface of LDs. The Plin genes are evolutionarily conserved in mammals and are believed to be derived from gene duplication of one ancestral gene (137). Five paralogous mammalian perilipin genes have been identified, which have been given the official names *Plin1* to *Plin5* based on their order of discovery.

1.4.1 Basic structures of perilipins in mice

Basic conserved motifs in Plin proteins are illustrated in Figure 6. Four of the mouse Plin proteins (*Plin1*, 2, 3 and 5) are similar in size, consisting of 425-517 amino acids, whereas *Plin4* contains a long central repetitive region with a total size of 1403 amino acids (138, 139). Plin proteins share several conserved regions, with the

signature motif being their N-terminal PAT domains present in all Plins, but with a less evident sequence homology in Plin4. The nomenclature 'PAT' derives from the original names of the first three identified members in the Plin family: Plin1 (perilipin), Plin2 (ADRP) and Plin3 (TIP47). The PAT domain is a hydrophobic structure consisting of about 100 amino acid residues. This region in Plin1 facilitates recruitment of HSL to the LD surface upon lipolytic stimulation (140).

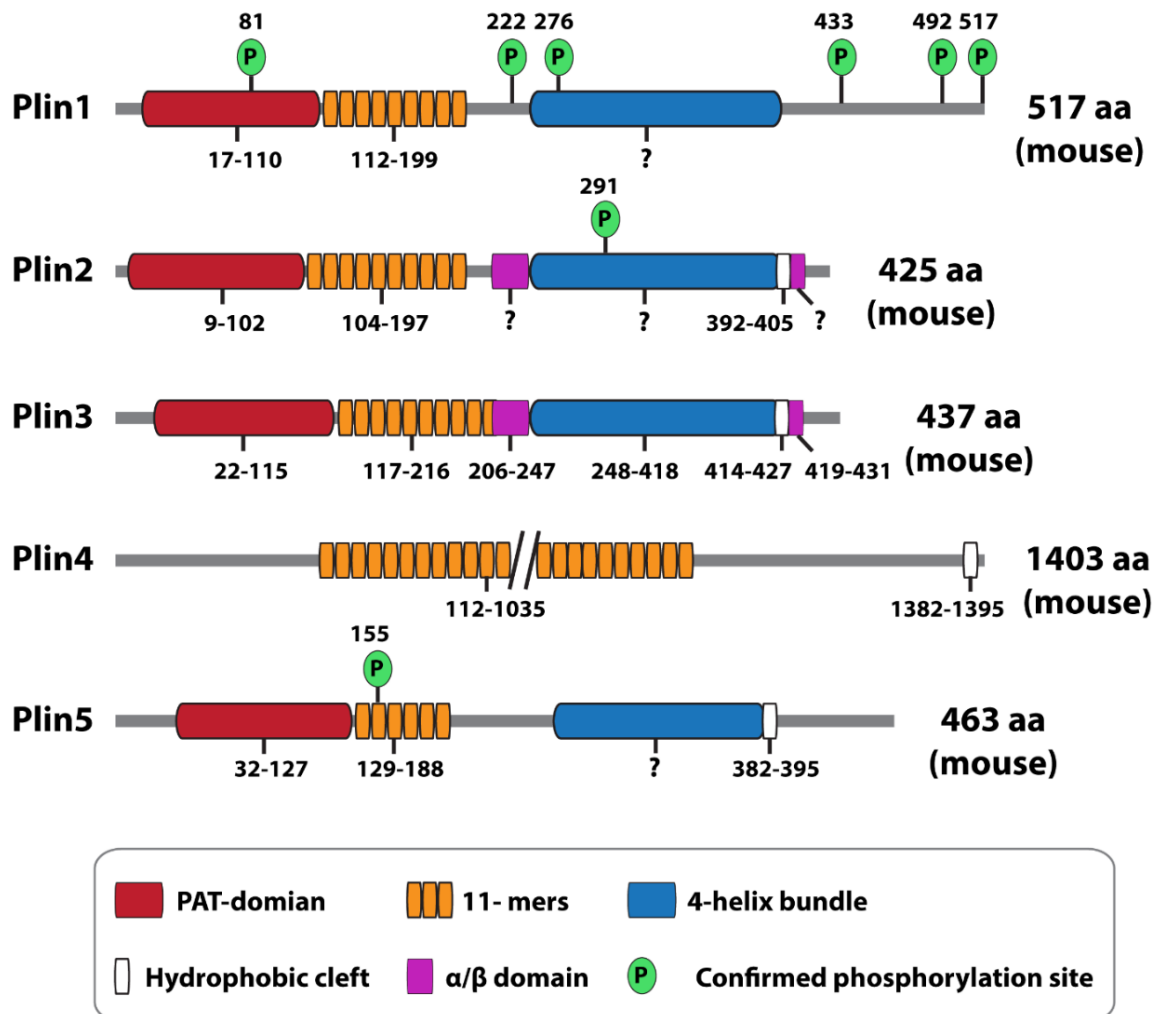


Figure 6. Basic structures of mouse perilipins. Plin1-5 share two conserved structures in their N-termini: the PAT domain (with limited sequence homology for Plin4) followed by 11-mer repeats. The PAT domain contains motifs that can interact with HSL. The 11-mer repeats are predicted to form amphipathic helical structure that can interact with phospholipids (LD surfaces). Plin4 has a very long repetitive region of 11-mers of about 900 residues. The C-termini are more divergent. The C-terminus of Plin3 contains a 4-helix bundle and α/β domains, which form a hydrophobic cleft. Similar cleft structures are predicted to present in Plin2, Plin4 and Plin5. Murine Plin1 is expressed as four subtypes (Plin1a-d) due to alternative mRNA splicing. The full-length Plin1a (often referred to as Plin1) contains six serine residues that can be phosphorylated by PKA. Phosphorylation of Plin1 at these various sites are important for Plin1 interactions with HSL and CGI-58

during lipolysis. Plin2 and Plin5 have one confirmed phosphorylatable site each, at serine 291 and 155, respectively. Phosphorylation of serine 155 in Plin5 enhances lipolytic activity.

A second conserved structure shared by all Plins is the repeated region following the N-terminal PAT domain. The number of repeats varies among Plin members and subtypes, with the longest repeating region found in Plin4 of about 900 residues. The repeated region is often described to consist of segments of 11-mer repeats (141). This is somewhat imprecise, as the sequence identity is greater when aligned as a 33-mer repeats (personal communication, Knut Tomas Dalen, Department of Nutrition, University of Oslo). Similar 11-mer repeats, with less sequence identity to those found in Plins, are present in apolipoproteins and other lipid binding proteins such as the Cide family members (141). The 11-mer regions are believed to form amphipathic helices that can interact with phospholipid-monolayer and are important for targeting of Plins and other LD binding proteins to LD surfaces (142).

The carboxyl terminal domains of the different Plins are more divergent and responsible for at least some of the subtype-specific functions among different Plin members. X-ray crystallography revealed that the C-terminal of Plin3 contain a four-helix bundle structure (143), which is also predicted to exist in Plin1, 2 and 5. Similar structures also exist in ApoE and are proposed to mediate transient interactions with lipoprotein particles, indicating that this region may interact with the LD surfaces as well. Additionally, the four-helix bundles and the following α/β domain form a hydrophobic cleft, which is suggested to bind hydrophobic moieties (LD core) rather than interact with the phospholipid-monolayer (143). Domains in the C-terminal regions of Plin1 and Plin5 can interact with ATGL or/and its co-activator ABHD5 and regulate lipolytic activity (details see section: 1.4.4).

1.4.2 Tissue distribution and transcriptional regulation of perilipins

Mammalian cells express several Plin proteins where the dominating Plin proteins at the LD surface differs among cell types (144). Plin1 is mainly expressed in white (52) and brown adipose tissue (145) and steroidogenic organs like adrenal cortex (146). Plin2 and Plin3 are both ubiquitously expressed (147). Expression of Plin3 is relatively stable, whereas expression of Plin2 is stimulated by fatty acids. Plin4 is expressed in white adipose tissue (148), heart (149) and skeletal muscle (150, 151).

Plin5 is mainly expressed in mitochondria-rich oxidative tissues with high capacity to oxidize fatty acids, such as brown adipose tissue, liver, skeletal muscle and myocardium (139). Each mammalian tissue expresses at least two types Plins, where combinations of expressed Plin members likely fulfill cell-specific requirements for LD regulation (152).

Expression of Plin1, Plin2, Plin4 and Plin5 are transcriptionally regulated by members of the peroxisome proliferator-activated receptors (PPARs), whereas Plin3 expression is likely unaffected by PPAR activity. Transcription of Plin1 and Plin4 are regulated by PPAR γ in white adipose tissue (153, 154). Plin2 is regulated by PPAR α in liver (155, 156) and PPAR β/δ in macrophages (157). Transcription of Plin5 is reported to be regulated by PPAR α in liver, heart and muscle (139, 158), by PPAR β/δ in muscle (150), and by PPAR γ in adipose tissue (158, 159). Lipid components released from LDs are potential ligands of these transcription factors (160), where transcription of *Plin* genes and control of LD lipolysis by Plin proteins form a feedback loop regulating LD balance and lipid flux. In addition to PPARs, other transcription factors such as LXRs (161) and SREBPs (162) may regulate transcriptions of Plins, but it is unclear if these are directly mediated.

1.4.3 LD targeting and post-translational regulation of perilipins

Perilipins bind to LD surface via poorly understood mechanisms, which are likely mediated by structural motifs of Plins and the biophysical properties of LDs. The conserved PAT domain and 11-mers are thought to be essential for LD targeting (163, 164), but these segments are not the only motifs involved in LD binding. Truncated Plin2 lacking the PAT domain can still bind to LDs, though less efficient compared with the wild-type Plin2 (165). The 11-mer repeats domain is predicted to form amphipathic alpha helices (141). Disruptive mutations in this region reduce LD binding affinity, suggesting that the 11-mers domain is sufficient for LD binding (142), at least for Plin1, Plin2 and Plin3. In addition to the conserved PAT domain and 11-mer repeats, nonconserved C-terminal structures are also involved in LD targeting. A hydrophobic central domain of Plin1 is predicted to form a hairpin structure that embeds into LD core (166). Mouse Plin2 with truncated N- and C-termini, but encompassed a domain between amino acid 189 and 205 still functions to target LDs and increases cellular LD content (167). The C-terminal structure of mouse Plin3 fall into a distinct L-shape with

a hydrophobic cleft consisting of four-helix bundles and α/β domain - a structure that is suggested to bind to the hydrophobic core of LDs (143).

The biophysical properties of the LD surfaces also influence the binding of Plins. Binding of Plin2 requires both hydrophobic and electrostatic interactions, and is influenced by the lipid composition of the LD surfaces (168). The head-group and acyl-chains of the LD phospholipids affect binding of Plin3 via interaction with its C-terminus (169). Subtypes of Plin1 bear identical N-termini, but have distinct preference to LDs with different core lipids: Plin1a and Plin1b prefer to bind TAG-LDs, Plin1c prefers to bind CE-LDs, while Plin1d has no such preference (61). The specific C-termini of different Plin1 subtypes and core lipids may together decide such specific targeting. Computer based molecular dynamics simulation studies suggest that neutral core lipids may interact with monolayer phospholipids and alter the biophysical properties of the latter (170), which may affect protein targeting to LD surfaces. This interaction may partly explain the core preference of Plins.

The stability of Plin proteins varies between Plin subtypes and depend on the state of LD-binding. The Plin1 and Plin2 proteins are stabilized when bound to a LD surface. With shrinking of core lipids and decreasing of phospholipid surfaces during LD mobilization, these proteins dissociated from LDs and are quickly degraded by proteasomes or lysosomes. In contrast, Plin3, Plin4 and Plin5 are stable in their cytosolic 'LD-free' form and may aggregate in small disc-like structures in cytosol. It has been suggested that these particles may contain tiny neutral lipid cores, but experimental evidence is difficult due to the detection limit of conventional light microscopy (171). These Plins can quickly relocate to LD surfaces during formation and expansion of LDs.

The protein levels of several of the Plins are not necessarily consistent with their mRNA levels. For instance, in matured adipocytes at basal state, Plin1 is the dominant Plin at the LD surface. Despite high levels of adipose Plin2 mRNAs, translated Plin2 protein is quickly degraded by proteasomes in the absence of available LD surfaces (172, 173). However, upon induction of lipolysis, Plin2 binds to small LDs adjacent to the larger Plin1-coated LDs and escape from degradation (174). This mechanism is believed to temporarily keep the released lipid components in Plin2-coated small LDs to buffer adipose lipid release during lipolytic stimulation.

Protein expression level is not the only factor that affects the function of Plins. Several of the Plin proteins are also regulated by phosphorylation (144, 152). Phosphorylation regulates Plin interactions with the LD surface or lipases/lipase co-activators (at least known for Plin1 and Plin5, see section 1.4.4.1 and 1.4.4.3), thereby switching their function from repressing to promoting of lipolysis. In mice, full length Plin1 (Plin1a) has six confirmed PKA phosphorylation sites at serine 81, 222, 276, 433, 492 and 517 (175). Whereas Plin5 has one confirmed site which can be phosphorylated by PKA at serine 155 (119, 176). Plin3 has one proposed phosphorylation site at serine 245 (143), yet the biological significance of this phosphorylation needs to be clarified. It has not been confirmed whether Plin2 is a substrate of PKA, though one identified phosphorylation site has been identified at serine 291 (177). Recent studies suggest that Plin2 is phosphorylated by AMPK upon induction of lipolysis (106).

1.4.4 Perilipins regulate lipolysis and lipid droplets: The classic barrier theory and beyond

After the discovery of adipose perilipin 1 in the 1990s, our view on fat mobilization changed dramatically. Our understanding of lipolysis in adipose and non-adipose tissues shifted from the catabolic activity of lipases alone, to a broader perspective involving regulation of their access to the LD surface and core lipids. Among the five mammalian Plin proteins, the role for Plin1 in adipose tissue is the best characterized. Our understanding of Plin2 and Plin5 function for non-adipose LD regulation is largely based on our knowledge of Plin1 function. So far, the role of Plin3 and Plin4 is still little understood. Although this thesis mainly focuses on Plin2 and Plin5, the 'classic' LD regulation model established for Plin1 in adipocytes will be described in the next chapter as a basis to understand the role of Plin2 and Plin5 in regulation of lipolysis in non-adipose tissues.

1.4.4.1 Perilipin 1: The classic barrier interacts with lipases

The first discovered Plin member, Perilipin1, was identified and characterized in adipocytes. Later observations of humans with rare null mutations in PLIN1 and characterization of *Plin1* knockout animal models have confirmed that an important function of Plin1 is to act as a barrier on the LD surface and regulate lipolysis by interfering with the access or/and activity of lipases. TAG is the major core lipid of

adipose LDs. As mentioned earlier, lipolysis of TAG involves three sequential hydrolytic steps catalyzed by three lipases (ATGL, HSL and MGL), where one fatty acid is released from the glycerol backbone in each step (for details, see section 1.3.2.2). Under basal state when lipolysis is repressed, Plin1 binds the ATGL co-activator alpha-beta hydrolase domain-containing 5 (ABHD5, also known as CGI-58) in its C-terminus (178), while ATGL (179) and HSL (140) are mostly distributed in the cytosol with little contact with LD surfaces. Plin1 is now believed to act as a physical barrier on the LD surface and prevent ATGL and HSL access to the core lipids. In addition, the Plin1-ABHD5 interaction segregates ATGL and ABHD5, which further inhibits ATGL enzymatic activity. Upon lipolytic stimulation (e.g., during starvation, exercise or with the presences of β -adrenergic activators), several of the factors described above (including Plin1, ATGL, ABHD5 and HSL) are phosphorylated by PKA. Plin1 is phosphorylated on up to six sites, which changes its role as a barrier against lipases. Phosphorylation of the Plin1 C-terminal region results in the release of ABHD5, which enables the ABHD5 to interact with ATGL and stimulate its lipolytic activity. The recruitment of ATGL to LD surface may involve ATGL phosphorylation, but probably independent of Plin1 (176). In parallel, phosphorylation of the N-terminal PAT domain of Plin1 enhances binding of phosphorylated HSL to the LD surface (140). In sum, a number of phosphorylation events induced by a lipolytic signal switches the function of Plin1 from anti-lipolytic to pro-lipolytic and increase the rate of TAG mobilization about 100-folds. The role of Plin1 in lipolysis regulation has been established by observation of whole animals and isolated *Plin1*^{+/+} and *Plin1*^{-/-} adipocytes (118, 180). *Plin1*^{-/-} adipocytes/mice are not only subjected to severely diminished lipid storage at basal state, but also have severely impaired ability to release fatty acids from TAG upon lipolytic stimulation. This implies a complete loss of hormonal regulation of adipose LD storage and mobilization. Through the interaction with lipases and lipase co-activators, Plin1 plays as a 'protector' on LD reservoirs.

This 'classic' dual-functional barrier model of Plin1 characterized in adipocytes is the basis for studying the function of other Plin members and non-adipose LD regulation.

1.4.4.2 Perilipin 2: A flexible barrier links lipolysis and lipophagy

Plin2 was discovered as an mRNA induced in differentiating adipocytes (181). Later studies have revealed that Plin2 is expressed broadly with moderate to high levels in the majority of tissues examined (147, 182). Plin2 functions as a dominant LD-coating protein in cells where Plin1 and Plin5 are expressed at low levels, with a clear LD protective role in liver. The Plin2 protein is unstable and rapidly degraded in its LD-free form in the cytosol, and only stable when bound to LDs (172). In mature, unstimulated adipocytes with Plin1 on LD surfaces, Plin2 seems to have lower LD binding-affinity compared to Plin1. In *Plin1*^{-/-} adipocytes, Plin2 become the major Plin on the surface of adipose LDs (118). Compared to wild-type cells, Plin2-coated LDs in *Plin1*^{-/-} adipocytes have elevated basal levels of lipolysis and nearly fails to increase lipolysis in response to lipolytic stimulation by activating PKA. This suggests that Plin2 neither has the 'dual-function' barrier role of Plin1, nor interacts with lipases or lipase co-factors like Plin1 (176, 183). Non-adipose cells overexpressing Plin2 have reduced recruitment of ATGL to LDs, which attenuates lipolysis and inhibits LD turnover (184), but liver cells lacking Plin2 have increased recruitment of ATGL and ABHD5 on LDs with concomitantly enhanced basal lipolysis (152, 185). These studies indicate that Plin2 may restrict binding of ATGL and protects LDs from lipolysis in a 'passive' manner, but perhaps less efficient than Plin1. In sum, Plin2 seems to act as a weak physical barrier that are neither strongly anti-lipolytic at basal state nor pro-lipolytic upon PKA activation.

More recently, an alternative role of Plin2 in regulation of LD mobilization has been identified in the lipophagy pathway. At basal state, Plin2 acts as a physical barrier that prevents encapsulation of hepatic LDs by autophagosomes and lipophagic degradation (186). In addition, Plin2 seems to be a substrate of CMA. Upon binding with hsc70, Plin2 is phosphorylated by AMPK and the complex is recognized by Lamp-2A on lysosomes and facilitates its lysosomal degradation (106). Removal of Plin2 from LDs by CMA is believed to expose the LD surface to facilitate both cytosolic lipolysis and lipophagy. Mutated Plin2 with reduced affinity to hsc70 is not removed from LDs in cultured fibroblasts, which prevents docking of cytosolic lipases and formation of autophagosomes both at the basal state and during nutrient deprivation (105).

Taken together, Plin2 seems to function as a flexible barrier that to some extent protects LDs from cytosolic lipases. Being a CMA substrate, Plin2 seems to regulate LD degradation by signaling to the lipophagy pathway. Due to its ubiquitous expression, Plin2 is likely important for LD degradation in multiple tissues. Many questions about Plin2 function remain to be answered. In this thesis, we investigated the role of Plin2 in regulation of fatty acid flux in skeletal muscle (**paper I**) and cholesterol balance in adrenal cortex (**paper II**).

1.4.4.3 Perilipin 5: A bridge connects lipid droplets and mitochondria

The expression of Plin5 is relatively restricted to oxidative tissues, with high expression found in heart, brown adipose tissue and muscle (139). Plin5 interacts with the same set of lipases and lipase co-activators as Plin1, but regulates these moieties differently. The N-terminal PAT domain of Plin5 binds HSL even at the basal state and attenuates its lipolytic activity (140). The C-terminal domain of Plin5 shares limited sequence homology to Plin1, but seems able to bind both ABHD5 (187) and ATGL (176). Interestingly, the binding site for ATGL overlaps with that for ABHD5, which enables Plin5 to exclusively recruit either ATGL or ABHD5 (188). This segregation of ATGL and ABHD5 is believed to preclude their interaction and effectively attenuate lipolysis under basal condition, even though both molecules are present on the LD surface. PKA is found to phosphorylate mouse Plin5 at serine 155 and promotes lipolysis (119, 189). The exact mechanism involved at the LD surface that promotes lipolysis are not understood, and it is unknown if ATGL, ABHD5 and HSL are released from phosphorylated Plin5.

A unique property of Plin5 is its ability to generate physical contacts between Plin5 coated LDs and mitochondria (190, 191). The C-terminal sequence of Plin5 is essential for the recruitment of mitochondria onto LD surfaces (190). It is believed that these contacts might facilitate fatty acid transfer from LDs to mitochondria and favor FA-oxidation (190, 192). However, a recent study in brown adipose tissue have suggested the opposite: LDs coated with Plin5 are attached with a subpopulation of mitochondria, which utilize primarily glucose and less fatty acid as substrate to generate ATP. The LD-mitochondria interaction may facilitate ATP supply for core lipid synthesis and favor LD growth (193).

Despite the close relationship between Plin5, LDs and mitochondria, transgenic mice with manipulated levels of Plin5 are characterized with mild metabolic disturbances. The most obvious phenotype is their altered LD content in myocardium and muscle. Levels of accumulated LDs are severely decreased in myocardium (194) and skeletal muscle (195) of *Plin5*^{-/-} mice. In contrast, overexpression of Plin5 in skeletal muscle increases muscle LD content (20, 196). Mice with cardiac-specific Plin5 overexpression have increased LD content in myocardium even at chow fed state (197). Therefore, Plin5 seems to be important for the growth and/or stability of LDs in these oxidative tissues. In contrast to the clear changes of LD content in oxidative tissues, the role of Plin5 in energy metabolism is complex and difficult to understand. Both Plin5 deletion and Plin5 overexpression are reported to increase fatty acid oxidation (158, 194, 198) and production of reactive oxygen species (194, 197). In addition to alternations in fatty acid metabolism, Plin5 null mice have increased whole-body utilization of carbohydrates, with impaired insulin action upon high-fat diet feeding (195). Plin5 is also a potential regulator of insulin secretion in pancreatic β -cells (199), and has been reported to translocate to the nucleus and alter gene transcriptions (200). These functions of Plin5 are beyond direct lipolytic regulation of LDs, and need to be investigated further.

Overall, Plin5 seems to be important for maintaining the LD-pool in oxidative tissues, though its role in energy metabolism remains unclear. In this work, we investigated the function of Plin5 in regulation of fatty acid flux in cardiomyocytes (**paper III**), and its role in cardiac metabolism and myocardial ischemia.

2 AIMS OF THE STUDY

Lipid droplets (LDs) are intracellular organelles that store neutral lipids such as TAG and CE. Perilipins coat the surface of LDs and regulates their degradation. Abnormalities in LD storage are observed in many metabolic disorders such as obesity, type II diabetes, atherosclerosis, and even cachexia. Hence, increased understanding of Plin functions and their role in metabolism and lipid-related diseases may reveal new targets for diagnosis, prognosis and treatment of metabolic diseases.

Two of the members of perilipin family, Plin2 and Plin5, are highly expressed in non-adipose tissues, such as in heart, muscle and adrenals, where they likely are important for LD regulation in these tissues. The main purpose of this thesis was to investigate how Plin2 and Plin5 affect LD storage, lipid flux and metabolisms in these tissues.

The specific objectives of the individual studies were:

- 1) Investigate the role of Plin2 for regulation of lipid droplet storage, fatty acid flux and energy metabolism in skeletal muscle (**paper I**).
- 2) Study the role of Plin2 for storage of adrenal cortical lipid droplets, cholesterol balance and steroidogenesis (**paper II**).
- 3) Study the role of Plin5 for cardiac lipid droplet storage, cardiac lipid flux, energy substrate metabolism and myocardial ischemia/hypoxia (**paper III**).

3 SUMMARY OF PAPERS

Paper I: Loss of perilipin 2 in cultured myotubes enhances lipolysis and redirects the metabolic energy balance from glucose oxidation towards fatty acid oxidation.

In this study, we established myoblast cultures from *Plin2*^{+/+} and *Plin2*^{-/-} mice and differentiated these into myotubes *in vitro* to characterize their ability to accumulate LDs and their ability to oxidize fatty acids and glucose. *Plin2*^{-/-} myotubes stored less LDs and incorporated less fatty acids into LDs compared to *Plin2*^{+/+} myotubes, a defect that was fully restored by addition of lipolysis inhibitors. LDs isolated from *Plin2*^{-/-} myotubes contained elevated levels of lipolytic products compared to LDs isolated from *Plin2*^{+/+} myotubes. These results are consistent with a constantly activated lipolytic activity in the absence of Plin2, which underline a role of Plin2 in protection of LDs against lipases. Plin2 deletion shifted energy metabolism in myotubes by increasing fatty acid oxidation and decreasing glucose utilization. Further, expression of transcription factors stimulating FA oxidation, *Ppara* and *Ppargc1a*, were upregulated, while expression of the FA storing related transcription factor *Pparg* was repressed in *Plin2*^{-/-} myotubes. Moreover, upregulation of genes related with fatty acid transport (*Cd36*) and downregulation of genes related with glucose transport (*Slc2a1*), glycolysis (*Pkm*, *Pdha1* and *Pdk4*) and glycogenolysis (*Pygm*), suggest that increased lipolytic activity in *Plin2*^{-/-} myotubes reprograms energy metabolism through alterations in expression of key transcription factors and oxidative genes. Somewhat unexpectedly, insulin-induced Akt phosphorylation and glycogen synthesis were similar in *Plin2*^{-/-} and *Plin2*^{+/+} myotubes, indicating that the insulin signaling pathway was unaffected by Plin2 deletion. In summary, our findings demonstrate that Plin2 protects TAG containing LDs against lipolysis and balances metabolism of energy substrates in skeletal muscle cells.

Paper II: Absence of Plin2 causes adrenal enlargement with increased accumulation of cholesteryl ester-containing lipid droplets.

Adrenal cortical cells mainly store CE-LDs. In this study, we examined adrenals in *Plin2*^{-/-} mice, and investigated the role of Plin2 for CE-LD storage and cellular cholesterol balance. *Plin2*^{-/-} mice had enlarged adrenals and stored larger and more CE-LDs in adrenal cortical cells compared to *Plin2*^{+/+} mice. Fasting depleted CE content in both *Plin2*^{+/+} and *Plin2*^{-/-} adrenals, which suggests that the lipolytic response in *Plin2*^{-/-} adrenals remained intact. Circulating corticosterone levels were unaffected

by *Plin2* deletion, indicating that *Plin2* is dispensable for stimulated CE mobilization. *Plin2*^{-/-} adrenals contained elevated levels of free cholesterol at basal state. In line with this, gene expression of LXR α , a key transcription factor that regulates cholesterol homeostasis, as well as downstream target genes responsible for cholesterol reverse transport (*ApoE* and *Abcg1*) were upregulated in *Plin2*^{-/-} adrenals. Moreover, mRNAs encoding enzymes catalyzing CE and phosphatidylcholine synthesis (*Soat1* and *Pcyt1a*) were increased in *Plin2*^{-/-} adrenals. Unexpectedly, *Plin2*^{-/-} adrenals accumulated ceroid-like structures and multilamellar bodies in the cortex, especially in old females. The increased content of phosphatidylglycerols in parallel implies that these lipids are components of the accumulated structures. *Plin2*^{-/-} adrenals contain higher level of *Lal* and *Npc1/2* mRNAs, suggestive of disturbed lipophagic activity. Taken together, our findings revealed that *Plin2* is important to balance the storage of CE-LDs and cellular cholesterol homeostasis in adrenal cortical cells.

Paper III: *Plin5* deficient cardiomyocytes have reduced lipid droplet storage but increased tolerance to hypoxia after fatty acid stimulation.

In this study, we used cardiomyocytes isolated from *Plin5*^{+/+} and *Plin5*^{-/-} mice as a model to investigate the role of *Plin5* in cardiac LD storage, energy metabolism and cellular tolerance to ischemia/hypoxia. *Plin5*^{-/-} cardiomyocytes had reduced ability to store fatty acids in LDs, which was restored by an ATGL inhibitor, indicating that *Plin5* preserves cardiac LD storage mainly by inhibiting lipolysis. When incubated with fatty acids, *Plin5*^{-/-} cardiomyocytes had a transient accumulation of fatty acid derived metabolites. *Plin5* deletion did not significantly influence complete fatty acid oxidation and glucose utilization. Expression of metabolic genes were essentially similar in *Plin5*^{+/+} and *Plin5*^{-/-} hearts. These data suggest that *Plin5* deletion affects cardiac LD storage and fatty acid buffering capacity, but with less effect on cardiac energy metabolism. After oleic acid treatment, *Plin5*^{-/-} cardiomyocytes had increased tolerance to hypoxia, which may be explained by a higher glycogen content compared to wild-type cells. *Plin5*^{-/-} mice had increased heart weight and increased cardiac expression of *Myh7* mRNA with age, suggesting that long-term effect of *Plin5* deletion may induce remodeling of the myocardium.

Overall, our results suggest that *Plin5* protects cardiac LDs against lipolysis. *Plin5*^{-/-} cardiomyocytes have decreased LD storage and reduced ability to buffer fatty acid flux, but with minor alternations in energy metabolism at normal basal conditions.

Our study indicates that expression of Plin5 and pre-accumulation of LDs may not always be protective in hypoxic cardiomyocytes.

4 METHODOLOGICAL CONSIDERATIONS

4.1 Ethical considerations

The use of animals for research pose ethical controversies and is therefore undergoing ethical evaluation prior to initiation of the experiments. All use of animals in this thesis was approved and registered by the Norwegian Animal Research Authority (Mattilsynet, approvals FOTS ids: #6305, #6922 and #10901) and confirmed to the ethical guidelines given in Directive 2010/63/EU of the European Parliament on the protection of animals used for scientific purposes. Animal experiments adhered to the guideline of 'The three Rs'. Multiple tissues were collected from each sacrificed animal to minimize the total number of mice needed. Some studies were performed in isolated cells as a substitute for experiments in living animals (**paper I and III**).

4.2 Studies of perilipins and lipid droplets in mice

Genetically modified animal models with loss-of-function mutations in single genes are widely used to study the function of genes. Compared to small interfering RNA (siRNA)-induced gene knockdown models with some residual expression of the targeted gene, gene knockout models are superior as they will have the targeted gene products completely eliminated, when designed properly. In this work, we utilized Plin2 and Plin5 null mice and wild-type controls to study the functions of these two proteins in living animals, isolated cells and extracted tissues. The two knockout models used in this study had their selection cassettes removed by crossing with Flp recombinase transgenic mice, followed by backcrossing into the C57B/6N strain for 10 generations prior to studies. This approach minimizes variations in genetic background between the control mice and knockout models. Removal of a Plin gene may result in compensative changes in the expression of other Plin genes. Therefore, the expression levels of other Plin members have been examined in the studied Plin null models.

Animal models are affected by the housing environment, with effects on e.g. metabolism and stress. The light cycle, food ingredients, environmental stress levels and pathogens should always be considered when performing animal studies. In our study, mice were housed with a stable light/dark cycle (12h/12h), with 55±5 % relative humidity at 22±2 °C with free access to water and rodent chow. The health status of the animals was monitored quarterly in accord with FELASA guidelines. None listed

pathogens were identified in the mice used in these studies. Blood and tissue samples were harvested in different ways depending on downstream analysis and the experimental purpose. For tissue collection, mice were euthanized by cervical dislocation at 08am-11am to minimize variations caused by circadian rhythms. For heart perfusion experiments and isolation of cardiomyocytes, mice were intraperitoneally injected with 50 µg/g body weight sodium pentobarbital plus heparin 8 IU/g body weight before harvesting the hearts, in order to prevent clotting during perfusion and keep viability of the cardiomyocytes. Experiments were performed in animals at 15-30 weeks of age, and in one occasion also at 5-6 weeks and 50-60 weeks to study the effect of aging (**paper II** and **III**). Details about animal management and phenotype screening of the Plin-knockout mice are illustrated in Figure 7.

Metabolic phenotyping of Plin-knockout mice

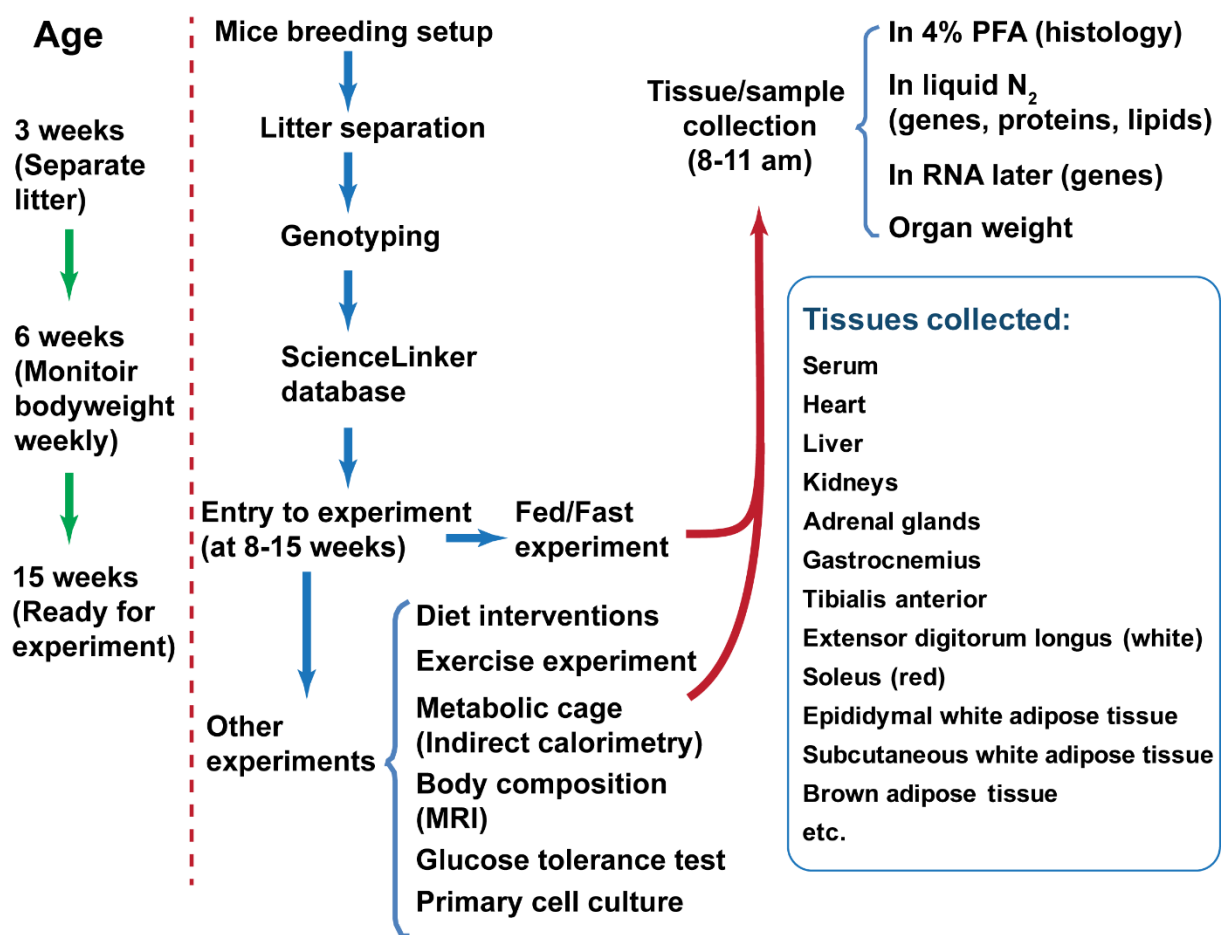


Figure 7. Metabolic phenotyping of Plin-knockout mice. Animal management and experimental procedures are illustrated in the flowchart. Multiple *in vivo* tests were carried out to examine the whole-body effect of Plin deletions. Various types of samples

were collected from Plin-knockout mice and their wild-type control animals and used to characterize their metabolic phenotypes in different tissues. Not all illustrated procedures were used in the manuscripts included in this thesis. The thesis focused on analysis of skeletal muscle, heart and adrenal glands.

Fed and Fast experiment – Mice fed with a standard chow diet (58% calories from carbohydrates, 18% from fat and 24% from protein) primarily utilize carbohydrates and less fatty acids for ATP production. Prolonged fasting reduces utilization of carbohydrates as fuel while increases the use of fatty acids, ketone bodies and amino acids. Comparison of the fed and fasted state is widely used to investigate energy metabolism. Fat mobilization from adipose tissue during fasting increases circulating fatty acids and alters systemic fatty acid flux within a short time-frame. Hence, fasting is a convenient strategy to investigate relationships between lipid flux and metabolism of lipid droplets. As variations in adipose mass influence the ability to release fatty acids during fasting, an important factor is body fat content, which is closely related to total body weight. In our study, mice at 15 weeks of age with matched bodyweights were fed *ad libitum* or subjected to 24 hours fasting prior to euthanasia and tissue collection.

In vivo ACTH stimulation test – In **paper II**, to study steroid hormone secretion of adrenal glands *in vivo*, we performed ACTH stimulation test in *Plin2^{+/+}* and *Plin2^{-/-}* mice. Adrenocorticotrophic hormone (ACTH) is a tropic hormone released by pituitary gland, which stimulates synthesis and release of steroid hormones in the adrenal cortex. Cortical steroid hormones released after administration of exogenous ACTH reflect the maximum (stimulated) steroidogenesis of the adrenal cortex. Many factors, such as stress, inflammation and circadian rhythms are known to affect secretion of steroid hormones (201), and should be controlled for during the test. In our study, ACTH was administered to animals via intraperitoneal injection at 9:00am. Blood samples were collected from lateral saphenous vein right before injection (0 hour, as baseline), and at 1 hour and 2 hours after injection. Serum levels of corticosterone, the principle glucocorticoids in mice, was determined with ELISA.

Ex-vivo perfused beating heart model - In **paper III**, to study the role of Plin5 in beating hearts exposed to ischemia, an *ex vivo* perfused heart model (Langendorff heart) was used to compare hearts collected from *Plin5^{+/+}* and *Plin5^{-/-}* mice. Hearts were retrogradely perfused through the aorta with Krebs-Henseleit buffer at constant

pressure and temperature, with continuous bubbling of 5% CO₂ and 95% O₂ (for additional details, see **paper III**). No-flow global ischemia and reperfusion were induced to mimic *in vivo* myocardial ischemia. Compared to *in vivo* heart models, heart function parameters measured in Langendorff hearts are artificial and do not fully represent the *in vivo* situation. In addition, energy substrates provided in Krebs-Henseleit buffer consists of high levels of glucose, which is different from the physiological situations *in vivo* where fatty acids are important fuel source. Due the limitations with our Langendorff experimental setup, we were unable to perfuse hearts with a fatty acid-containing buffer to better mimic the *in vivo* energy metabolism. On the positive side, the Langendorff heart model excludes most systemic effects such as hormones and blood vessel resistance, which makes it a simplified and reproducible model to study myocardial ischemia (202). Using the Langendorff heart model, we compared the *ex-vivo* heart function in *Plin5*^{+/+} and *Plin5*^{-/-} hearts before and after ischemia. In the end of the experiment, hearts were sliced and sections incubated with TTC (triphenyl tetrazolium chloride), a colorless redox indicator. Viable tissue will catalyze TTC to TPF (1,3,5-triphenylformazan) and show a brick-red color, while dead tissue will show pale white color without having the reaction. The overall infarct size was estimated as: pale white area/total area x 100% of five cross sections from the middle of each heart.

4.3 Studies of perilipins and lipid droplets in cell culture models

Even though *in vivo* models are better to represent true physiology, it is sometimes more informative to examine Plins and LDs at a cellular level to shed a light on their role in cell biology. In animal models, systemic effects such as substrate availability, hormone actions as well as cross talk between tissues are only partly understood and not easy to control. Furthermore, due the complicated experimental design and limitations of the study, some experiments, such as radioactive traced metabolic flux assays and application of lipase inhibitors, are difficult to carried out *in vivo*. To bypass these problems, we established cell culture models from *Plin2* and *Plin5* mice to study these two proteins under simplified but more precisely controlled conditions. In **paper I**, cultured myotubes were established form myoblasts of *Plin2*^{+/+} and *Plin2*^{-/-} mice. In **paper III**, adult cardiomyocytes were isolated from hearts of *Plin5*^{+/+} and *Plin5*^{-/-} mice.

Cultured myotubes from *Plin2*^{+/+} and *Plin2*^{-/-} mice – In **paper I**, to study the role of Plin2 in energy metabolism of skeletal muscle, we established *in vitro* cultured myotubes from myoblasts (muscle satellite cells) isolated from hind legs of *Plin2*^{+/+} and *Plin2*^{-/-} mice. The method used for myoblast enrichment and differentiation to myotubes was modified from Hessvik et.al. (203). Compared to myoblasts, differentiated myotubes have elevated expression levels of genes involved in fatty acid and glucose utilization, and their metabolic properties are more close to true mature skeletal muscles (204, 205) and suitable for studies of energy metabolism (206). Increased passaging of myoblasts decreases their ability to utilize fatty acids and glucose when differentiated into myotubes (207). Therefore, to be comparable, myotubes were established from myoblasts at low passage numbers. It is known that metabolic properties of skeletal muscles are fiber type dependent. Type I fibers contain more LDs and oxidize preferentially fatty acids rather than glucose and are dominating in “oxidative muscles”. Type IIb fibers contain fewer LDs and utilize preferentially glucose rather than fatty acids, and are dominating in “glycolytic muscles”. Type IIa fibers are more or less intermediate. Even though fiber types and have distinct metabolic characters, it has been reported that satellite cells isolated from different donor muscle types uniformly establish myoblast cultures with a preference to differentiate into myotubes with a dominating content of intermediate type IIa fibers (208).

Primary myotubes cultured *in vitro* have many morphological and physiological characters that resemble *in vivo* skeletal muscle fibers. They have a striated appearance and similar calcium flow upon stimulated contraction (209). Even some of the metabolic characters from the donor, such as partial properties of diabetes, obesity and endurance training (210, 211) can be preserved in myotubes established from donor myoblasts. These profiles make cultured myotubes a useful model to study muscle physiology and various muscle-related diseases *in vitro*. Of note, there are some limitations with this *in vitro* model when used for metabolic studies. *In vitro* cultured myotubes have less mitochondrial content and lower oxidative capacity compared to skeletal muscle *in vivo* (212). In addition, muscle energy expenditure, fuel preference and fiber type plasticity are affected by contractile activities, which occur infrequently in cultured myotubes unless artificially induced, e.g., by electrical pulse stimulation (EPS) (213). In **paper I**, we showed that expression of certain Plins were different in cultured myotubes compared to *in vivo* muscle tissue, with low expression

of Plin4 and Plin5 in myotubes. These properties indicate that certain characteristics of *in vitro* cultured myotubes are less comparable with matured muscle fibers *in vivo*. Importantly, we confirmed that expression of Plin2 in myotubes remained high and that removal of Plin2 in *Plin2*^{-/-} myotubes did not affect expression of other Plins. In sum, even though cultured myotubes has some limitations, they seem to be a suitable model to study the metabolic functions of Plin2 *in vitro*.

Isolated cardiomyocytes from adult *Plin5*^{+/+} and *Plin5*^{-/-} mice – Several models are available to study *in vitro* cultured cardiomyocyte-like cells. Mice HL-1 and rat H9c2 cell lines are commercially available immortalized cardiomyocyte cell lines that have been well characterized (214). These ‘standardized’ cell lines are relatively easy to culture and tend to give comparable results. However, endogenous expression of Plin5 is low in these cell lines. Although high levels of Plin5 expression can be achieved by gene transfer (transfection and transduction) and artificial overexpression, the lack of intrinsic Plin5 expression renders these models less optimal to study the role of Plin5 for cardiac energy metabolism. A better alternative is primary cardiomyocytes. Fetal or neonatal primary cardiomyocytes are relatively easy to isolate and many of their *in vivo* properties can be maintained in culture for weeks. However, altered expression of ion channels and fiber type genes, as well as a shift in energy metabolism during cardiac development, makes neonatal cardiomyocytes less representative for the adult myocardium (215). Adult cardiomyocyte isolation is more difficult, but have been available since the 1970s (216). Isolation and culture techniques have been improved since then and viable rod-shaped cardiomyocytes can be kept in culture for several weeks. However, many of their initial *in vivo* properties are maintained shortly, and is gradually lost after hours or days of culturing (217). Nevertheless, when used short after isolation, adult cardiomyocytes are better models of myocardium compared to cell lines and neonatal cardiomyocytes, and the preferred choice for short-term metabolic studies. In our study (**paper III**), we chose to utilize isolated adult cardiomyocytes from *Plin5*^{+/+} and *Plin5*^{-/-} mice as an *in vitro* model to study cardiac Plin5 and LDs.

Cardiomyocytes were isolated from adult mice according to the method described by O’Connell et al. (218), with minor modifications. In this procedure, BDM (2,3-Butanedione monoxime), a myosin inhibitor which inhibits contractility and reduces energy expenditure of cardiomyocytes, was added to increase the yield of

viable cardiomyocytes (219). A high concentration of BDM was applied during isolation and the following one to two hours of stabilization, until cardiomyocytes were attached to the laminin coated surfaces. After that, BDM was added in lower concentrations to allow spontaneous beating of cardiomyocytes to better mimic the *in vivo* energy metabolism. Serum was supplemented during plating to help cells to recover from the enzymatic digestion and physical disruption during isolation. However, serum contains exogenous hormones and growth factors which may affect cell metabolism and encourage growth of non-cardiomyocyte cell types (215). For this reason, serum was replaced with BSA after cell attachment. Compared to *in vivo* myocardium and ex-vivo beating hearts (Langendorff model), isolated cardiomyocytes have significantly decreased beating rhythms and reduced energy expenditure. In **paper III**, we demonstrate that upon fatty acid stimulation, *Plin5*^{-/-} cardiomyocytes accumulated less LDs than *Plin5*^{+/+} cells, which resembles well *in vivo* myocardium during fasting (194). In addition, despite of a rapid decline in *Plin5* mRNA levels in cardiomyocytes compared to heart tissue, *Plin5* mRNA expression was maintained at high levels during 20 hours of *in vitro* culturing. More importantly, the transcription levels of the other *Plins* were similar in isolated *Plin5*^{+/+} and *Plin5*^{-/-} cardiomyocytes. Overall, our results show that adult cardiomyocytes are a suitable model to study cardiac *Plin5* and LDs *in vitro*, at least when they are cultured for a short period of time (up to 20 hours).

Hypoxia-reoxygenation in primary cardiomyocytes - The pathophysiological cellular environment during myocardial ischemia is characterized by reduced availability of oxygen and energy substrates, accumulation of CO₂ and acidification. In **paper III**, we investigated how lack of *Plin5* and altered LD accumulation affected ischemia-reperfusion injury by exposing isolated cardiomyocytes to hypoxia-reoxygenation as a mimic of *in vivo* ischemia-reperfusion. Lactate dehydrogenase (LDH) is a cytosolic enzyme that is retained in cells when the plasma membranes is intact. However, damaged cells leak out LDH as a result of increased membrane permeability, where the severity of cell damage is proportional with the amount of LDH released. For this reason, measurement of LDH release to conditioned medium is widely used to estimate cell damage. In **paper III**, we examined the degree of cell damage induced by hypoxia by measuring LDH in the media collected at the pre-incubation, hypoxia and re-oxygenation stages. Notably, as living cells contain high concentrations of LDH, detached cells were removed from the collected media

samples by centrifugation prior to measurement of LDH activity. The total LDH content was calculated as the sum of LDH released to the media and LDH remaining in the cell lysate. LDH released during pre-incubation, referred to as the baseline LDH release, was similar for all groups. Therefore, the released LDH in the subsequent hypoxia and re-oxygenation steps represent cell damage induced by hypoxia/re-oxygenation.

Isolation of LDs from cultured cells – Lipids are basic components of almost all cellular structures, but the main accessible lipid reservoir is LD. Regulation of LDs mainly occurs on LD surfaces. To understand how perilipins regulate flux of lipids in and out of LDs, a good strategy is to analyze lipid components of purified LDs. Several approaches may be used to disrupt plasma membranes and release intracellular components. To isolate fragile organelles such as LDs, a gentle, yet efficient method, without the use of detergents that will otherwise disrupt the LDs, are preferred. In **paper I**, we used a N₂ disruption vessel followed by gradient ultracentrifugation to isolate LDs from myotubes, according to a method modified from Ding, et al. (220). With its low shearing force and high yield, the N₂ cell disruption vessel is superior to most other cell disruption methods for organelle isolations. The optimal pressure to use varies with cell types and organelles to be isolated. For soft cells and fragile organelles, lower pressure is preferred to avoid excessive disruption. The speed of ultracentrifugation should be adjusted according to the LD size. Small LDs will need high speed to float, whereas large LDs require low speed to avoid dispersion. In addition, LDs tend to melt at higher temperatures. Therefore, all procedures after harvesting of the cells should be performed at 4°C, where handling in between steps should be quick without letting the samples heat up. Isolated LDs can be used for either lipid or protein analysis. In our study, LDs isolated from cultured myotubes were analyzed with thin-layer chromatography (TLC) to identify major lipid components.

4.4 **Histology and quantification of lipid droplets**

Changed LD morphology is an indicator of altered lipid metabolism. In **paper I, II and III**, we used histological methods to visualize LDs.

Tissue fixation and sectioning - Traditionally, paraffin sections are preferred by many researchers for histological studies due to their supreme ability to preserve detailed cell structures. Importantly, the use of ethanol and xylene during sample dehydration extracts neutral lipids from the LD core, resulting in LDs shown as empty

holes in the sections. In addition, the LDs-remnants are often deformed in shape and are unsuitable for LD quantification. This method is therefore sub-optimal to study LD morphology. In contrast, sections prepared from frozen samples (cryosections) show less details of fine cell structures compared to paraffin sections, but cell structures are less deformed where more original components are preserved, including the core lipids of LDs. Except for white adipose tissue, it is relatively easy to prepare cryosections from various types of tissues. In our studies, tissues were fixed with 4%PFA, cryopreserved with 10%-30% sucrose solution, embedded with OCT and snap frozen in liquid nitrogen vapor. 20 μ m-thick free-floating sections were prepared with a cryostat and kept in appropriate buffer prior to examination of the LD morphology.

Staining method to visualize LDs - Bodipy 493/503 was used to stain LDs in cultured cells and tissue sections. Bodipy 493/503 is a lipophilic fluorescent dye that stains neutral lipids with high specificity, superior to other staining methods such as Oil Red O staining and Nile Red staining (221). Oil red O staining involves the use of isopropanol, which extracts core lipids, destroys LD structures and gives relatively high staining background. The wide spectral signal of Nile Red makes it less selective to stain small LDs and difficult to use in combination with other dyes. Bodipy is relatively soluble in water-containing solutions, does not alter LD morphology, and has a narrow emission spectrum with very low background staining. We have demonstrated (in **paper II** and **paper III**) that Bodipy is compatible with many other fluorescent dyes, such as Hoechst 33342 (stains nuclei) and CF568 conjugated Phalloidin (stains F-actins to show cell skeleton), making it possible to stain LDs, nuclei and the cell skeleton in a single triple staining approach. One limitation with Bodipy staining is its susceptibility for photobleaching. To avoid this, sections should be kept away from light during storage, and not be exposed to intense laser or light during imaging. Preview of Bodipy stained structures should be avoided as much as possible, especially when images are needed for LD quantification. In our studies, the channel used to excite Phalloidin signals was used to preview and focus sections when taking confocal images. Additionally, staining of sections and obtained signal intensity will differ somewhat between experiments. To ensure that microscopy images were comparable, all sections in the same experiment were stained simultaneously and setup parameters for microscopy were kept constant during imaging within each experiment.

Another imaging method we have used in this thesis is transmission electron microscopy (TEM). In **paper II**, we used TEM to examine fine structures of adrenal glands. Due to the complexity of sample preparation and sectioning, the use of this method was restricted to investigate ultra-structures, e.g. fine structure of organelles and membranes in adrenals.

Quantification of LDs with ImageJ - Software based automatic quantification of LDs in tissue section images is efficient, reproducible and less susceptible to subjective biases from investigators. ImageJ is an open source software with various plugins available for image based analysis. This software was therefore selected to quantify LDs in this thesis. A method was established and validated in our lab to automatically quantify the number and size of LDs (Figure 8), combined with counting of nuclei as an estimation of cell numbers in the images. Fluorescent staining of LDs and nuclei with separate dyes enabled complete separation of these two structures in different channels, which made it possible to analyze LDs and nuclei with no overlaps. All images selected for quantification were representative and without overlapped fields. For each experiment, a representative image was selected to set software parameters, including mathematical filters to increase signal-to-noise ratio and threshold value to generate binary images. The optimized setup was subsequently used during analysis of all images within one experiment. Binary images generated based on the set thresholds were processed with the 'Watershed' plugin to automatically segregate adjacent particles. Finally, the individual size and total number of particles were reported by the software with the 'Analyze Particles' plugin. The final calculated results were represented as 'average LD size', 'LD number per cell' and 'LD areas per cell'.

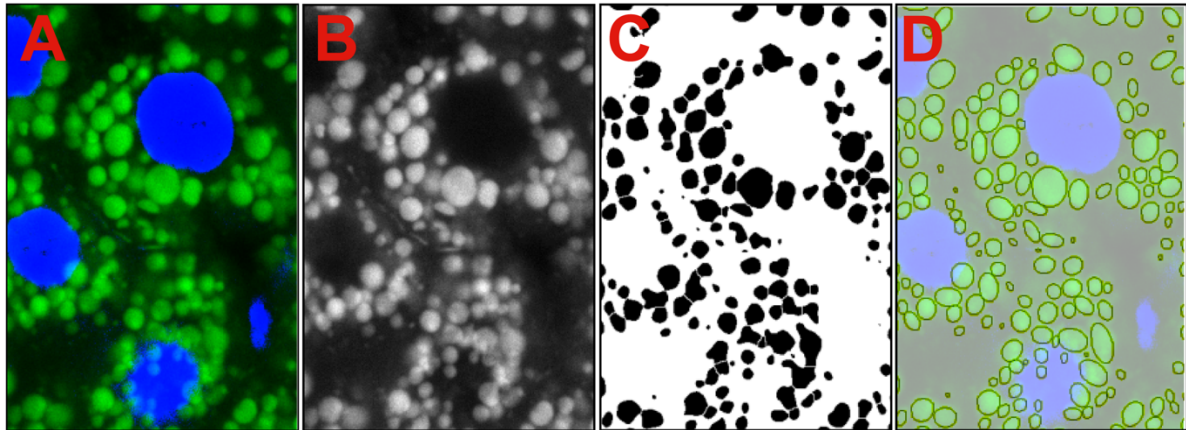


Figure 8. Image processing with ImageJ for quantification of LDs. A) Confocal microscopy image (adrenal cortex as an example) contains green channel for LDs and blue channel for nuclei. B) Separated green channel from A) only shows LDs. C) Image processed from B). Mathematical filters were applied to increase signal-to-noise ratio. The ‘Threshold’ plugin was applied to decode the image into a binary format, and the ‘Watershed’ plugin was applied to segregate adjacent particles. D) LD particles recognized by the software (indicated as circles) were overlapped with original image A) to check accuracy. The size of individual LDs and total LD number in the image were reported by ImageJ. Nuclei (blue signal in A) were quantified with the same principles.

4.5 Radioactive traced fatty acid and glucose metabolic flux assays

Radioactive traced metabolic flux assay is a sensitive method to track uptake, cellular storage, and metabolism of labeled compounds. In **paper I** and **paper III**, [1-¹⁴C]-oleic acid and D-[¹⁴C(U)]-glucose were used as tracers to study metabolism of fatty acids and glucose, respectively. Cellular substrate accumulation, ¹⁴C-ASM (acid soluble metabolites) and ¹⁴CO₂ were measured to compare the metabolic properties of *Plin2*^{-/-} myotubes and *Plin5*^{-/-} cardiomyocytes against wild-type controls.

Substrate accumulation – Substrates accumulated by cells reflect their storage and uptake efficiency. To measure cellular accumulation of fatty acids and glucose, attached cells seeded in flat bottom 96-well plates were incubated with media supplemented with ¹⁴C labeled oleic acid or ¹⁴C labeled glucose (both 1 μCi/ml). In **paper I**, cellular substrate accumulation was determined with scintillation proximity assay (SPA) (222) in cultured myotubes for up to 24 hours. The SPA method can be used to continuously monitor accumulation of ¹⁴C-labelled molecules in adherent cells. The adherent cells are in close proximity to the detectors and when tracers are enriched during incubation, the ¹⁴C signal of internalized tracers can be distinguished from the background signal in the culture medium. An advantage of the SPA method

is the possibility for continuous measurement of living cells. A limitation is lower counting efficiency and sensitivity. In **paper III**, we measured the metabolic properties of cardiomyocytes. Here, the cellular substrate accumulation was measured with conventional liquid scintillation counting of cell lysates. This method is more sensitive compared to SPA, but is limited to one measurement for each sample without the possibility for continuous measurements. For both methods, cells were washed in 0.2%BSA in PBS followed by two more washes in cold PBS to remove tracers attached on cell surfaces prior to final harvest. Cell lysates were used to determine acid soluble metabolites (ASM) and cellular protein content. Media was collected to determine the levels of remaining substrates.

Complete substrate oxidation - Complete oxidation of glucose and fatty acids results in CO₂ released by the cells. After incubating cells with ¹⁴C-labeled substrates, we collected ¹⁴CO₂ produced during 2 hours of incubation to estimate complete substrate oxidation according to the method reported by Wensaas, A. J., et al. (222), with some modifications. It has been suggested that a considerable amount of fatty acids taken up by the cells are incorporated into LDs before being oxidized (114). Therefore, the labelling condition of LD-pool should be considered during a radioactive traced fatty acid flux assay. We demonstrated that for cardiomyocytes (and probably also for skeletal muscle cells and other cell types having significant fatty acid turnover through LDs), pre-labelling of cellular LD-pool is a prerequisite to use ¹⁴CO₂ as a correct estimation of completely oxidized fatty acids (**paper III**, Figure 3). To avoid misinterpretations of the measured signal, ¹⁴CO₂ derived from fatty acid tracers should be sampled after complete labelling of LDs (**paper I**), or at different stages of labelling (**paper III**).

Incomplete fatty acid oxidation - Acid soluble metabolites (ASM) are defined as molecules that are not co-precipitated with BSA after addition of perchloric acid (HClO₄). BSA binds fatty acids with chain length longer than 6 carbons and co-precipitates by perchloric acid. The [1-¹⁴C]-oleic acid tracer used in our experiments was labelled on the first carbon and all intermediate metabolites are therefore traceable until the labeled carbon is oxidized and released as ¹⁴CO₂. Therefore, all intermediate metabolites generated during oxidation of ¹⁴C-fatty acids, such as fatty acids shorter than 6 carbons, acetyl-CoA (C1-C2), TCA cycle intermediates, but not gaseous ¹⁴CO₂, are present in ASM (223). Together, these molecules represent degradation products

of fatty acids during incomplete oxidation. The sum of ASM and CO₂ reflects the cellular capacity to oxidize fatty acids. An alternative and more advanced method to measure fatty acid metabolic flux is ¹³C metabolic flux analysis (224). This method relies on nuclear magnetic resonance, mass spectrometry and big data analysis, which is more complex and currently not established in our lab.

4.6 Analysis of genes, proteins and lipids

To understand the phenotypes of Plin-knockout mice at a molecular level, expression levels of genes (mRNA), proteins and lipids were analyzed.

Gene expression levels were analyzed with real-time quantitative PCR (qPCR) using an intercalating dye (SYBR Green) to quantify the generated double stranded nucleotides. With this method, the Ct value of the reaction is reversely correlated with the amount of the target sequence among the total amount of cDNA. If not performed correctly, the data generated may display big variations due to intrinsic variations of samples *per se* or random and systemic error caused by experimental setups and uneven pipetting. To minimize experimental variation, RNAs was isolated with the same protocol and the RNA integrity was checked with a NanoDrop 1000 spectrophotometer. The same amount of RNA was used for simultaneous cDNA synthesis of all samples in the same experiment. Equal amount of cDNAs were subsequently used in down-stream qPCR reactions. Data analysis of gene expression was performed with RQ Manager 1.2 (Applied Biosystems, Life Technologies) using the relative quantification method ($\Delta\Delta C_t$ method). Results were presented as gene expression levels relative to expression of a reference gene ($2^{-\Delta\Delta C_t}$). Selection of a suitable reference gene is difficult. In **paper I** and **paper II**, the expression levels of Tata-binding protein mRNA (gene: *Tbp*) was verified not to differ between groups of myotubes or adrenal gland samples, and was used as a reference gene. However, in heart tissue and cardiomyocytes (**paper III**), the mRNA levels of *Tbp* displayed more variations between groups, and therefore mRNAs of the evenly expressed Glyceraldehyde 3-phosphate dehydrogenase (*Gapdh*) and Ribosomal protein lateral stalk subunit P0 (*Rplp0*) were selected as reference genes. The size of the amplified PCR product varies depending on primers designed for each gene, which will affect the fluorescent signal intensity of the intercalated SYBR Green and affect the determined Ct value. Therefore, $2^{-\Delta\Delta C_t}$ values are not directly comparable between

genes. Gene expression results were represented as fold-differences relative to means of wild-type controls (**paper I** and **paper III**).

Immunoblot (Western blot) is commonly used to analyze protein expression levels. This method is semi-quantitative, since the signal intensity depends on epitope expression levels and antibody binding efficiency. The epitope-specific affinity and specificity of the primary antibody are the main factors affecting the reliability of an immunoblot. The antibody affinity dictates the sensitivity and proteins with low expression levels may only be detected with high affinity antibodies. Specificity of antibodies decides detection accuracy. A common problem for commercially available antibodies is their big variations in specificity. The specificity of antibodies used in our studies have been tested previously. In *Plin2*^{+/+} and *Plin2*^{-/-} myotubes, β -actin was verified to be similarly expressed independent of treatments or groups and was used as loading control (**paper I**). Gapdh was used as loading control in *Plin2*^{+/+} and *Plin2*^{-/-} adrenal glands (**paper II**) due to its consistent expression in that organ.

Lipid components were analyzed with thin-layer chromatography (TLC) or advanced lipidomic analysis. TLC is a fast and economically favorable method to quantify the content of major lipid species. In **paper I**, lipid components of LDs isolated from myotubes were analyzed by TLC to compare the difference of lipolytic products derived from TAG (DAG, MAG and FFA). Due to its higher sensitivity than enzymatic-based colorimetric lipid analyses, TLC was used in **paper III** to quantify the content of TAG from heart tissue samples. In **paper II**, TLC was used to identify major lipid species in adrenal glands and quantify the content of CE and free cholesterol. Compared to TLC, lipidomic analysis is more advanced, with higher sensitivity and throughput with an ability to detect unclassified lipids. However, it is more expensive and requires special instruments (high performance liquid chromatography (HPLC) coupled to time of flight-mass spectrometry (TOF-MS)). In this thesis, untargeted lipidomic analysis was used to identify unknown lipids in adrenals (**paper II**).

4.7 Statistics

The animals used in these experiments have identical genetic background (backcrossed >10 times), except for the intended genetic modification (deletion of the various Plin genes). Therefore, low individual variation is expected within a group. The number of animals used in the animal studies were based on previous power

calculations where small numbers (four to nine animals per group) are found to be sufficient to detect biological variance between groups. In **paper I, II and III**, all data were analyzed with Prism 7 (Graphpad Software, CA, USA). Data in this thesis are found to be (or close to be) normal distributed. In **paper III**, parameters reflecting heart function in heart perfusion experiments were analyzed with 2-way ANOVA. Unpaired two-tailed Student's t-test was used to analyze the remaining data. $p < 0.05$ was defined as significantly different. Data in bar graphs and dot plot graphs are presented as means \pm SD. Data in line graphs are presented as means \pm SEM.

5 GENERAL DISCUSSION

5.1 Perilipins, lipolysis and lipid droplets

The morphology of LDs varies considerably between cell types. Even within an isolated cell, the morphology of LDs will change depending on nutritional conditions and the cellular metabolic states. These changes are reflected as alterations in LD size, number, localization and interactions with other organelles (22). The morphology of LDs is regulated by various LD-associated proteins, such as perilipins (Plins) - a family of LD-associated proteins expressed in a tissue- and cell-specific manner. Different Plins have different ability to balance the LD pool, and hence, the morphology of LDs will differ in cell types dependent on the type of Plin proteins expressed. Expression and function of Plins are regulated by transcription factors (such as PPARs), post-translational modifications (such as phosphorylation / dephosphorylation) as well as factors affecting stability of Plin proteins (proteasomal / lysosomal degradation). The model for Plin1-mediated LD regulation in white adipocytes suggests that Plin1 function as a physical barrier at the LD surface and regulate LD-metabolisms through control of lipolysis (section 1.4.4). Plin family members share conserved sequential and structural motifs, implying that the same LD regulation may also apply to other Plins, albeit likely with Plin type-dependent specificities. The main purpose of this thesis work has been to understand the individual roles of Plin2 and Plin5 and their impact on lipid flux and energy metabolism.

5.1.1 Plin2 and TAG-LDs in skeletal muscle cells

The levels of Plin2 protein in various tissue types are closely related to the content of LDs (182, 225). Global deletion of Plin2 in mice initially revealed few differences from wild-type mice, except reduced hepatic content of lipids (226). Later studies have suggested that lack of Plin2 protects against high-fat diet induced adipose and hepatic LD accumulation (227), whereas cardiac Plin2 overexpression promotes LD accumulation in cardiomyocytes (228). These observations underline a role for Plin2 as a LD protector in various cell types. However, the role of Plin2 in the regulation of LDs in skeletal muscle cells and its contribution to muscle metabolism of energy substrates have not been thoroughly investigated.

In **paper I**, we showed that stimulation of cultured myotubes with oleic acid resulted in increased expression of Plin2 mRNA and protein in wild-type myotubes,

with a simultaneous increase in cellular LD content. Our data is consistent with similar observations in other cell types, where fatty acids both activates Plin2 gene transcription and provide LD surfaces to stabilize the Plin2 protein (158, 172, 229). In contrast, accumulation of TAG containing LDs following oleic acid stimulation was largely blunted in *Plin2*^{-/-} myotubes compared to wild-type cells, revealed by a reduction of LD content by light microscopy and a decrease in cellular accumulation of ¹⁴C labeled oleic acid (TAG) in *Plin2*^{-/-} myotubes. These observations suggest that the presence of Plin2 stabilizes TAG containing LDs in skeletal muscle cells. In agreement with our findings, a similar decrease in LD content has been reported in C2C12 myotubes where Plin2 has been temporarily and incompletely removed by siRNA silencing (230), while Plin2 overexpression increased LDs and TAG content, further supporting that Plin2 promotes LD storage in muscle cells.

Our study contributed with further mechanistic insight in how Plin2 preserve skeletal LDs by regulating lipolytic rate. ATGL is the principle lipase that hydrolyze TAG (231) and *Atgl*^{-/-} mice have elevated levels of TAG (LDs) in skeletal muscle cells (116). It has been reported earlier that ectopic expression of Plin2 in HEK293 cells decrease associations of ATGL with LDs (184), whereas knockdown of Plin2 in AML12 liver cells increases the association of ATGL with LD and enhances lipolysis (184, 185). These observations suggest that Plin2 protects LDs by inhibiting ATGL action. By using TLC, we demonstrated that LDs isolated from *Plin2*^{-/-} myotubes contained a higher proportion of lipolytic products such as DAG, MAG and free fatty acids compared to LDs isolated from *Plin2*^{+/+} myotubes, implying an elevated lipolytic activity in *Plin2*^{-/-} myotubes. In line with this, pharmaceutical inhibition of ATGL or/and HSL restored formation of TAG-containing LDs in *Plin2*^{-/-} cells similar to levels observed in *Plin2*^{+/+} myotubes. Retraction of the reversible ATGL inhibitor Atglistatin returned *Plin2*^{-/-} myotubes to a state with elevated lipolysis and increased fatty acid release compared to *Plin2*^{+/+} myotubes. Taken together, our results are in line with a notion that Plin2 promotes LD accumulation in skeletal muscle cells by protecting TAG containing LDs against ATGL/HSL mediated lipolysis.

5.1.2 Plin2 and CE-LDs in adrenal cortex

LDs in most cell types are primarily filled with TAG and serve as a cellular storage reservoir of energy-dense fatty acids. In contrast, LDs of steroidogenic adrenal

cortical cells mainly consist of CE (11). Early studies have demonstrated that these adrenal LDs are coated with Plin1 and Plin2 (146, 232), implying these two proteins may play important roles in regulation of CE-containing LDs in adrenal cortical cells. Previous studies on Plin2 have mostly focused on its function in regulation of TAG-containing LDs in tissues such as liver, adipose tissue and skeletal muscle. To our knowledge, studies to reveal the functional role of adrenal Plins are lacking.

In **paper II**, we showed that adrenals express high levels of Plin2 mRNA and protein, which conforms previous examines on adrenal LD coating proteins by immunostaining (232) and proteomic analysis of CE containing LDs (64). However, despite that most reported animal and cell models with reduced or deleted Plin expressions are associated with a reduction of LD content, we observed a significant increase in adrenal LD content in *Plin2*^{-/-} mice. In parallel with increased content of LDs, *Plin2*^{-/-} adrenals accumulated more CE compared to *Plin2*^{+/+}. TAG was not detectable by TLC in either *Plin2*^{+/+} or *Plin2*^{-/-} adrenals. These results indicate that removal of Plin2 alters the relative levels of accumulated core lipids in adrenals, but does not change the type of accumulated lipid species.

We further showed that fasting induced mobilization of adrenal CE and reduced the cortical LD content. This resembled the fasting response of TAG containing LDs in white adipocytes, which are mainly coated and regulated by Plin1 (152). Importantly, even though Plin2 deficiency led to increased storage of CE containing LDs, *Plin2*^{-/-} adrenal cortical cells responded normal to fasting with a decrease in CE-LD content compared to unstimulated cells. Plin2 seems not required for mobilization of adrenal LDs upon stress, suggesting that Plin1 might be the dominant Plin responsible for regulation of LD lipolysis in adrenal cortical cells during fasting.

In addition to increased CE, we detected elevated levels of free cholesterol in *Plin2*^{-/-} adrenals at basal state (chow fed state). In parallel, we observed increased gene expressions related with cholesterol esterification (*Soat1*), implying that *Plin2*^{-/-} adrenals have enhanced synthesis of CE. In contrast, expression of genes related with cholesterol uptake (*Scarb1*, *Ldlr*,) and *de novo* cholesterol synthesis (*Hmgcr*) were marginally changed or unaltered by deletion of Plin2. Hence, the increased CE-LDs observed in the lack of Plin2 are likely not caused by increased cholesterol uptake or cholesterol biosynthesis, but due to enhanced cholesterol esterification.

Notably, removal of Plin2 increased mRNA levels of Plin1, Plin4 and Plin5. The consistent increase of these Plin mRNAs indicate elevated PPAR activity. PPARs are known to be activated by various LD degradation products (such as fatty acids) (150, 233) and regulate transcriptions of Plins (150, 153-156). Even though mRNA levels of PPAR α and PPAR γ were unchanged by Plin2 deletion, there was a substantial upregulation of PPAR δ . In line with increased PPAR activity, TLC revealed an increase in free fatty acids in *Plin2*^{-/-} adrenals compared to *Plin2*^{+/+}. All these results imply that LD degradation was increased in *Plin2*^{-/-} adrenals at the basal state. However, protein levels of Plins were not consistent with their mRNAs. We observed reduced Plin1 but increased Plin3 proteins in the lack of Plin2. How deletion of Plin2 affects the protein levels of other Plins and alters CE balance are unclear. Plin3 is known to functionally compensate for the loss of Plin2 for LD accumulation in embryonic fibroblasts (234), whereas Plin1 is essential for the translocation of HSL to LDs (180). Possibly, the altered LD surface protein pattern with increased Plin3 and decreased Plin1 favor LD storage and attenuates HSL mediated CE lipolysis at the basal state. Somewhat unexpectedly, it seems that in *Plin2*^{-/-} adrenals, both synthesis and degradation of CE-LDs are increased.

5.1.3 Plin5 and TAG-LDs in cardiomyocytes

Expression of Plin5 is restricted to oxidative tissues and is especially high in myocardium. Content of LDs in cardiomyocytes is very low at basal state, but cardiac LD levels can increase under physiological and pathological conditions, such as fasting (235), heart failure, diabetes and obesity (236-238) – all conditions when circulating fatty acid levels are elevated.

Previous studies in genetically modified mouse models with altered Plin5 expression demonstrate that Plin5 is required for accumulation of cardiac LDs. *Plin5*^{-/-} mice have reduced cardiac TAG and LD content compared to *Plin5*^{+/+} mice (194), a difference that is more pronounced after fasting. In contrast, Plin5 overexpression results in excessive accumulation of LDs in myocardium even at basal state, which is reduced (119) or unaffected by fasting (197). In isolated and *in vitro* cultured cardiomyocytes (**paper III**), we observed few visible LDs in the absence of fatty acid supplementation in the media, independent of Plin5 expression. This indicates that exogenous fatty acid is essential for accumulation or maintenance of cardiac LDs,

which is in line with previous report (239). When cardiomyocytes were stimulated with oleic acid, *Plin5*^{+/+} cells formed numerous LDs, while LD levels remained low in *Plin5*^{-/-} cardiomyocytes. The severely reduced LD storage by *Plin5* deletion in isolated cardiomyocytes are in agreement with similar observations *in vivo* (194).

Available literature points to alternative mechanisms for the reduced cardiac TAG content in *Plin5*^{-/-} mice. Currently, the most accepted hypothesis is that *Plin5* protects LDs against lipolysis (mainly by ATGL and HSL) and therefore preserves LDs (119). However, *in vivo* injection of radioactive tracers suggests that cardiac fatty acid uptake is reduced in mice lacking *Plin5* (240). Moreover, *Plin5* seems to be important for recruitment of mitochondria to the LD surface to provide ATP for synthesis of TAG lipids in brown adipocytes (193). Albeit is unknown if the same applies to cardiomyocytes, in our isolated cardiomyocyte model, we found that incubation with oleic acid combined with inhibition of ATGL totally restored accumulation of LDs in *Plin5*^{-/-} cardiomyocytes, while as inhibition of ATGL *per se* did not accumulate LDs without the presence of fatty acids. Hence, our findings support that *Plin5* inhibits ATGL activity and thereby protects LDs from lipolytic degradation, and suggest that fatty acid uptake in cardiomyocytes is unaffected by *Plin5* deletion.

An interesting phenomenon not reported earlier in the literature, is the heterogeneous pattern of LD labeling in isolated *Plin5*^{+/+} and *Plin5*^{-/-} cardiomyocytes cultured *in vitro* (**Paper III**, Figure 2). Following fatty acid stimulation, a small population of *Plin5*^{+/+} cardiomyocytes accumulated no visible LDs, a majority accumulated intermediary levels, while another minority accumulated numerous and large LDs. In contrast, most *Plin5*^{-/-} cardiomyocytes accumulated no visible LDs, but occasionally a few cells had LD levels comparable with *Plin5*^{+/+} cardiomyocytes. These observations demonstrate that *Plin5* can promote and maintain LD storage in cardiomyocytes, but it is neither mandatory nor sufficient for LD formation. Moreover, our findings suggest that different populations of cardiomyocytes with different levels of *Plin5* expression or different lipid metabolic properties are present within one heart. This heterogeneity among cardiomyocytes warrants further investigation.

5.1.4 LD morphology and direction of lipid flux

Although changes in LD morphology usually indicate alternations in cellular lipid metabolism, it does not necessarily reflect the rate of lipid oxidation and direction of

lipid flux. A limitation with morphologic studies of LDs, is the use of static methods to study highly dynamic biological processes of lipid trafficking and metabolism. The two most important biological processes affecting LD morphology are esterification and lipolysis of core lipids and balances of surface phospholipids. Regulation of lipolysis is tightly linked to Plins, but other mechanisms independent of Plins should also be considered, including interactions between LD and other organelles, such as ER, mitochondria, lysosomes, and other LDs (LD-LD interactions) mediated by other proteins important for LD biology and cellular lipid homeostasis (241). The contribution from these other proteins have not been investigated in this thesis and will not be discussed further. In addition to study changes in LD morphology, examination of LD turnover and lipid flux are necessary to understand how LDs affect cellular metabolic status. A combination of LD morphology studies and lipid flux analysis was used in this thesis.

5.2 Perilipins regulate lipid flux

Since Plins control storage and release of core lipids, they affect intracellular lipid flux from LDs. Deletion of Plin1 results in reduced fatty acid storage and enhanced β -oxidation in adipose tissue (242), underlining the importance of Plin1 for regulation of fatty acid flux in adipocytes. However, Plin1 is absent in most non-adipocytes, where LDs are mainly coated with other perilipin family members, in particular, Plin2 and Plin5. Our studies demonstrate that these two proteins balance LD accumulation and are responsible for regulation of lipid flux in non-adipose cells, such as skeletal muscle cells (**Paper I**), adrenal cortical cells (**Paper II**), and cardiomyocytes (**Paper III**).

5.2.1 Plin2 and fatty acid flux in skeletal muscle cells

Altered expression of Plin2 has been shown to affect intracellular fatty acid flux in different cell types. Plin2 overexpression in rat hepatocytes reduces fatty acid turnover and preserves TAG. Plin2 knockdown enhances hepatic TAG hydrolysis and fatty acid release, which further activates PPAR α , a key transcription factor regulating fatty acid utilization (243). Knockdown of Plin2 in C2C12 cells decreases incorporation of palmitic acid into TAG, increases its incorporation into DAG and phospholipids, which result in reduced accumulation of LDs and a concomitant increase in fatty acid flux directed to β -oxidation (230). In agreement with these studies, in **paper I** we showed that complete ablation of Plin2 resulted in increased fatty acid oxidation in

myotubes established from *Plin2*^{-/-} mice. Compared to *Plin2*^{+/+} myotubes, *Plin2*^{-/-} myotubes had reduced incorporation of oleic acid into TAG and DAG but unaltered incorporation into phospholipids. It has been suggested that palmitic acid is less efficiently incorporated into LD compared to oleic acid (114), which may partly explain the difference in metabolism among the two fatty acid tracers used in these studies. We further showed that inhibition of ATGL, the principle lipase hydrolyzing TAG, resulted in comparable accumulation of fatty acids and formation of TAG containing LDs in *Plin2*^{+/+} and *Plin2*^{-/-} myotubes, indicating that the ability to take up fatty acids is unaffected by Plin2 deletion. Unaltered fatty acid uptake upon Plin2 deletion has also been reported in primary hepatocytes (226).

The altered fatty acid flux upon Plin2 deletion leads to increased oxidation of oleic acid and elevated levels of CO₂ and ASM in cultured *Plin2*^{-/-} myotubes, in agreement with previous findings after Plin2 knockdown in C2C12 myotubes (230). Interestingly, we also found that production of CO₂ and ASM were repressed by inhibition of lipolysis with Atglistatin (ATGL inhibitor) or CAY-10499 (HSL inhibitor), which indicates that increased oxidation of fatty acids in *Plin2*^{-/-} myotubes occurs due to elevated lipolytic activity. The repression of fatty acid oxidation by lipolysis inhibitors also implies that a large fraction of fatty acids routed to oxidation are derived from stored LDs, which is in agreement with previous notion that a large fraction of fatty acids taken up by cells are shuttled through LDs before being directed to oxidation (115). Taken together, in skeletal muscle cells, Plin2 balances the flux of fatty acids between storage in LDs and oxidation in mitochondria by its regulation on lipolytic activity.

5.2.2 **Plin2 and cholesterol flux in adrenal cortical cells**

Previous studies on perilipins have focused on balance of intracellular fatty acid flux and regulation of fatty acid metabolism. In contrast, little is known about their role for cholesterol balance. In **paper II**, we demonstrate for the first time that Plin2 is important for balancing cholesterol flux and CE-storage in adrenal cortical cells.

Adrenals lacking Plin2 contains elevated levels of both CE containing LDs and its lipolytic products cholesterol and fatty acids, which complicates the judgement on the direction of intracellular cholesterol flux in the absence of Plin2. The net increase in CE-containing LDs in the lack of Plin2 indicates that lipolysis of core lipids is

repressed, similar to what is normally observed for various models with overexpression of Plins (184, 196, 197, 230). At the same time, the increased cellular free cholesterol in *Plin2*^{-/-} adrenals suggests that degradation of CE is enhanced. We found no experimental evidence for increased cholesterol uptake or enhanced cholesterol biosynthesis, judged by unaltered gene expression levels of SR-B1 (*Scarb1*) and LDLR (*Ldlr*), important for exogenous cholesterol uptake, and *Hmgcr*, a key enzyme for *de novo* cholesterol synthesis, in the lack of Plin2. The elevated levels of free cholesterol and increased mRNAs of LXR α , ABCG1 and ApoE, suggest that cholesterol efflux is enhanced in *Plin2*^{-/-} adrenals at the basal state, possibly as an attempt to reduce intracellular cholesterol levels and reset cholesterol balance (244, 245).

Changes in adrenal cholesterol flux have been reported to affect steroidogenesis in several mouse models. LXR α is a key transcription regulator balancing intracellular cholesterol levels. *LXR α* ^{-/-} mice have impaired cholesterol efflux in adrenals, which leads to accumulation of intracellular free cholesterol, enhanced LD storage, increased steroidogenesis and elevated basal levels of plasma corticosterone (246). HSL is responsible for the majority of neutral cholesterol esterase activity in adrenals (101). *Hsl*^{-/-} mice have severely impaired ability to mobilize CE-LD through activation of lipolysis and have unchanged basal circulating corticosterone levels, but moderately impaired secretion of corticosterone upon exogenous ACTH stimulation (247). This demonstrates that the mobilization of cholesterol for steroid hormone synthesis is not fully dependent on HSL mediated lipolysis of LDs. We found that *Plin2* deficiency had no effect on plasma corticosterone levels, neither at basal fed state, after 24 hours of fasting, nor following an exogenous ACTH stimulation. Possibly, enhanced cellular efflux of cholesterol compensates to balance cholesterol to a level that is sufficient to maintain proper steroidogenesis. Alternatively, the excessive free cholesterol may not be directly accessible for mitochondria and steroidogenesis, e.g. by being sequestered in autolysosomes or/and LDs.

An interesting characteristic of *Plin2*^{-/-} adrenals is the abnormal accumulation of ceroid-like structures containing multilamellar bodies. The close relationship between these aggregates and LDs, revealed by high resolution confocal microscopy and electron microscopy, indicates an adrenal cortical cell origin (**paper II**). Structures similar to those found in *Plin2* adrenals also accumulate in tissues affected by lysosomal disorders (248), suggesting that *Plin2* deficiency results in accumulation of

end-stage autolysosomes in adrenal cortical cells. Unexpectedly, adrenals in *Plin2*^{-/-} mice accumulated considerable amount of phosphatidylglycerol (PG) with age. PG is suggested to be present in multilamellar bodies (249) and formation of such structures is enhanced when cholesterol accumulates in autolysosomes (250). Moreover, increased levels of PG have been suggested to promote autophagy (251, 252). Our findings therefore indicate that end-stage autolysosomes accumulate in adrenal cortical cells in the absence of Plin2, which are filled with PG and possibly free cholesterol, indicative of altered lipophagic activity. Deletion of Plin2 enhances lipophagic degradation of TAG-LDs in liver (186), but it is unclear if the same applies to CE-LDs. Accumulation of autolysosomes can be explained by either increased flux of CE-LDs into autolysosomes and enhanced autophagy, or reduced lysosomal function and accumulation of autophagy cargo. Further investigations will be needed to understand mechanistically why multilamellar bodies and PG accumulate in adrenals with Plin2 deficiency.

Taken together, Plin2 seems dispensable for mobilization of CE containing LDs for steroidogenesis in adrenal cortical cells. However, deletion of Plin2 leads to elevated levels of cellular free cholesterol and accumulation of end-stage autolysosomes, which may eventually increase cell damage. Our findings demonstrate that Plin2 is important for balancing cellular cholesterol flux in adrenal cortical cells, possibly by interfering with the lipophagic machinery.

5.2.3 **Plin5 and fatty acid flux in cardiomyocytes**

Plin5 is the dominant Plin protein in myocardium and influences LD formation and lipid flux in cardiomyocytes. In **paper III**, we showed that lack of Plin5 significantly reduced storage of fatty acids in cardiac LDs, which is consistent with observations in heart tissue during fasting (194, 240). We found that LD storage is restored when lipolysis is inhibited by Atglistatin, indicating that Plin5 facilitates storage of fatty acids in LDs by repressing ATGL activity. The finding that LD storage in the presence of Atglistatin is comparable between *Plin5*^{+/+} and *Plin5*^{-/-} cardiomyocytes suggests that fatty acid uptake is unaffected by Plin5 deletion. Others have reported reduced fatty acid uptake *in vivo* under certain conditions (240, 253). The discrepancy in observed fatty acid uptake between studies might be attributed to differences in experimental

conditions (*in vitro* versus *in vivo*), cells studied (cardiomyocytes versus hepatocytes) and fatty acid tracers (oleic acid versus palmitic acid) used in different studies.

The majority of fatty acids taken up by cardiomyocytes is used as substrates for β -oxidation followed by oxidative phosphorylation in mitochondria for generation of ATP. Some studies have reported increased fatty acid oxidation (194) and impaired mitochondria oxidative capacity in cardiomyocytes lacking Plin5 (254). In our isolated adult cardiomyocyte model (**paper III**), $^{14}\text{CO}_2$ production from *Plin5*^{-/-} cardiomyocytes revealed a non-significant trend of increased fatty acid oxidation during the first few hours of fatty acid stimulation, whereas $^{14}\text{CO}_2$ production was similar to wild-type cells with prolonged incubation with oleic acid. These results suggest that the overall capacity of complete fatty acid oxidation is not significantly affected by Plin5 deletion in adult cardiomyocytes. We demonstrated that complete labeling of the LD pool prior to measurement of $^{14}\text{CO}_2$ is a prerequisite to correctly measure fatty acid oxidation rate (for details see: methodological considerations 4.5 and **paper III**, Figure 3). Since a majority of fatty acids are incorporated into LDs before being directed to oxidation, the higher release of $^{14}\text{CO}_2$ from *Plin5*^{-/-} cardiomyocytes than *Plin5*^{+/+} during the first hours after addition of radioactive fatty acids implies a faster turnover of fatty acid flux through LDs, which is in agreement with previous notion that Plin5 slows LD turnover (144).

Accumulation of intermediate metabolites generated during fatty acid oxidation are associated with elevated ROS production and insulin resistance (255, 256). Such metabolic intermediates are reflected as ASM in radioactive traced fatty acid oxidation assays (223). In **paper III**, we showed that the levels of ASM was relatively stable in *Plin5*^{+/+} cardiomyocytes, whereas in *Plin5*^{-/-} cardiomyocytes, there was a transient increase of ASM during the first 6 hours of fatty acid stimulation. These results suggest that removal of Plin5 leads to a temporal accumulation of fatty acid derived metabolic intermediates when cells are suddenly exposed to elevated levels of fatty acids. Interestingly, administration of the ATGL inhibitor Atglistatin, which restores LD accumulation in *Plin5*^{-/-} cardiomyocytes, decreased ASM content in *Plin5*^{-/-} cardiomyocytes to levels measured in *Plin5*^{+/+} cardiomyocytes. This result implies that LD expansion helps to prevent accumulation of fatty acid-derived metabolic intermediates. Importantly, our experiments demonstrated that the fatty acid buffering ability of LDs has a limit. In **paper III**, we showed that accumulation of ^{14}C -oleic acid labelled LDs increased dramatically during the first 6 hours, but from then on

maintained essentially at the same level, indicating that LD pools in both *Plin5*^{+/+} and *Plin5*^{-/-} cells were saturated after approximately 6 hours of oleic acid stimulation. Interestingly, the above-mentioned differences in CO₂ and ASM levels between *Plin5*^{+/+} and *Plin5*^{-/-} cardiomyocytes are more prominent during the first 6 hours of fatty acid stimulation, and they disappeared at 20 hours of incubation, in line with a steady-state LD content. Our findings correspond well with findings in adipose tissue (126), suggesting that it is not the LDs content per se, but their ability to expand that is important for buffering of fatty acid flux. Certainly, Plin5 is an important factor regulating LD expandability, and therefore buffers fatty acid flux in cardiomyocytes.

In sum, Plin5 inhibits ATGL mediated lipolysis and favors expansion of the cardiac LD-pool. When cardiomyocytes are exposed to increased levels of fatty acids, the expansion of LDs buffers against intracellular fatty acid flux and prevents pileup of metabolic intermediates generated through excessive fatty acid metabolism, and thereby minimizes lipotoxicity. Hence, Plin5 is a key regulator of fatty acid flux in cardiomyocytes.

5.3 Perilipins and energy homeostasis

A common feature of cell and animal models with manipulated Plin expression is alternations in energy homeostasis. One example is *Plin1*^{-/-} mice, which exhibit reduced respiratory exchange ratio (RER) due to enhanced whole body utilization of fatty acids (118). Lack of Plin1 in white adipose tissue reduce the ability to store TAG, which not only increases the oxidation of fatty acids in adipocytes, but also enhances fatty acid utilization in several other non-adipose tissues. In comparison, the metabolic effect upon deletion of the more widely expressed Plin2 and Plin5 is less clear, and might be even different depending on the tissues examined.

5.3.1 Plin2 and energy metabolism in skeletal muscle

The metabolic consequences of Plin2 deletion in mice is minor, yet complex. Plin2 null mice on a normal chow diet have normal bodyweight and adipose mass, with no alterations in plasma lipid profiles and glucose levels compared to wild-type littermates (226). However, when challenged with nutritional stress such as obesogenic diet, Plin2 null mice seems to be protected against obesity, liver steatosis and insulin resistance (227). In mice subjected to diet-induced insulin resistance, inhibition of Plin2 expression with antisense oligonucleotide enhances insulin action in

liver, without affecting insulin sensitivity in muscle and adipose tissue (257). In contrast, improved insulin sensitivity and glucose disposal in obese individuals following weight loss or antidiabetic treatments correlate with upregulated expression of Plin2 in (human) skeletal muscle (258). A recent study comparing mice with liver-specific and whole-body Plin2 deletion conclude that hepatic Plin2 is needed for diet induced liver steatosis and fibrosis, whereas extra-hepatic Plin2 contribute more to obesity and insulin resistance (259). Considering that Plin2 has a wide distribution that covers many types of cells, and that Plin2 protein levels are regulated by fatty acid flux and available LD surfaces, the whole-body effect and cross-talks between different tissues (especially liver, skeletal muscle and adipose tissue) may complicate our understanding on the importance of Plin2 for metabolism. To minimize the effect of tissue cross-talk, we established *in vitro* cultured myotubes to directly study the metabolic function of Plin2 in skeletal muscle cells (**paper I**).

In our *in vitro* myotube model, we found that *Plin2*^{-/-} myotubes have reduced ability to store fatty acids in LDs due to enhanced lipolysis. As a consequence, Plin2 deficiency leads to increased fatty acid oxidation. The uptake, intracellular transport, and cytosolic binding of fatty acids, as well as many enzymatic steps in fatty acid metabolism are under transcriptional control by PPARs (233) which are activated by fatty acids and fatty acid derived molecules (260, 261). In the lack of Plin2, we observed upregulated gene expression of *Ppara* and *Ppargc1a*, which control genes important for fatty acid oxidation (262) and mitochondrial biogenesis (263). Moreover, transcription of *Pparg*, which favors lipid storage, was downregulated. In line with changes in these transcription factors, mRNA levels of PPAR downstream target genes such as *Cd36*, *Cpt2* and *Ucp2/3* were all upregulated, indicating that Plin2 deletion increases intracellular fatty acid metabolites that activate PPARs. Interestingly, enhanced fatty acid oxidation has also been reported in muscle overexpressing *Ppara* (264) and C2C12 myotubes overexpressing *Ppargc1a* (265), suggesting that upregulation of these two transcription factors are important for increased fatty acid oxidation in *Plin2*^{-/-} myotubes. These results imply that enhanced lipolysis in myotubes lacking Plin2 not only generates more fatty acids for mitochondrial oxidation, but also upregulates the oxidative ability of myotubes through the activation of PPARs.

Perhaps as a consequence of increased fatty acid utilization, we observed decreased glucose oxidation in *Plin2*^{-/-} myotubes compared to *Plin2*^{+/+} (**paper I**).

Cellular accumulation of glucose also decreased in *Plin2*^{-/-} myotubes, independently of fatty acid stimulation. Consistent with these findings, gene and protein expressions facilitating glucose uptake (*Slc2a1*), glycolysis (*Pkm*) and glucose oxidation (*Pdha1*) were downregulated. In contrast, we detected upregulated gene expression of *Pdk4*, which phosphorylates and inactivates PDH, a key regulator of glucose oxidation. As a sign of elevated *Pdk4* activity, phosphorylated *Pdha1* protein was elevated in *Plin2*^{-/-} myotubes, despite the total *Pdha1* protein levels of *Plin2*^{-/-} myotubes tend to be lower than in *Plin2*^{+/+}. Overall, these data demonstrate that both transcriptional and posttranslational mechanisms are activated in *Plin2*^{-/-} myotubes to repress glucose utilization.

The redirected fuel preference from glucose toward fatty acids in *Plin2* deficient myotubes fits energy substrate competition first described by Randal (Randal cycle) (29), where excessive Acetyl-CoA produced from fatty acid β -oxidation inhibits utilization of glucose. Interestingly, opposite to what we have observed in our *Plin2*^{-/-} myotube model, knockdown of the ATGL co-activator ABHD5 (also known as CGI-58) in human primary myotubes results in increased LD storage and decreased fatty acid oxidation, enhanced glucose oxidation and elevated glycogen synthesis (266). These opposite metabolic effects suggest that lipolytic rate and LD turnover influence the utilization of energy substrates (fatty acids or glucose) and energy homeostasis.

It is generally believed that excessive lipid storage in peripheral tissues and elevated fatty acid oxidation inhibits insulin signaling (267). However, studies are inconclusive regarding changes in insulin sensitivity in the lack of *Plin2* (230, 257, 268). In our *in vitro* model, *Plin2*^{-/-} myotubes utilized less glucose without affecting insulin-stimulated glycogen synthesis or the ability to phosphorylate Akt, despite that the total Akt expression was lower in *Plin2*^{-/-} myotubes. These data suggest that the response to insulin stimulation is unaffected by *Plin2* deletion, which is in agreement with the previously reported normal insulin signaling in *Plin2* knockdown C2C12 myotubes (230). Possibly, in the lack of *Plin2*, the increased fatty acid flux to mitochondrial oxidation compensates for the increased LD leakage and alleviates lipotoxicity, which may otherwise impair insulin signaling.

Taken together, our data support that *Plin2* balances storage and oxidation of fatty acids in skeletal muscle and thereby indirectly affects glucose utilization.

Enhanced fatty acid oxidation results in a secondary decrease in glucose disposal in myotubes lacking Plin2 independent of insulin actions, but likely through substrate competition, as first described by Randal et al.

5.3.2 **Plin5 in energy metabolism of cardiomyocytes and myocardial ischemia**

A unique feature of the Plin5 protein is its ability to facilitate physical association between LDs and mitochondria (190, 269). The Plin5-dependent association between LDs and mitochondria suggests that Plin5 may function to coordinate transfer of LD-derived fatty acids to mitochondria for efficient oxidation (269, 270). However, a recent study in brown adipocytes suggests that Plin5 recruits mitochondria for ATP synthesis and facilitates LD growth (193). Whether the same occurs in cardiomyocytes is unclear. Similar to BAT, fatty acids serve as a primary fuel in the myocardium, which makes it reasonable to expect that lack of Plin5 in cardiomyocytes may potentially disturb fatty acid oxidation and affect cardiac energy metabolism. Alterations in cardiac LD content is associated with different pathological conditions such as myocardial ischemia (271-273) and heart failure (238). Plin5 knockout and Plin5 overexpression models show alterations in cardiac LD content. However, other cardiac alternations in these models seem to be surprisingly mild and ambiguous. Although *Plin5*^{-/-} mice have reduced cardiac LD content, they have maintained almost normal heart function unless the mice are challenged with stress (240). Only one study has reported that Plin5 null mice are subjected to declined cardiac contractile function with age (194). In contrast, mice with Plin5 overexpression develops cardiac hypertrophy and severe steatosis in myocardium that resembles the phenotypes of the *Atgl*^{-/-} mice, but their heart function is also relatively normal (197). In **paper III**, we analyzed aged *Plin5*^{-/-} mice and observed increased heart weight and higher mRNA levels of *Myh7* in old (55 weeks) mice compared to young (15 weeks) mice. However, mRNA levels of *Nppa* and *Nppb*, two genes encoding natriuretic peptides that usually increase with heart failure, were unaltered by Plin5 deletion. Our finding indicates that Plin5 deficiency induces remodeling of myocardium with age, but does not necessarily lead to heart failure. These observations imply that the requirement for Plin5 in cardiomyocytes for fatty acid metabolism is minor, or alternatively, is well compensated for.

Regarding myocardial fatty acid oxidation, Plin5 is reported to enhance (196, 253), reduce (119, 194, 198), or not affect (274) fatty acid oxidation. These

discrepancies among experiments performed in various laboratories are likely caused by differences in the models used, the experimental conditions, and adaptive/compensative differences between isolated cardiomyocytes and *in vivo* beating hearts. In **paper III**, we used ^{14}C labeled oleic acid as a tracer in isolated cardiomyocytes and observed a transient increase in incomplete fatty acid oxidation intermediates (cellular ASM) in *Plin5*^{-/-} cardiomyocytes exposed to a sudden increase of extracellular fatty acids. In contrast, the release of $^{14}\text{CO}_2$ generated from complete fatty acid oxidation was comparable between *Plin5*^{+/+} and *Plin5*^{-/-} cardiomyocytes. Importantly, we discovered that with or without pre-labeling of the LD-pool largely affected $^{14}\text{CO}_2$ measurement results, which may partly explain discrepancies reported for fatty acid oxidation between studies. Moreover, various fatty acids may be directed towards alternative metabolic pathways (114). We used ^{14}C -oleic acid as fatty acid tracer in our study (**paper III**), whereas many other studies used ^{14}C -palmitic acid. Compared to wild-type hearts, heart from *Plin5*^{-/-} mice has marginal changes in the expression of genes encoding proteins important for fatty acid metabolism (e.g. upregulation of *Cd36*), implying that *Plin5* deletion has limited changes in myocardial fatty acid oxidation.

Cardiomyocytes consume large amount of ATP and are sensitive to hypoxia. Two major fuels for cardiomyocytes are fatty acids and glucose, where fatty acids contribute to 50-70% of cardiac ATP production, and the remaining is mostly provided by glucose (9, 275). Both energy substrates can be stored in limited amounts intracellularly, with fatty acid stored as TAG in LDs and glucose stored as glycogen. During hypoxia, low oxygen prevents utilization of fatty acids and cardiomyocytes must rely on catabolism of glycogen (glycogenolysis) and glucose (glycolysis) to sustain ATP production (276, 277). Two *in vivo* studies conclude that the presence of *Plin5*, which preserved cardiac LDs, protects the heart during myocardium ischemia (240, 278). A third, *in vitro* study, suggests that LD accumulation sequesters free fatty acids and Ca^{2+} and protects cardiomyocytes during hypoxia (279). Unexpectedly, in our study using isolated cardiomyocytes (**paper III**), we found that pretreatment with oleic acid improved tolerance to hypoxia in *Plin5*^{-/-} cardiomyocytes (LD-poor) but not *Plin5*^{+/+} (LD-rich). Further, LDH release (cell damage) from *Plin5*^{+/+} cardiomyocytes with low LD content (pretreated with BSA) or high LD content (pretreated with oleic acid) was similar. Moreover, facilitated LD accumulation using oleic acid combined with

Atglistatin worsened cell damage independent of Plin5 expression. Interestingly, after oleic acid treatment, glycogen content was maintained at higher levels in *Plin5*^{-/-} cardiomyocytes compared to *Plin5*^{+/+} cardiomyocytes. As higher cardiac glycogen content is believed to be beneficial during ischemia (hypoxia) (280), this may partly explain the alleviated damage of *Plin5*^{-/-} cardiomyocytes under a hypoxic stress. Our results suggest that glycogen levels are more important than LD content for cardiomyocytes during hypoxia, but how Plin5 signals to glycogen metabolism needs further investigation.

In sum, our data suggests that deletion of Plin5 in myocardium induces minor changes in cardiac energy metabolism at basal state. *Plin5*^{-/-} cardiomyocytes treated with oleic acid maintained higher levels of glycogen compared with *Plin5*^{+/+} cardiomyocytes, which may improve tolerance to hypoxic stress.

6 CONCLUSION

The work included in this thesis expands our understanding of Plin function for regulation of lipid droplets and cellular lipid flux in various cell types. We have examined the metabolic consequences of removal of two important Plin family members in non-adipocytes, Plin2 and Plin5, in skeletal muscle cells, adrenal cortical cells and cardiomyocytes.

In **paper I**, our characterization of Plin2-null myotubes complements parallel investigations of Plin2 function in skeletal muscles. We demonstrated that Plin2 protects LDs against lipolysis. Increased fatty acid leakage from LDs devoid of Plin2 redirects muscle fatty acid flux: TAG storage is decreased, while fatty acid oxidation is increased. Expression of transcription factors such as PPAR α , PPAR γ and PGC-1 α are altered and likely contribute to reprogramming of cell metabolism. Change in fatty acid flux affects metabolism of glucose and represses its utilization.

In **paper II**, our characterization of adrenals in Plin2-null mice has revealed new knowledge regarding adrenal cholesterol balance. *Plin2*^{-/-} mice have normal adrenal steroidogenesis, but adrenals are enlarged, with increased CE-LD content and elevated levels of free cholesterol. The *Plin2*^{-/-} adrenals have activated cholesterol efflux to eliminate excess cholesterol. Plin2-null mice also accumulate ceroid-like structures, multilamellar bodies and phosphatidylcholine in the adrenal cortex/medulla boundary, which are signs of disturbed lysosomal activity. These observations indicate that adrenal Plin2 is important to balance cellular cholesterol flux, probably by interfering with lipophagy.

In **paper III**, our characterization of Plin5-null cardiomyocytes and animals demonstrates that Plin5 protects cardiac LDs by repressing enzymatic activity of ATGL. Plin5 is not essential for the formation of LDs in cardiomyocytes, nor critical for fatty acid oxidation, but Plin5 deletion reduces the buffering capacity of cardiac LDs and accelerates fatty acid turnover. We also show that Plin5 deficient cardiomyocytes maintain higher levels of cellular glycogen than wild-type cells when exposed to oleic acid, which may alleviate cell damage induced by hypoxia. The levels of LD accumulation alone have no effect on hypoxia in *Plin5*^{+/+} or *Plin5*^{-/-} cardiomyocytes. Plin5 deficiency results in remodeling of the myocardium with age, although this does not seem to increase the risk of heart failure in old *Plin5*^{-/-} mice.

In summary, the studies included in this thesis suggest that an important role of LDs is to serve as intracellular reservoirs for fatty acids and cholesterol. Plin2 and Plin5 at LD surface function as protectors of these lipid reservoirs. The complex yet delicate interplay between Plins, the lipolytic machinery and other proteins on LDs regulates intracellular fatty acid flux, balances cholesterol homeostasis, and affects metabolism of energy substrates. Improved understanding of these mechanisms may potentially lead to discovery of new targets for diagnosis and treatment of lipid-related metabolic diseases.

7 REFERENCES

1. Fahy E, Cotter D, Sud M, Subramaniam S. Lipid classification, structures and tools. *Biochimica et biophysica acta*. 2011;1811(11):637-47.
2. Greenberg AS, Coleman RA, Kraemer FB, McManaman JL, Obin MS, Puri V, et al. The role of lipid droplets in metabolic disease in rodents and humans. *The Journal of clinical investigation*. 2011;121(6):2102-10.
3. Krahmer N, Farese RV, Jr., Walther TC. Balancing the fat: lipid droplets and human disease. *EMBO molecular medicine*. 2013;5(7):973-83.
4. Gross DA, Silver DL. Cytosolic lipid droplets: from mechanisms of fat storage to disease. *Critical reviews in biochemistry and molecular biology*. 2014;49(4):304-26.
5. Petan T, Jarc E, Jusovic M. Lipid Droplets in Cancer: Guardians of Fat in a Stressful World. *Molecules (Basel, Switzerland)*. 2018;23(8).
6. van Herpen NA, Schrauwen-Hinderling VB. Lipid accumulation in non-adipose tissue and lipotoxicity. *Physiology & behavior*. 2008;94(2):231-41.
7. Schuster S, Cabrera D, Arrese M, Feldstein AE. Triggering and resolution of inflammation in NASH. *Nature reviews Gastroenterology & hepatology*. 2018;15(6):349-64.
8. Li X, Li Z, Zhao M, Nie Y, Liu P, Zhu Y, et al. Skeletal Muscle Lipid Droplets and the Athlete's Paradox. *Cells*. 2019;8(3).
9. Lopaschuk GD, Ussher JR, Folmes CD, Jaswal JS, Stanley WC. Myocardial fatty acid metabolism in health and disease. *Physiological reviews*. 2010;90(1):207-58.
10. Schulze PC, Drosatos K, Goldberg IJ. Lipid Use and Misuse by the Heart. *Circulation research*. 2016;118(11):1736-51.
11. Shen WJ, Azhar S, Kraemer FB. Lipid droplets and steroidogenic cells. *Experimental cell research*. 2016;340(2):209-14.
12. Goldberg IJ, Eckel RH, Abumrad NA. Regulation of fatty acid uptake into tissues: lipoprotein lipase- and CD36-mediated pathways. *Journal of lipid research*. 2009;50 Suppl:S86-90.
13. van der Vusse GJ. Albumin as fatty acid transporter. *Drug metabolism and pharmacokinetics*. 2009;24(4):300-7.
14. Pearce J. Fatty acid synthesis in liver and adipose tissue. *The Proceedings of the Nutrition Society*. 1983;42(2):263-71.
15. D'Andrea S. Lipid droplet mobilization: The different ways to loosen the purse strings. *Biochimie*. 2016;120:17-27.
16. Carmen GY, Victor SM. Signalling mechanisms regulating lipolysis. *Cellular signalling*. 2006;18(4):401-8.
17. Janero DR, Siuta-Mangano P, Miller KW, Lane MD. Synthesis, processing, and secretion of hepatic very low density lipoprotein. *Journal of cellular biochemistry*. 1984;24(2):131-52.
18. McGarry JD, Foster DW. Regulation of hepatic fatty acid oxidation and ketone body production. *Annual review of biochemistry*. 1980;49:395-420.
19. Rui L. Energy metabolism in the liver. *Comprehensive Physiology*. 2014;4(1):177-97.
20. Harris LA, Skinner JR, Shew TM, Pietka TA, Abumrad NA, Wolins NE. Perilipin 5-Driven Lipid Droplet Accumulation in Skeletal Muscle Stimulates the Expression of Fibroblast Growth Factor 21. *Diabetes*. 2015;64(8):2757-68.
21. Nguyen TB, Olzmann JA. Lipid droplets and lipotoxicity during autophagy. *Autophagy*. 2017;13(11):2002-3.

22. Thiam AR, Beller M. The why, when and how of lipid droplet diversity. *Journal of cell science*. 2017;130(2):315-24.
23. Soupene E, Kuypers FA. Mammalian long-chain acyl-CoA synthetases. *Experimental biology and medicine (Maywood, NJ)*. 2008;233(5):507-21.
24. Bonnefont JP, Djouadi F, Prip-Buus C, Gobin S, Munnich A, Bastin J. Carnitine palmitoyltransferases 1 and 2: biochemical, molecular and medical aspects. *Molecular aspects of medicine*. 2004;25(5-6):495-520.
25. Berg JM, Tymoczko JL, Stryer L. *Biochemistry, Fifth Edition*: W.H. Freeman; 2002.
26. Poirier Y, Antonenkov VD, Glumoff T, Hiltunen JK. Peroxisomal beta-oxidation--a metabolic pathway with multiple functions. *Biochimica et biophysica acta*. 2006;1763(12):1413-26.
27. Reddy JK, Hashimoto T. Peroxisomal beta-oxidation and peroxisome proliferator-activated receptor alpha: an adaptive metabolic system. *Annual review of nutrition*. 2001;21:193-230.
28. Powers JM, Moser HW. Peroxisomal disorders: genotype, phenotype, major neuropathologic lesions, and pathogenesis. *Brain pathology (Zurich, Switzerland)*. 1998;8(1):101-20.
29. Randle PJ, Garland PB, Hales CN, Newsholme EA. The glucose fatty-acid cycle. Its role in insulin sensitivity and the metabolic disturbances of diabetes mellitus. *Lancet (London, England)*. 1963;1(7285):785-9.
30. Hue L, Taegtmeyer H. The Randle cycle revisited: a new head for an old hat. *American journal of physiology Endocrinology and metabolism*. 2009;297(3):E578-91.
31. Lecerf JM, de Lorgeril M. Dietary cholesterol: from physiology to cardiovascular risk. *The British journal of nutrition*. 2011;106(1):6-14.
32. Hui DY, Howles PN. Carboxyl ester lipase: structure-function relationship and physiological role in lipoprotein metabolism and atherosclerosis. *Journal of lipid research*. 2002;43(12):2017-30.
33. Wang LJ, Song BL. Niemann-Pick C1-Like 1 and cholesterol uptake. *Biochimica et biophysica acta*. 2012;1821(7):964-72.
34. Iqbal J, Hussain MM. Intestinal lipid absorption. *American journal of physiology Endocrinology and metabolism*. 2009;296(6):E1183-94.
35. Shelness GS, Sellers JA. Very-low-density lipoprotein assembly and secretion. *Current opinion in lipidology*. 2001;12(2):151-7.
36. Osono Y, Woollett LA, Herz J, Dietschy JM. Role of the low density lipoprotein receptor in the flux of cholesterol through the plasma and across the tissues of the mouse. *The Journal of clinical investigation*. 1995;95(3):1124-32.
37. Fielding CJ, Fielding PE. Molecular physiology of reverse cholesterol transport. *Journal of lipid research*. 1995;36(2):211-28.
38. Landschulz KT, Pathak RK, Rigotti A, Krieger M, Hobbs HH. Regulation of scavenger receptor, class B, type I, a high density lipoprotein receptor, in liver and steroidogenic tissues of the rat. *The Journal of clinical investigation*. 1996;98(4):984-95.
39. Trigatti BL, Rigotti A, Braun A. Cellular and physiological roles of SR-BI, a lipoprotein receptor which mediates selective lipid uptake. *Biochimica et biophysica acta*. 2000;1529(1-3):276-86.
40. Sandhu J, Li S, Fairall L, Pfisterer SG, Gurnett JE, Xiao X, et al. Aster Proteins Facilitate Nonvesicular Plasma Membrane to ER Cholesterol Transport in Mammalian Cells. *Cell*. 2018;175(2):514-29.e20.

41. Azhar S, Leers-Sucheta S, Reaven E. Cholesterol uptake in adrenal and gonadal tissues: the SR-BI and 'selective' pathway connection. *Frontiers in bioscience : a journal and virtual library*. 2003;8:s998-1029.
42. Geelen MJ, Gibson DM, Rodwell VW. Hydroxymethylglutaryl-CoA reductase--the rate-limiting enzyme of cholesterol biosynthesis. A report of a meeting held at Nijenrode Castle, Breukelen, The Netherlands, August 24, 1985. *FEBS letters*. 1986;201(2):183-6.
43. Mitsche MA, McDonald JG, Hobbs HH, Cohen JC. Flux analysis of cholesterol biosynthesis in vivo reveals multiple tissue and cell-type specific pathways. *eLife*. 2015;4:e07999.
44. Zhao C, Dahlman-Wright K. Liver X receptor in cholesterol metabolism. *The Journal of endocrinology*. 2010;204(3):233-40.
45. Shen WJ, Azhar S, Kraemer FB. SR-B1: A Unique Multifunctional Receptor for Cholesterol Influx and Efflux. *Annual review of physiology*. 2018;80:95-116.
46. Barter P, Rye KA. Cholesteryl ester transfer protein: its role in plasma lipid transport. *Clinical and experimental pharmacology & physiology*. 1994;21(9):663-72.
47. Mok HY, von Bergmann K, Grundy SM. Effects of continuous and intermittent feeding on biliary lipid outputs in man: application for measurements of intestinal absorption of cholesterol and bile acids. *Journal of lipid research*. 1979;20(3):389-98.
48. Afonso MS, Machado RM, Lavrador MS, Quintao ECR, Moore KJ, Lottenberg AM. Molecular Pathways Underlying Cholesterol Homeostasis. *Nutrients*. 2018;10(6).
49. Rosol TJ, Yarrington JT, Latendresse J, Capen CC. Adrenal gland: structure, function, and mechanisms of toxicity. *Toxicologic pathology*. 2001;29(1):41-8.
50. Grouleff J, Irudayam SJ, Skeby KK, Schiott B. The influence of cholesterol on membrane protein structure, function, and dynamics studied by molecular dynamics simulations. *Biochimica et biophysica acta*. 2015;1848(9):1783-95.
51. Sokolov A, Radhakrishnan A. Accessibility of cholesterol in endoplasmic reticulum membranes and activation of SREBP-2 switch abruptly at a common cholesterol threshold. *The Journal of biological chemistry*. 2010;285(38):29480-90.
52. Greenberg AS, Egan JJ, Wek SA, Garty NB, Blanchette-Mackie EJ, Londos C. Perilipin, a major hormonally regulated adipocyte-specific phosphoprotein associated with the periphery of lipid storage droplets. *The Journal of biological chemistry*. 1991;266(17):11341-6.
53. Olofsson S-O, Boström P, Andersson L, Rutberg M, Perman J, Borén J. Lipid droplets as dynamic organelles connecting storage and efflux of lipids. *Biochimica et Biophysica Acta (BBA) - Molecular and Cell Biology of Lipids*. 2009;1791(6):448-58.
54. Welte MA, Gould AP. Lipid droplet functions beyond energy storage. *Biochimica et Biophysica Acta (BBA) - Molecular and Cell Biology of Lipids*. 2017;1862(10, Part B):1260-72.
55. Fujimoto T, Parton RG. Not just fat: the structure and function of the lipid droplet. *Cold Spring Harbor perspectives in biology*. 2011;3(3).
56. Suzuki M, Shinohara Y, Ohsaki Y, Fujimoto T. Lipid droplets: size matters. *Journal of electron microscopy*. 2011;60 Suppl 1:S101-16.
57. Bartz R, Li WH, Venables B, Zehmer JK, Roth MR, Welti R, et al. Lipidomics reveals that adiposomes store ether lipids and mediate phospholipid traffic. *Journal of lipid research*. 2007;48(4):837-47.
58. Walther TC, Farese RV. The life of lipid droplets. *Biochimica et Biophysica Acta (BBA) - Molecular and Cell Biology of Lipids*. 2009;1791(6):459-66.

59. Schreiber R, Taschler U, Preiss-Landl K, Wongsiriroj N, Zimmermann R, Lass A. Retinyl ester hydrolases and their roles in vitamin A homeostasis. *Biochimica et Biophysica Acta (BBA) - Molecular and Cell Biology of Lipids*. 2012;1821(1):113-23.
60. Parker RO, Crouch RK. Retinol dehydrogenases (RDHs) in the visual cycle. *Experimental eye research*. 2010;91(6):788-92.
61. Hsieh K, Lee YK, Londos C, Raaka BM, Dalen KT, Kimmel AR. Perilipin family members preferentially sequester to either triacylglycerol-specific or cholesteryl-ester-specific intracellular lipid storage droplets. *Journal of cell science*. 2012;125(Pt 17):4067-76.
62. Thiam AR, Farese RV, Jr., Walther TC. The biophysics and cell biology of lipid droplets. *Nature reviews Molecular cell biology*. 2013;14(12):775-86.
63. Yang L, Ding Y, Chen Y, Zhang S, Huo C, Wang Y, et al. The proteomics of lipid droplets: structure, dynamics, and functions of the organelle conserved from bacteria to humans. *Journal of lipid research*. 2012;53(7):1245-53.
64. Khor VK, Ahrends R, Lin Y, Shen WJ, Adams CM, Roseman AN, et al. The proteome of cholesteryl-ester-enriched versus triacylglycerol-enriched lipid droplets. *PloS one*. 2014;9(8):e105047.
65. Walther TC, Farese RV, Jr. Lipid droplets and cellular lipid metabolism. *Annual review of biochemistry*. 2012;81:687-714.
66. Taneva S, Dennis MK, Ding Z, Smith JL, Cornell RB. Contribution of each membrane binding domain of the CTP:phosphocholine cytidyltransferase-alpha dimer to its activation, membrane binding, and membrane cross-bridging. *The Journal of biological chemistry*. 2008;283(42):28137-48.
67. Ding Z, Taneva SG, Huang HK, Campbell SA, Semenc L, Chen N, et al. A 22-mer segment in the structurally pliable regulatory domain of metazoan CTP: phosphocholine cytidyltransferase facilitates both silencing and activating functions. *The Journal of biological chemistry*. 2012;287(46):38980-91.
68. Olzmann JA, Carvalho P. Dynamics and functions of lipid droplets. *Nature reviews Molecular cell biology*. 2019;20(3):137-55.
69. Liu P, Ying Y, Zhao Y, Mundy DI, Zhu M, Anderson RG. Chinese hamster ovary K2 cell lipid droplets appear to be metabolic organelles involved in membrane traffic. *The Journal of biological chemistry*. 2004;279(5):3787-92.
70. Bersuker K, Olzmann JA. Establishing the lipid droplet proteome: Mechanisms of lipid droplet protein targeting and degradation. *Biochimica et biophysica acta*. 2017;1862(10 Pt B):1166-77.
71. Krahmer N, Hilger M, Kory N, Wilfling F, Stoehr G, Mann M, et al. Protein correlation profiles identify lipid droplet proteins with high confidence. *Molecular & cellular proteomics : MCP*. 2013;12(5):1115-26.
72. Heid H, Rickelt S, Zimbelmann R, Winter S, Schumacher H, Dorflinger Y, et al. On the formation of lipid droplets in human adipocytes: the organization of the perilipin-vimentin cortex. *PloS one*. 2014;9(2):e90386.
73. Long AP, Mannes Schmidt AK, VerBrugge B, Dortch MR, Minkin SC, Prater KE, et al. Lipid droplet de novo formation and fission are linked to the cell cycle in fission yeast. *Traffic (Copenhagen, Denmark)*. 2012;13(5):705-14.
74. Choudhary V, Ojha N, Golden A, Prinz WA. A conserved family of proteins facilitates nascent lipid droplet budding from the ER. *The Journal of cell biology*. 2015;211(2):261-71.

75. Coleman R, Bell RM. Triacylglycerol synthesis in isolated fat cells. Studies on the microsomal diacylglycerol acyltransferase activity using ethanol-dispersed diacylglycerols. *The Journal of biological chemistry*. 1976;251(15):4537-43.
76. Beck B, Drevon CA. Properties and subcellular distribution of acyl-CoA: cholesterol acyltransferase (ACAT) in guinea-pig liver. *Scandinavian journal of gastroenterology*. 1978;13(1):97-105.
77. Hashimoto S, Fogelman AM. Smooth microsomes. a trap for cholesteryl ester formed in hepatic microsomes. *The Journal of biological chemistry*. 1980;255(18):8678-84.
78. Ploegh HL. A lipid-based model for the creation of an escape hatch from the endoplasmic reticulum. *Nature*. 2007;448(7152):435-8.
79. Van Maldergem L, Magre J, Khallouf TE, Gedde-Dahl T, Jr., Delepine M, Trygstad O, et al. Genotype-phenotype relationships in Berardinelli-Seip congenital lipodystrophy. *Journal of medical genetics*. 2002;39(10):722-33.
80. Cartwright BR, Binns DD, Hilton CL, Han S, Gao Q, Goodman JM. Seipin performs dissectible functions in promoting lipid droplet biogenesis and regulating droplet morphology. *Molecular biology of the cell*. 2015;26(4):726-39.
81. Salo VT, Belevich I, Li S, Karhinen L, Vihinen H, Vigouroux C, et al. Seipin regulates ER-lipid droplet contacts and cargo delivery. *The EMBO journal*. 2016;35(24):2699-716.
82. Salo VT, Li S, Vihinen H, Holtta-Vuori M, Szkalicity A, Horvath P, et al. Seipin Facilitates Triglyceride Flow to Lipid Droplet and Counteracts Droplet Ripening via Endoplasmic Reticulum Contact. *Developmental cell*. 2019.
83. Kadereit B, Kumar P, Wang WJ, Miranda D, Snapp EL, Severina N, et al. Evolutionarily conserved gene family important for fat storage. *Proceedings of the National Academy of Sciences of the United States of America*. 2008;105(1):94-9.
84. Wolins NE, Quaynor BK, Skinner JR, Schoenfish MJ, Tzekov A, Bickel PE. S3-12, Adipophilin, and TIP47 package lipid in adipocytes. *The Journal of biological chemistry*. 2005;280(19):19146-55.
85. Wolins NE, Brasaemle DL, Bickel PE. A proposed model of fat packaging by exchangeable lipid droplet proteins. *FEBS letters*. 2006;580(23):5484-91.
86. McFie PJ, Banman SL, Kary S, Stone SJ. Murine diacylglycerol acyltransferase-2 (DGAT2) can catalyze triacylglycerol synthesis and promote lipid droplet formation independent of its localization to the endoplasmic reticulum. *The Journal of biological chemistry*. 2011;286(32):28235-46.
87. Wilfling F, Wang H, Haas JT, Kraemer N, Gould TJ, Uchida A, et al. Triacylglycerol synthesis enzymes mediate lipid droplet growth by relocalizing from the ER to lipid droplets. *Developmental cell*. 2013;24(4):384-99.
88. Fujimoto Y, Itabe H, Kinoshita T, Homma KJ, Onoduka J, Mori M, et al. Involvement of ACSL in local synthesis of neutral lipids in cytoplasmic lipid droplets in human hepatocyte HuH7. *Journal of lipid research*. 2007;48(6):1280-92.
89. Poppelreuther M, Rudolph B, Du C, Grossmann R, Becker M, Thiele C, et al. The N-terminal region of acyl-CoA synthetase 3 is essential for both the localization on lipid droplets and the function in fatty acid uptake. *Journal of lipid research*. 2012;53(5):888-900.
90. Kraemer N, Guo Y, Wilfling F, Hilger M, Lingrell S, Heger K, et al. Phosphatidylcholine synthesis for lipid droplet expansion is mediated by localized activation of CTP:phosphocholine cytidyltransferase. *Cell metabolism*. 2011;14(4):504-15.

91. Khelef N, Buton X, Beatini N, Wang H, Meiner V, Chang TY, et al. Immunolocalization of acyl-coenzyme A:cholesterol O-acyltransferase in macrophages. *The Journal of biological chemistry*. 1998;273(18):11218-24.
92. Zweytick D, Leitner E, Kohlwein SD, Yu C, Rothblatt J, Daum G. Contribution of Are1p and Are2p to steryl ester synthesis in the yeast *Saccharomyces cerevisiae*. *European journal of biochemistry*. 2000;267(4):1075-82.
93. Gross DA, Zhan C, Silver DL. Direct binding of triglyceride to fat storage-inducing transmembrane proteins 1 and 2 is important for lipid droplet formation. *Proceedings of the National Academy of Sciences of the United States of America*. 2011;108(49):19581-6.
94. Jacquier N, Choudhary V, Mari M, Toulmay A, Reggiori F, Schneider R. Lipid droplets are functionally connected to the endoplasmic reticulum in *Saccharomyces cerevisiae*. *Journal of cell science*. 2011;124(Pt 14):2424-37.
95. Fei W, Shui G, Zhang Y, Kraemer N, Ferguson C, Kapterian TS, et al. A role for phosphatidic acid in the formation of "supersized" lipid droplets. *PLoS genetics*. 2011;7(7):e1002201.
96. Murphy S, Martin S, Parton RG. Quantitative analysis of lipid droplet fusion: inefficient steady state fusion but rapid stimulation by chemical fusogens. *PloS one*. 2010;5(12):e15030.
97. Gao G, Chen FJ, Zhou L, Su L, Xu D, Xu L, et al. Control of lipid droplet fusion and growth by CIDE family proteins. *Biochimica et biophysica acta*. 2017;1862(10 Pt B):1197-204.
98. Zimmermann R, Strauss JG, Haemmerle G, Schoiswohl G, Birner-Gruenberger R, Riederer M, et al. Fat mobilization in adipose tissue is promoted by adipose triglyceride lipase. *Science (New York, NY)*. 2004;306(5700):1383-6.
99. Ong KT, Mashek MT, Bu SY, Greenberg AS, Mashek DG. Adipose triglyceride lipase is a major hepatic lipase that regulates triacylglycerol turnover and fatty acid signaling and partitioning. *Hepatology (Baltimore, Md)*. 2011;53(1):116-26.
100. Haemmerle G, Zimmermann R, Zechner R. Letting lipids go: hormone-sensitive lipase. *Current opinion in lipidology*. 2003;14(3):289-97.
101. Kraemer FB, Shen WJ, Natu V, Patel S, Osuga J, Ishibashi S, et al. Adrenal neutral cholesteryl ester hydrolase: identification, subcellular distribution, and sex differences. *Endocrinology*. 2002;143(3):801-6.
102. Garcia EJ, Vevea JD, Pon LA. Lipid droplet autophagy during energy mobilization, lipid homeostasis and protein quality control. *Frontiers in bioscience (Landmark edition)*. 2018;23:1552-63.
103. Martinez-Lopez N, Garcia-Macia M, Sahu S, Athonvarangkul D, Liebling E, Merlo P, et al. Autophagy in the CNS and Periphery Coordinate Lipophagy and Lipolysis in the Brown Adipose Tissue and Liver. *Cell metabolism*. 2016;23(1):113-27.
104. Sathyanarayan A, Mashek MT, Mashek DG. ATGL Promotes Autophagy/Lipophagy via SIRT1 to Control Hepatic Lipid Droplet Catabolism. *Cell reports*. 2017;19(1):1-9.
105. Kaushik S, Cuervo AM. Degradation of lipid droplet-associated proteins by chaperone-mediated autophagy facilitates lipolysis. *Nature cell biology*. 2015;17(6):759-70.
106. Kaushik S, Cuervo AM. AMPK-dependent phosphorylation of lipid droplet protein PLIN2 triggers its degradation by CMA. *Autophagy*. 2016;12(2):432-8.
107. Pereira-Dutra FS, Teixeira L, de Souza Costa MF, Bozza PT. Fat, fight, and beyond: The multiple roles of lipid droplets in infections and inflammation. *Journal of leukocyte biology*. 2019.

108. Liu L, Zhang K, Sandoval H, Yamamoto S, Jaiswal M, Sanz E, et al. Glial lipid droplets and ROS induced by mitochondrial defects promote neurodegeneration. *Cell*. 2015;160(1-2):177-90.
109. Cermelli S, Guo Y, Gross SP, Welte MA. The lipid-droplet proteome reveals that droplets are a protein-storage depot. *Current biology : CB*. 2006;16(18):1783-95.
110. Zhang N, Yin P, Zhou L, Li H, Zhang L. ARF1 activation dissociates ADRP from lipid droplets to promote HCV assembly. *Biochemical and biophysical research communications*. 2016;475(1):31-6.
111. Schaffer JE. Lipotoxicity: when tissues overeat. *Current opinion in lipidology*. 2003;14(3):281-7.
112. Hashimoto T, Segawa H, Okuno M, Kano H, Hamaguchi HO, Haraguchi T, et al. Active involvement of micro-lipid droplets and lipid-droplet-associated proteins in hormone-stimulated lipolysis in adipocytes. *Journal of cell science*. 2012;125(Pt 24):6127-36.
113. Khor VK, Shen WJ, Kraemer FB. Lipid droplet metabolism. *Current opinion in clinical nutrition and metabolic care*. 2013;16(6):632-7.
114. Bakke SS, Moro C, Nikolic N, Hessvik NP, Badin PM, Lauvhaug L, et al. Palmitic acid follows a different metabolic pathway than oleic acid in human skeletal muscle cells; lower lipolysis rate despite an increased level of adipose triglyceride lipase. *Biochimica et biophysica acta*. 2012;1821(10):1323-33.
115. Kanaley JA, Shadid S, Sheehan MT, Guo Z, Jensen MD. Relationship between plasma free fatty acid, intramyocellular triglycerides and long-chain acylcarnitines in resting humans. *The Journal of physiology*. 2009;587(Pt 24):5939-50.
116. Haemmerle G, Lass A, Zimmermann R, Gorkiewicz G, Meyer C, Rozman J, et al. Defective lipolysis and altered energy metabolism in mice lacking adipose triglyceride lipase. *Science (New York, NY)*. 2006;312(5774):734-7.
117. Haemmerle G, Moustafa T, Woelkart G, Buttner S, Schmidt A, van de Weijer T, et al. ATGL-mediated fat catabolism regulates cardiac mitochondrial function via PPAR-alpha and PGC-1. *Nature medicine*. 2011;17(9):1076-85.
118. Tansey JT, Sztalryd C, Gruia-Gray J, Roush DL, Zee JV, Gavrilova O, et al. Perilipin ablation results in a lean mouse with aberrant adipocyte lipolysis, enhanced leptin production, and resistance to diet-induced obesity. *Proceedings of the National Academy of Sciences of the United States of America*. 2001;98(11):6494-9.
119. Pollak NM, Jaeger D, Kolleritsch S, Zimmermann R, Zechner R, Lass A, et al. The interplay of protein kinase A and perilipin 5 regulates cardiac lipolysis. *The Journal of biological chemistry*. 2015;290(3):1295-306.
120. Lund J, Helle SA, Li Y, Lovsletten NG, Stadheim HK, Jensen J, et al. Higher lipid turnover and oxidation in cultured human myotubes from athletic versus sedentary young male subjects. *Scientific reports*. 2018;8(1):17549.
121. Farmer BC, Kluemper J, Johnson LA. Apolipoprotein E4 Alters Astrocyte Fatty Acid Metabolism and Lipid Droplet Formation. *Cells*. 2019;8(2).
122. Frayn KN. Adipose tissue as a buffer for daily lipid flux. *Diabetologia*. 2002;45(9):1201-10.
123. Fielding B. Tracing the fate of dietary fatty acids: metabolic studies of postprandial lipaemia in human subjects. *The Proceedings of the Nutrition Society*. 2011;70(3):342-50.
124. Longo M, Zatterale F, Naderi J, Parrillo L, Formisano P, Raciti GA, et al. Adipose Tissue Dysfunction as Determinant of Obesity-Associated Metabolic Complications. *International journal of molecular sciences*. 2019;20(9).

125. Vigouroux C, Caron-Debarle M, Le Dour C, Magre J, Capeau J. Molecular mechanisms of human lipodystrophies: from adipocyte lipid droplet to oxidative stress and lipotoxicity. *The international journal of biochemistry & cell biology*. 2011;43(6):862-76.
126. Virtue S, Vidal-Puig A. Adipose tissue expandability, lipotoxicity and the Metabolic Syndrome — An allostatic perspective. *Biochimica et Biophysica Acta (BBA) - Molecular and Cell Biology of Lipids*. 2010;1801(3):338-49.
127. Jung UJ, Choi MS. Obesity and its metabolic complications: the role of adipokines and the relationship between obesity, inflammation, insulin resistance, dyslipidemia and nonalcoholic fatty liver disease. *International journal of molecular sciences*. 2014;15(4):6184-223.
128. Strawford A, Antelo F, Christiansen M, Hellerstein MK. Adipose tissue triglyceride turnover, de novo lipogenesis, and cell proliferation in humans measured with 2H₂O. *American journal of physiology Endocrinology and metabolism*. 2004;286(4):E577-88.
129. Ryden M, Andersson DP, Bernard S, Spalding K, Arner P. Adipocyte triglyceride turnover and lipolysis in lean and overweight subjects. *Journal of lipid research*. 2013;54(10):2909-13.
130. Shepherd SO, Strauss JA, Wang Q, Dube JJ, Goodpaster B, Mashek DG, et al. Training alters the distribution of perilipin proteins in muscle following acute free fatty acid exposure. *The Journal of physiology*. 2017;595(16):5587-601.
131. Ferrara D, Montecucco F, Dallegri F, Carbone F. Impact of different ectopic fat depots on cardiovascular and metabolic diseases. *Journal of cellular physiology*. 2019.
132. Al-Hasani H, Joost HG. Nutrition-/diet-induced changes in gene expression in white adipose tissue. *Best practice & research Clinical endocrinology & metabolism*. 2005;19(4):589-603.
133. Funai K, Semenkovich CF. Skeletal muscle lipid flux: running water carries no poison. *American journal of physiology Endocrinology and metabolism*. 2011;301(2):E245-51.
134. Kienesberger PC, Pulnikunnil T, Nagendran J, Dyck JR. Myocardial triacylglycerol metabolism. *Journal of molecular and cellular cardiology*. 2013;55:101-10.
135. Gluchowski NL, Becuwe M, Walther TC, Farese RV, Jr. Lipid droplets and liver disease: from basic biology to clinical implications. *Nature reviews Gastroenterology & hepatology*. 2017;14(6):343-55.
136. Martin S, Parton RG. Caveolin, cholesterol, and lipid bodies. *Seminars in cell & developmental biology*. 2005;16(2):163-74.
137. Lu X, Gruia-Gray J, Copeland NG, Gilbert DJ, Jenkins NA, Londos C, et al. The murine perilipin gene: the lipid droplet-associated perilipins derive from tissue-specific, mRNA splice variants and define a gene family of ancient origin. *Mammalian genome : official journal of the International Mammalian Genome Society*. 2001;12(9):741-9.
138. Scherer PE, Bickel PE, Kotler M, Lodish HF. Cloning of cell-specific secreted and surface proteins by subtractive antibody screening. *Nature biotechnology*. 1998;16(6):581-6.
139. Dalen KT, Dahl T, Holter E, Arntsen B, Londos C, Sztalryd C, et al. LSDP5 is a PAT protein specifically expressed in fatty acid oxidizing tissues. *Biochimica et biophysica acta*. 2007;1771(2):210-27.
140. Wang H, Hu L, Dalen K, Dorward H, Marcinkiewicz A, Russell D, et al. Activation of hormone-sensitive lipase requires two steps, protein phosphorylation and binding to the PAT-1 domain of lipid droplet coat proteins. *The Journal of biological chemistry*. 2009;284(46):32116-25.

141. Bussell R, Jr., Eliezer D. A structural and functional role for 11-mer repeats in alpha-synuclein and other exchangeable lipid binding proteins. *Journal of molecular biology*. 2003;329(4):763-78.
142. Rowe ER, Mimmack ML, Barbosa AD, Haider A, Isaac I, Ouberai MM, et al. Conserved Amphipathic Helices Mediate Lipid Droplet Targeting of Perilipins 1–3. *The Journal of biological chemistry*. 2016;291(13):6664-78.
143. Hickenbottom SJ, Kimmel AR, Londos C, Hurley JH. Structure of a lipid droplet protein; the PAT family member TIP47. *Structure (London, England : 1993)*. 2004;12(7):1199-207.
144. Sztalryd C, Brasaemle DL. The perilipin family of lipid droplet proteins: Gatekeepers of intracellular lipolysis. *Biochimica et Biophysica Acta (BBA) - Molecular and Cell Biology of Lipids*. 2017;1862(10, Part B):1221-32.
145. Souza SC, Christoffolete MA, Ribeiro MO, Miyoshi H, Strissel KJ, Stancheva ZS, et al. Perilipin regulates the thermogenic actions of norepinephrine in brown adipose tissue. *Journal of lipid research*. 2007;48(6):1273-9.
146. Servetnick DA, Brasaemle DL, Gruia-Gray J, Kimmel AR, Wolff J, Londos C. Perilipins are associated with cholesteryl ester droplets in steroidogenic adrenal cortical and Leydig cells. *The Journal of biological chemistry*. 1995;270(28):16970-3.
147. Brasaemle DL, Barber T, Wolins NE, Serrero G, Blanchette-Mackie EJ, Londos C. Adipose differentiation-related protein is an ubiquitously expressed lipid storage droplet-associated protein. *Journal of lipid research*. 1997;38(11):2249-63.
148. Wolins NE, Skinner JR, Schoenfish MJ, Tzekov A, Bensch KG, Bickel PE. Adipocyte protein S3-12 coats nascent lipid droplets. *The Journal of biological chemistry*. 2003;278(39):37713-21.
149. Chen W, Chang B, Wu X, Li L, Sleeman M, Chan L. Inactivation of Plin4 downregulates Plin5 and reduces cardiac lipid accumulation in mice. *American journal of physiology Endocrinology and metabolism*. 2013;304(7):E770-9.
150. Bindsboll C, Berg O, Arntsen B, Nebb HI, Dalen KT. Fatty acids regulate perilipin5 in muscle by activating PPARdelta. *Journal of lipid research*. 2013;54(7):1949-63.
151. Pourteymour S, Lee S, Langleite TM, Eckardt K, Hjorth M, Bindsboll C, et al. Perilipin 4 in human skeletal muscle: localization and effect of physical activity. *Physiological reports*. 2015;3(8).
152. Kimmel AR, Sztalryd C. The Perilipins: Major Cytosolic Lipid Droplet-Associated Proteins and Their Roles in Cellular Lipid Storage, Mobilization, and Systemic Homeostasis. *Annual review of nutrition*. 2016;36:471-509.
153. Arimura N, Horiba T, Imagawa M, Shimizu M, Sato R. The peroxisome proliferator-activated receptor gamma regulates expression of the perilipin gene in adipocytes. *The Journal of biological chemistry*. 2004;279(11):10070-6.
154. Dalen KT, Schoonjans K, Ulven SM, Weedon-Fekjaer MS, Bentzen TG, Koutnikova H, et al. Adipose tissue expression of the lipid droplet-associating proteins S3-12 and perilipin is controlled by peroxisome proliferator-activated receptor-gamma. *Diabetes*. 2004;53(5):1243-52.
155. Dalen KT, Ulven SM, Arntsen BM, Solaas K, Nebb HI. PPARalpha activators and fasting induce the expression of adipose differentiation-related protein in liver. *Journal of lipid research*. 2006;47(5):931-43.

156. Edvardsson U, Ljungberg A, Linden D, William-Olsson L, Peilot-Sjogren H, Ahnmark A, et al. PPARalpha activation increases triglyceride mass and adipose differentiation-related protein in hepatocytes. *Journal of lipid research*. 2006;47(2):329-40.
157. Chawla A, Lee CH, Barak Y, He W, Rosenfeld J, Liao D, et al. PPARdelta is a very low-density lipoprotein sensor in macrophages. *Proceedings of the National Academy of Sciences of the United States of America*. 2003;100(3):1268-73.
158. Wolins NE, Quaynor BK, Skinner JR, Tzekov A, Croce MA, Gropler MC, et al. OXPAT/PAT-1 is a PPAR-induced lipid droplet protein that promotes fatty acid utilization. *Diabetes*. 2006;55(12):3418-28.
159. Barquissau V, Beuzelin D, Pisani DF, Beranger GE, Mairal A, Montagner A, et al. White-to-brite conversion in human adipocytes promotes metabolic reprogramming towards fatty acid anabolic and catabolic pathways. *Molecular metabolism*. 2016;5(5):352-65.
160. Pegorier JP, Le May C, Girard J. Control of gene expression by fatty acids. *The Journal of nutrition*. 2004;134(9):2444s-9s.
161. Kotokorpi P, Venteclef N, Ellis E, Gustafsson JA, Mode A. The human ADFP gene is a direct liver-X-receptor (LXR) target gene and differentially regulated by synthetic LXR ligands. *Molecular pharmacology*. 2010;77(1):79-86.
162. Langhi C, Marquart TJ, Allen RM, Baldan A. Perilipin-5 is regulated by statins and controls triglyceride contents in the hepatocyte. *Journal of hepatology*. 2014;61(2):358-65.
163. Miura S, Gan JW, Brzostowski J, Parisi MJ, Schultz CJ, Londos C, et al. Functional conservation for lipid storage droplet association among Perilipin, ADRP, and TIP47 (PAT)-related proteins in mammals, *Drosophila*, and *Dictyostelium*. *The Journal of biological chemistry*. 2002;277(35):32253-7.
164. Jacquier N, Mishra S, Choudhary V, Schneiter R. Expression of oleosin and perilipins in yeast promotes formation of lipid droplets from the endoplasmic reticulum. *Journal of cell science*. 2013;126(Pt 22):5198-209.
165. Najt CP, Lwande JS, McIntosh AL, Senthivayagam S, Gupta S, Kuhn LA, et al. Structural and functional assessment of perilipin 2 lipid binding domain(s). *Biochemistry*. 2014;53(45):7051-66.
166. Subramanian V, Garcia A, Sekowski A, Brasaemle DL. Hydrophobic sequences target and anchor perilipin A to lipid droplets. *Journal of lipid research*. 2004;45(11):1983-91.
167. McManaman JL, Zabaronick W, Schaack J, Orlicky DJ. Lipid droplet targeting domains of adipophilin. *Journal of lipid research*. 2003;44(4):668-73.
168. Sletten A, Seline A, Rudd A, Logsdon M, Listenberger LL. Surface features of the lipid droplet mediate perilipin 2 localization. *Biochemical and biophysical research communications*. 2014;452(3):422-7.
169. Mirheydari M, Rathnayake SS, Frederick H, Arhar T, Mann EK, Cocklin S, et al. Insertion of perilipin 3 into a glycerophospholipid monolayer depends on lipid headgroup and acyl chain species. *Journal of lipid research*. 2016;57(8):1465-76.
170. Bacle A, Gautier R, Jackson CL, Fuchs PFJ, Vanni S. Interdigitation between Triglycerides and Lipids Modulates Surface Properties of Lipid Droplets. *Biophysical journal*. 2017;112(7):1417-30.
171. Bartholomew SR, Bell EH, Summerfield T, Newman LC, Miller EL, Patterson B, et al. Distinct cellular pools of perilipin 5 point to roles in lipid trafficking. *Biochimica et biophysica acta*. 2012;1821(2):268-78.

172. Xu G, Sztalryd C, Lu X, Tansey JT, Gan J, Dorward H, et al. Post-translational regulation of adipose differentiation-related protein by the ubiquitin/proteasome pathway. *The Journal of biological chemistry*. 2005;280(52):42841-7.
173. Masuda Y, Itabe H, Odaki M, Hama K, Fujimoto Y, Mori M, et al. ADRP/adipophilin is degraded through the proteasome-dependent pathway during regression of lipid-storing cells. *Journal of lipid research*. 2006;47(1):87-98.
174. Takahashi Y, Shinoda A, Kamada H, Shimizu M, Inoue J, Sato R. Perilipin2 plays a positive role in adipocytes during lipolysis by escaping proteasomal degradation. *Scientific reports*. 2016;6:20975.
175. Egan JJ, Greenberg AS, Chang MK, Londos C. Control of endogenous phosphorylation of the major cAMP-dependent protein kinase substrate in adipocytes by insulin and beta-adrenergic stimulation. *The Journal of biological chemistry*. 1990;265(31):18769-75.
176. Wang H, Bell M, Sreenivasan U, Hu H, Liu J, Dalen K, et al. Unique regulation of adipose triglyceride lipase (ATGL) by perilipin 5, a lipid droplet-associated protein. *The Journal of biological chemistry*. 2011;286(18):15707-15.
177. Bartz R, Zehmer JK, Zhu M, Chen Y, Serrero G, Zhao Y, et al. Dynamic activity of lipid droplets: protein phosphorylation and GTP-mediated protein translocation. *Journal of proteome research*. 2007;6(8):3256-65.
178. Subramanian V, Rothenberg A, Gomez C, Cohen AW, Garcia A, Bhattacharyya S, et al. Perilipin A mediates the reversible binding of CGI-58 to lipid droplets in 3T3-L1 adipocytes. *The Journal of biological chemistry*. 2004;279(40):42062-71.
179. Yang X, Lu X, Lombes M, Rha GB, Chi YI, Guerin TM, et al. The G(0)/G(1) switch gene 2 regulates adipose lipolysis through association with adipose triglyceride lipase. *Cell metabolism*. 2010;11(3):194-205.
180. Sztalryd C, Xu G, Dorward H, Tansey JT, Contreras JA, Kimmel AR, et al. Perilipin A is essential for the translocation of hormone-sensitive lipase during lipolytic activation. *The Journal of cell biology*. 2003;161(6):1093-103.
181. Jiang HP, Serrero G. Isolation and characterization of a full-length cDNA coding for an adipose differentiation-related protein. *Proceedings of the National Academy of Sciences of the United States of America*. 1992;89(17):7856-60.
182. Heid HW, Moll R, Schwetlick I, Rackwitz HR, Keenan TW. Adipophilin is a specific marker of lipid accumulation in diverse cell types and diseases. *Cell and tissue research*. 1998;294(2):309-21.
183. Patel S, Yang W, Kozusko K, Saudek V, Savage DB. Perilipins 2 and 3 lack a carboxy-terminal domain present in perilipin 1 involved in sequestering ABHD5 and suppressing basal lipolysis. *Proceedings of the National Academy of Sciences of the United States of America*. 2014;111(25):9163-8.
184. Listenberger LL, Ostermeyer-Fay AG, Goldberg EB, Brown WJ, Brown DA. Adipocyte differentiation-related protein reduces the lipid droplet association of adipose triglyceride lipase and slows triacylglycerol turnover. *Journal of lipid research*. 2007;48(12):2751-61.
185. Bell M, Wang H, Chen H, McLenithan JC, Gong DW, Yang RZ, et al. Consequences of lipid droplet coat protein downregulation in liver cells: abnormal lipid droplet metabolism and induction of insulin resistance. *Diabetes*. 2008;57(8):2037-45.
186. Tsai TH, Chen E, Li L, Saha P, Lee HJ, Huang LS, et al. The constitutive lipid droplet protein PLIN2 regulates autophagy in liver. *Autophagy*. 2017;13(7):1130-44.

187. Granneman JG, Moore HP, Mottillo EP, Zhu Z. Functional interactions between Mldp (LSDP5) and Abhd5 in the control of intracellular lipid accumulation. *The Journal of biological chemistry*. 2009;284(5):3049-57.
188. Granneman JG, Moore HP, Mottillo EP, Zhu Z, Zhou L. Interactions of perilipin-5 (Plin5) with adipose triglyceride lipase. *The Journal of biological chemistry*. 2011;286(7):5126-35.
189. Kolleritsch S, Kien B, Schoiswohl G, Diwoky C, Schreiber R, Heier C, et al. Low cardiac lipolysis reduces mitochondrial fission and prevents lipotoxic heart dysfunction in Perilipin 5 mutant mice. *Cardiovascular research*. 2019.
190. Wang H, Sreenivasan U, Hu H, Saladino A, Polster BM, Lund LM, et al. Perilipin 5, a lipid droplet-associated protein, provides physical and metabolic linkage to mitochondria. *Journal of lipid research*. 2011;52(12):2159-68.
191. Pribasniig M, Kien B, Pusch L, Haemmerle G, Zimmermann R, Wolinski H. Extended-resolution imaging of the interaction of lipid droplets and mitochondria. *Biochimica et biophysica acta Molecular and cell biology of lipids*. 2018;1863(10):1285-96.
192. Varghese M, Kimler VA, Ghazi FR, Rathore GK, Perkins GA, Ellisman MH, et al. Adipocyte lipolysis affects Perilipin 5 and cristae organization at the cardiac lipid droplet-mitochondrial interface. *Scientific reports*. 2019;9(1):4734.
193. Benador IY, Veliova M, Mahdaviani K, Petcherski A, Wikstrom JD, Assali EA, et al. Mitochondria Bound to Lipid Droplets Have Unique Bioenergetics, Composition, and Dynamics that Support Lipid Droplet Expansion. *Cell metabolism*. 2018;27(4):869-85.e6.
194. Kuramoto K, Okamura T, Yamaguchi T, Nakamura TY, Wakabayashi S, Morinaga H, et al. Perilipin 5, a lipid droplet-binding protein, protects heart from oxidative burden by sequestering fatty acid from excessive oxidation. *The Journal of biological chemistry*. 2012;287(28):23852-63.
195. Mason RR, Mokhtar R, Matzaris M, Selathurai A, Kowalski GM, Mokbel N, et al. PLIN5 deletion remodels intracellular lipid composition and causes insulin resistance in muscle. *Molecular metabolism*. 2014;3(6):652-63.
196. Bosma M, Sparks LM, Hooiveld GJ, Jorgensen JA, Houten SM, Schrauwen P, et al. Overexpression of PLIN5 in skeletal muscle promotes oxidative gene expression and intramyocellular lipid content without compromising insulin sensitivity. *Biochimica et biophysica acta*. 2013;1831(4):844-52.
197. Wang H, Sreenivasan U, Gong DW, O'Connell KA, Dabkowski ER, Hecker PA, et al. Cardiomyocyte-specific perilipin 5 overexpression leads to myocardial steatosis and modest cardiac dysfunction. *Journal of lipid research*. 2013;54(4):953-65.
198. Montgomery MK, Mokhtar R, Bayliss J, Parkington HC, Suturin VM, Bruce CR, et al. Perilipin 5 Deletion Unmasks an Endoplasmic Reticulum Stress-Fibroblast Growth Factor 21 Axis in Skeletal Muscle. *Diabetes*. 2018;67(4):594-606.
199. Trevino MB, Machida Y, Hallinger DR, Garcia E, Christensen A, Dutta S, et al. Perilipin 5 regulates islet lipid metabolism and insulin secretion in a cAMP-dependent manner: implication of its role in the postprandial insulin secretion. *Diabetes*. 2015;64(4):1299-310.
200. Gallardo-Montejano VI, Saxena G, Kusminski CM, Yang C, McAfee JL, Hahner L, et al. Nuclear Perilipin 5 integrates lipid droplet lipolysis with PGC-1alpha/SIRT1-dependent transcriptional regulation of mitochondrial function. *Nature communications*. 2016;7:12723.
201. Acconcia F, Marino M. Steroid Hormones: Synthesis, Secretion, and Transport. In: Belfiore A, LeRoith D, editors. *Principles of Endocrinology and Hormone Action*. Cham: Springer International Publishing; 2016. p. 1-31.

202. Liao R, Podesser BK, Lim CC. The continuing evolution of the Langendorff and ejecting murine heart: new advances in cardiac phenotyping. *American journal of physiology Heart and circulatory physiology*. 2012;303(2):H156-67.
203. Hessvik NP, Boekschoten MV, Baltzersen MA, Kersten S, Xu X, Andersen H, et al. LXR β is the dominant LXR subtype in skeletal muscle regulating lipogenesis and cholesterol efflux. *American journal of physiology Endocrinology and metabolism*. 2010;298(3):E602-13.
204. Muoio DM, Way JM, Tanner CJ, Winegar DA, Kliewer SA, Houmard JA, et al. Peroxisome proliferator-activated receptor- α regulates fatty acid utilization in primary human skeletal muscle cells. *Diabetes*. 2002;51(4):901-9.
205. Al-Khalili L, Chibalin AV, Kannisto K, Zhang BB, Permert J, Holman GD, et al. Insulin action in cultured human skeletal muscle cells during differentiation: assessment of cell surface GLUT4 and GLUT1 content. *Cellular and molecular life sciences : CMLS*. 2003;60(5):991-8.
206. Berggren JR, Tanner CJ, Houmard JA. Primary cell cultures in the study of human muscle metabolism. *Exercise and sport sciences reviews*. 2007;35(2):56-61.
207. Nehlin JO, Just M, Rustan AC, Gaster M. Human myotubes from myoblast cultures undergoing senescence exhibit defects in glucose and lipid metabolism. *Biogerontology*. 2011;12(4):349-65.
208. LaFramboise WA, Guthrie RD, Scalise D, Elborne V, Bombach KL, Armanious CS, et al. Effect of muscle origin and phenotype on satellite cell muscle-specific gene expression. *Journal of molecular and cellular cardiology*. 2003;35(10):1307-18.
209. Smolina N, Kostareva A, Bruton J, Karpushev A, Sjoberg G, Sejersen T. Primary Murine Myotubes as a Model for Investigating Muscular Dystrophy. *BioMed research international*. 2015;2015:594751.
210. Bourlier V, Saint-Laurent C, Louche K, Badin PM, Thalamas C, de Glisezinski I, et al. Enhanced glucose metabolism is preserved in cultured primary myotubes from obese donors in response to exercise training. *The Journal of clinical endocrinology and metabolism*. 2013;98(9):3739-47.
211. Lund J, Rustan AC, Lovsletten NG, Mudry JM, Langleite TM, Feng YZ, et al. Exercise in vivo marks human myotubes in vitro: Training-induced increase in lipid metabolism. *PLoS one*. 2017;12(4):e0175441.
212. Aas V, Bakke SS, Feng YZ, Kase ET, Jensen J, Bajpeyi S, et al. Are cultured human myotubes far from home? *Cell and tissue research*. 2013;354(3):671-82.
213. Nikolic N, Aas V. Electrical Pulse Stimulation of Primary Human Skeletal Muscle Cells. *Methods in molecular biology (Clifton, NJ)*. 2019;1889:17-24.
214. Kuznetsov AV, Javadov S, Sickinger S, Frotschnig S, Grimm M. H9c2 and HL-1 cells demonstrate distinct features of energy metabolism, mitochondrial function and sensitivity to hypoxia-reoxygenation. *Biochimica et biophysica acta*. 2015;1853(2):276-84.
215. Mitcheson JS, Hancox JC, Levi AJ. Cultured adult cardiac myocytes: future applications, culture methods, morphological and electrophysiological properties. *Cardiovascular research*. 1998;39(2):280-300.
216. Powell T, Twist VW. A rapid technique for the isolation and purification of adult cardiac muscle cells having respiratory control and a tolerance to calcium. *Biochemical and biophysical research communications*. 1976;72(1):327-33.
217. Louch WE, Sheehan KA, Wolska BM. Methods in cardiomyocyte isolation, culture, and gene transfer. *Journal of molecular and cellular cardiology*. 2011;51(3):288-98.

218. O'Connell TD, Rodrigo MC, Simpson PC. Isolation and culture of adult mouse cardiac myocytes. *Methods in molecular biology* (Clifton, NJ). 2007;357:271-96.
219. Kivisto T, Makiranta M, Oikarinen EL, Karhu S, Weckstrom M, Sellin LC. 2,3-Butanedione monoxime (BDM) increases initial yields and improves long-term survival of isolated cardiac myocytes. *The Japanese journal of physiology*. 1995;45(1):203-10.
220. Ding Y, Zhang S, Yang L, Na H, Zhang P, Zhang H, et al. Isolating lipid droplets from multiple species. *Nature protocols*. 2013;8(1):43-51.
221. Spangenburg EE, Pratt SJP, Wohlers LM, Lovering RM. Use of BODIPY (493/503) to visualize intramuscular lipid droplets in skeletal muscle. *Journal of biomedicine & biotechnology*. 2011;2011:598358.
222. Wensaas AJ, Rustan AC, Lovstedt K, Kull B, Wikstrom S, Drevon CA, et al. Cell-based multiwell assays for the detection of substrate accumulation and oxidation. *Journal of lipid research*. 2007;48(4):961-7.
223. Huynh FK, Green MF, Koves TR, Hirschey MD. Measurement of fatty acid oxidation rates in animal tissues and cell lines. *Methods in enzymology*. 2014;542:391-405.
224. Wiechert W. ¹³C metabolic flux analysis. *Metabolic engineering*. 2001;3(3):195-206.
225. Straub BK, Gyoengyoesi B, Koenig M, Hashani M, Pawella LM, Herpel E, et al. Adipophilin/perilipin-2 as a lipid droplet-specific marker for metabolically active cells and diseases associated with metabolic dysregulation. *Histopathology*. 2013;62(4):617-31.
226. Chang BH, Li L, Paul A, Taniguchi S, Nannegari V, Heird WC, et al. Protection against fatty liver but normal adipogenesis in mice lacking adipose differentiation-related protein. *Molecular and cellular biology*. 2006;26(3):1063-76.
227. McManaman JL, Bales ES, Orlicky DJ, Jackman M, MacLean PS, Cain S, et al. Perilipin-2-null mice are protected against diet-induced obesity, adipose inflammation, and fatty liver disease. *Journal of lipid research*. 2013;54(5):1346-59.
228. Ueno M, Suzuki J, Hirose M, Sato S, Imagawa M, Zenimaru Y, et al. Cardiac overexpression of perilipin 2 induces dynamic steatosis: prevention by hormone-sensitive lipase. *American journal of physiology Endocrinology and metabolism*. 2017;313(6):E699-e709.
229. Gao J, Ye H, Serrero G. Stimulation of adipose differentiation related protein (ADRP) expression in adipocyte precursors by long-chain fatty acids. *Journal of cellular physiology*. 2000;182(2):297-302.
230. Bosma M, Hesselink MK, Sparks LM, Timmers S, Ferraz MJ, Mattijssen F, et al. Perilipin 2 improves insulin sensitivity in skeletal muscle despite elevated intramuscular lipid levels. *Diabetes*. 2012;61(11):2679-90.
231. Smirnova E, Goldberg EB, Makarova KS, Lin L, Brown WJ, Jackson CL. ATGL has a key role in lipid droplet/adiposome degradation in mammalian cells. *EMBO reports*. 2006;7(1):106-13.
232. Fong TH, Yang CC, Greenberg AS, Wang SM. Immunocytochemical studies on lipid droplet-surface proteins in adrenal cells. *Journal of cellular biochemistry*. 2002;86(3):432-9.
233. Poulsen L, Siersbaek M, Mandrup S. PPARs: fatty acid sensors controlling metabolism. *Seminars in cell & developmental biology*. 2012;23(6):631-9.
234. Sztalryd C, Bell M, Lu X, Mertz P, Hickenbottom S, Chang BH, et al. Functional compensation for adipose differentiation-related protein (ADFP) by Tip47 in an ADFP null embryonic cell line. *The Journal of biological chemistry*. 2006;281(45):34341-8.

235. Suzuki J, Shen WJ, Nelson BD, Selwood SP, Murphy GM, Jr., Kanehara H, et al. Cardiac gene expression profile and lipid accumulation in response to starvation. *American journal of physiology Endocrinology and metabolism*. 2002;283(1):E94-e102.
236. Christoffersen C, Bollano E, Lindegaard ML, Bartels ED, Goetze JP, Andersen CB, et al. Cardiac lipid accumulation associated with diastolic dysfunction in obese mice. *Endocrinology*. 2003;144(8):3483-90.
237. Ruberg FL. Myocardial lipid accumulation in the diabetic heart. *Circulation*. 2007;116(10):1110-2.
238. Schulze PC. Myocardial lipid accumulation and lipotoxicity in heart failure. *Journal of lipid research*. 2009;50(11):2137-8.
239. Trent CM, Yu S, Hu Y, Skoller N, Huggins LA, Homma S, et al. Lipoprotein lipase activity is required for cardiac lipid droplet production. *Journal of lipid research*. 2014;55(4):645-58.
240. Drevinge C, Dalen KT, Mannila MN, Tang MS, Stahlman M, Klevstig M, et al. Perilipin 5 is protective in the ischemic heart. *International journal of cardiology*. 2016;219:446-54.
241. Schuldiner M, Bohnert M. A different kind of love – lipid droplet contact sites. *Biochimica et Biophysica Acta (BBA) - Molecular and Cell Biology of Lipids*. 2017;1862(10, Part B):1188-96.
242. Saha PK, Kojima H, Martinez-Botas J, Sunehag AL, Chan L. Metabolic adaptations in the absence of perilipin: increased beta-oxidation and decreased hepatic glucose production associated with peripheral insulin resistance but normal glucose tolerance in perilipin-null mice. *The Journal of biological chemistry*. 2004;279(34):35150-8.
243. Sapiro JM, Mashek MT, Greenberg AS, Mashek DG. Hepatic triacylglycerol hydrolysis regulates peroxisome proliferator-activated receptor alpha activity. *Journal of lipid research*. 2009;50(8):1621-9.
244. Venkateswaran A, Laffitte BA, Joseph SB, Mak PA, Wilpitz DC, Edwards PA, et al. Control of cellular cholesterol efflux by the nuclear oxysterol receptor LXR alpha. *Proceedings of the National Academy of Sciences of the United States of America*. 2000;97(22):12097-102.
245. Laffitte BA, Repa JJ, Joseph SB, Wilpitz DC, Kast HR, Mangelsdorf DJ, et al. LXRs control lipid-inducible expression of the apolipoprotein E gene in macrophages and adipocytes. *Proceedings of the National Academy of Sciences of the United States of America*. 2001;98(2):507-12.
246. Cummins CL, Volle DH, Zhang Y, McDonald JG, Sion B, Lefrancois-Martinez AM, et al. Liver X receptors regulate adrenal cholesterol balance. *The Journal of clinical investigation*. 2006;116(7):1902-12.
247. Li H, Brochu M, Wang SP, Rochdi L, Cote M, Mitchell G, et al. Hormone-sensitive lipase deficiency in mice causes lipid storage in the adrenal cortex and impaired corticosterone response to corticotropin stimulation. *Endocrinology*. 2002;143(9):3333-40.
248. Platt FM, Boland B, van der Spoel AC. The cell biology of disease: lysosomal storage disorders: the cellular impact of lysosomal dysfunction. *The Journal of cell biology*. 2012;199(5):723-34.
249. Ridsdale R, Na CL, Xu Y, Greis KD, Weaver T. Comparative proteomic analysis of lung lamellar bodies and lysosome-related organelles. *PloS one*. 2011;6(1):e16482.
250. Lajoie P, Guay G, Dennis JW, Nabi IR. The lipid composition of autophagic vacuoles regulates expression of multilamellar bodies. *Journal of cell science*. 2005;118(Pt 9):1991-2003.

251. Zhang J, Xu D, Nie J, Han R, Zhai Y, Shi Y. Comparative gene identification-58 (CGI-58) promotes autophagy as a putative lysophosphatidylglycerol acyltransferase. *The Journal of biological chemistry*. 2014;289(47):33044-53.
252. Hsu P, Shi Y. Regulation of autophagy by mitochondrial phospholipids in health and diseases. *Biochimica et biophysica acta Molecular and cell biology of lipids*. 2017;1862(1):114-29.
253. Keenan SN, Meex RC, Lo JCY, Ryan A, Nie S, Montgomery MK, et al. Perilipin 5 Deletion in Hepatocytes Remodels Lipid Metabolism and Causes Hepatic Insulin Resistance in Mice. *Diabetes*. 2019;68(3):543-55.
254. Andersson L, Drevinge C, Mardani I, Dalen KT, Stahlman M, Klevstig M, et al. Deficiency in perilipin 5 reduces mitochondrial function and membrane depolarization in mouse hearts. *The international journal of biochemistry & cell biology*. 2017;91(Pt A):9-13.
255. Muoio DM, Neuffer PD. Lipid-induced mitochondrial stress and insulin action in muscle. *Cell metabolism*. 2012;15(5):595-605.
256. Lopaschuk GD. Fatty Acid Oxidation and Its Relation with Insulin Resistance and Associated Disorders. *Annals of nutrition & metabolism*. 2016;68 Suppl 3:15-20.
257. Varela GM, Antwi DA, Dhir R, Yin X, Singhal NS, Graham MJ, et al. Inhibition of ADRP prevents diet-induced insulin resistance. *American journal of physiology Gastrointestinal and liver physiology*. 2008;295(3):G621-8.
258. Phillips SA, Choe CC, Ciaraldi TP, Greenberg AS, Kong AP, Baxi SC, et al. Adipocyte differentiation-related protein in human skeletal muscle: relationship to insulin sensitivity. *Obesity research*. 2005;13(8):1321-9.
259. Orlicky DJ, Libby AE, Bales ES, McMahan RH, Monks J, La Rosa FG, et al. Perilipin-2 promotes obesity and progressive fatty liver disease in mice through mechanistically distinct hepatocyte and extra-hepatocyte actions. *The Journal of physiology*. 2019;597(6):1565-84.
260. Kliewer SA, Sundseth SS, Jones SA, Brown PJ, Wisely GB, Koble CS, et al. Fatty acids and eicosanoids regulate gene expression through direct interactions with peroxisome proliferator-activated receptors alpha and gamma. *Proceedings of the National Academy of Sciences of the United States of America*. 1997;94(9):4318-23.
261. Zechner R, Zimmermann R, Eichmann TO, Kohlwein SD, Haemmerle G, Lass A, et al. FAT SIGNALS--lipases and lipolysis in lipid metabolism and signaling. *Cell metabolism*. 2012;15(3):279-91.
262. Georgiadi A, Kersten S. Mechanisms of gene regulation by fatty acids. *Advances in nutrition (Bethesda, Md)*. 2012;3(2):127-34.
263. Lin J, Wu H, Tarr PT, Zhang CY, Wu Z, Boss O, et al. Transcriptional co-activator PGC-1 alpha drives the formation of slow-twitch muscle fibres. *Nature*. 2002;418(6899):797-801.
264. Finck BN, Bernal-Mizrachi C, Han DH, Coleman T, Sambandam N, LaRiviere LL, et al. A potential link between muscle peroxisome proliferator- activated receptor-alpha signaling and obesity-related diabetes. *Cell metabolism*. 2005;1(2):133-44.
265. Wende AR, Huss JM, Schaeffer PJ, Giguere V, Kelly DP. PGC-1alpha coactivates PDK4 gene expression via the orphan nuclear receptor ERRalpha: a mechanism for transcriptional control of muscle glucose metabolism. *Molecular and cellular biology*. 2005;25(24):10684-94.
266. Badin PM, Loubiere C, Coonen M, Louche K, Tavernier G, Bourlier V, et al. Regulation of skeletal muscle lipolysis and oxidative metabolism by the co-lipase CGI-58. *Journal of lipid research*. 2012;53(5):839-48.

267. Chow L, From A, Seaquist E. Skeletal muscle insulin resistance: the interplay of local lipid excess and mitochondrial dysfunction. *Metabolism: clinical and experimental*. 2010;59(1):70-85.
268. Chang BH, Li L, Saha P, Chan L. Absence of adipose differentiation related protein upregulates hepatic VLDL secretion, relieves hepatosteatosis, and improves whole body insulin resistance in leptin-deficient mice. *Journal of lipid research*. 2010;51(8):2132-42.
269. Bosma M, Minnaard R, Sparks LM, Schaart G, Losen M, de Baets MH, et al. The lipid droplet coat protein perilipin 5 also localizes to muscle mitochondria. *Histochemistry and cell biology*. 2012;137(2):205-16.
270. Kimmel AR, Sztalryd C. Perilipin 5, a lipid droplet protein adapted to mitochondrial energy utilization. *Current opinion in lipidology*. 2014;25(2):110-7.
271. Jodalen H, Stangeland L, Grong K, Vik-Mo H, Lekven J. Lipid accumulation in the myocardium during acute regional ischaemia in cats. *Journal of molecular and cellular cardiology*. 1985;17(10):973-80.
272. Cal R, Castellano J, Revuelta-Lopez E, Aledo R, Barriga M, Farre J, et al. Low-density lipoprotein receptor-related protein 1 mediates hypoxia-induced very low density lipoprotein-cholesteryl ester uptake and accumulation in cardiomyocytes. *Cardiovascular research*. 2012;94(3):469-79.
273. Drevinge C, Karlsson LO, Stahlman M, Larsson T, Perman Sundelin J, Grip L, et al. Cholesteryl esters accumulate in the heart in a porcine model of ischemia and reperfusion. *PloS one*. 2013;8(4):e61942.
274. Mohktar RA, Montgomery MK, Murphy RM, Watt MJ. Perilipin 5 is dispensable for normal substrate metabolism and in the adaptation of skeletal muscle to exercise training. *American journal of physiology Endocrinology and metabolism*. 2016;311(1):E128-37.
275. van der Vusse GJ, van Bilsen M, Glatz JF. Cardiac fatty acid uptake and transport in health and disease. *Cardiovascular research*. 2000;45(2):279-93.
276. Wambolt RB, Henning SL, English DR, Dyachkova Y, Lopaschuk GD, Allard MF. Glucose utilization and glycogen turnover are accelerated in hypertrophied rat hearts during severe low-flow ischemia. *Journal of molecular and cellular cardiology*. 1999;31(3):493-502.
277. Pascual F, Coleman RA. Fuel availability and fate in cardiac metabolism: A tale of two substrates. *Biochimica et Biophysica Acta (BBA) - Molecular and Cell Biology of Lipids*. 2016;1861(10):1425-33.
278. Zheng P, Xie Z, Yuan Y, Sui W, Wang C, Gao X, et al. Plin5 alleviates myocardial ischaemia/reperfusion injury by reducing oxidative stress through inhibiting the lipolysis of lipid droplets. *Scientific reports*. 2017;7:42574.
279. Barba I, Chavarria L, Ruiz-Meana M, Mirabet M, Agullo E, Garcia-Dorado D. Effect of intracellular lipid droplets on cytosolic Ca²⁺ and cell death during ischaemia-reperfusion injury in cardiomyocytes. *The Journal of physiology*. 2009;587(Pt 6):1331-41.
280. Depre C, Vanoverschelde JL, Taegtmeyer H. Glucose for the heart. *Circulation*. 1999;99(4):578-88.



Loss of perilipin 2 in cultured myotubes enhances lipolysis and redirects the metabolic energy balance from glucose oxidation towards fatty acid oxidation

Yuan Z. Feng,* Jenny Lund,^{1,*} Yuchuan Li,^{1,†} Irlin K. Knabenes,* Siril S. Bakke,* Eili T. Kase,* Yun K. Lee,[§] Alan R. Kimmel,[§] G. Hege Thoresen,*^{***} Arild Christian Rustan,* and Knut Tomas Dalen^{2,†,††}

Department of Pharmaceutical Biosciences,* School of Pharmacy, Faculty of Mathematics and Natural Sciences, Department of Nutrition,[†] and The Norwegian Transgenic Center,^{††} Institute of Basic Medical Sciences, Department of Pharmacology,** Institute of Clinical Medicine, Faculty of Medicine, University of Oslo, Oslo, Norway; and Laboratory of Cellular and Developmental Biology,[§] National Institute of Diabetes and Digestive and Kidney Diseases, National Institutes of Health, Bethesda, MD

ORCID ID: 0000-0002-0270-5982 (K.T.D.)

Abstract Lipid droplet (LD) coating proteins are essential for the formation and stability of intracellular LDs. Plin2 is an abundant LD coating protein in skeletal muscle, but its importance for muscle function is unclear. We show that myotubes established from *Plin2*^{-/-} mice contain reduced content of LDs and accumulate less oleic acid (OA) in triacylglycerol (TAG) due to elevated LD hydrolysis in comparison with *Plin2*^{+/+} myotubes. The reduced ability to store TAG in LDs in *Plin2*^{-/-} myotubes is accompanied by a shift in energy metabolism. *Plin2*^{-/-} myotubes are characterized by increased oxidation of OA, lower glycogen synthesis, and reduced glucose oxidation in comparison with *Plin2*^{+/+} myotubes, perhaps reflecting competition between FAs and glucose as part of the Randle cycle. In accord with these metabolic changes, *Plin2*^{-/-} myotubes have elevated expression of *Ppara* and *Ppargc1a*, transcription factors that stimulate expression of genes important for FA oxidation, whereas genes involved in glucose uptake and oxidation are suppressed. Loss of *Plin2* had no impact on insulin-stimulated Akt phosphorylation. Our results suggest that Plin2 is essential for protecting the pool of skeletal muscle LDs to avoid an uncontrolled hydrolysis of stored TAG and to balance skeletal muscle energy metabolism.—Feng, Y. Z., J. Lund, Y. Li, I. K. Knabenes, S. S. Bakke, E. T. Kase, Y. K. Lee, A. R. Kimmel, G. H. Thoresen, A. C. Rustan, and K. T. Dalen.

This work was supported by grants from the Medical Faculty at the University of Oslo, Henning and the Johan Throne-Holst Foundation (Y.L. and K.T.D.), the Intramural Research Programs of the National Institutes of Health (NIH), the National Institute of Diabetes and Digestive and Kidney Diseases (NIDDK) (K.T.D. and A.R.K.), the Novo Nordisk Foundation (K.T.D.), Aktieselskabet Freia Chocolate Fabrik's Medical Foundation, and Anders Jahre's Foundation (K.T.D., A.C.R., G.H.T.). The authors declare that they have no conflicts of interest with the contents of this article.

In Memoriam: The impetus for developing the *Plin2*-null model to ascertain *Plin2* function in the context of muscle function, LD accumulation, and insulin signaling originated from many scientific discussions among Constantine Londos (NIDDK/NIH), A.R.K., and K.T.D. in 2005. Dean was an inspiration and is deeply missed.

Manuscript received 5 August 2017.

Published, JLR Papers in Press, August 19, 2017
DOI <https://doi.org/10.1194/jlr.M079764>

Loss of perilipin 2 in cultured myotubes enhances lipolysis and redirects the metabolic energy balance from glucose oxidation towards fatty acid oxidation. *J. Lipid Res.* 2017. 58: 2147–2161.

Supplementary key words Plin2 • triacylglycerol • lipid droplet • lipolysis and fatty acid metabolism • fatty acid/metabolism • insulin signaling • muscle

Energy to drive contraction of skeletal muscle fibers is obtained primarily by oxidation of glucose or FAs. Skeletal muscle cells store these two energy sources as cytosolic glycogen or triacylglycerol (TAG)-containing lipid droplets (LDs), respectively. Incorporation of glucose into glycogen and its degradation for energy utilization are relatively more understood processes than are storage and metabolism of muscular lipids. Aerobic glucose utilization occurs in the cytosol catalyzed by the glycolytic enzymes, whereas FAs are

Abbreviations: ASM, acid-soluble metabolite; Acox1, acyl-CoA oxidase 1; ATGL, adipose triglyceride lipase; Akt, thymoma viral proto-oncogene/AKT serine/threonine kinase; Cpt2, carnitine palmitoyltransferase 2; CE, cholesteryl ester; Cd36, CD36 antigen/FA transporter; DAG, diacylglycerol; Fabp3, FA binding protein 3; Glut1 and Glut4, glucose transporter 1 and 4; Pygm, glycogen phosphorylase, muscle-associated; Gys1, glycogen synthase 1; Hk1 and Hk2, hexokinase 1 and 2; HSL, hormone sensitive lipase; LD, lipid droplet; Acadl, acyl-CoA dehydrogenase, long-chain; Acadm, acyl-CoA dehydrogenase, C-4 to C-12 straight chain; Acadvl, acyl-CoA dehydrogenase, very long chain; MAG, monoacylglycerol; OA, oleic acid; Ppargc1a, PPAR coactivator 1 alpha; PL, phospholipid; Pdk4, pyruvate dehydrogenase kinase isozyme 4; Pdha1, pyruvate dehydrogenase alpha 1; Pkm, pyruvate kinase muscle; Plin, perilipin; Slc2a1 and Slc2a4, solute carrier family 2 member 1 and 4; TAG, triacylglycerol Tbp, TATA box binding protein; Ucp2 and Ucp3, uncoupling protein 2 and 3.

¹J. Lund and Y. Li contributed equally to this work.

²To whom correspondence should be addressed.
e-mail: k.t.dalen@medisin.uio.no

mainly utilized through mitochondrial β -oxidation. In addition to hormonal regulation and transcription input of these two separate oxidative pathways, competitive and feedback interactions among their various substrates and products also directs glucose/FA oxidative balance and may be mechanistically important for tissue insulin sensitivity (1). Likewise, a high content of intramyocellular TAG, suggestive of increased FA availability, is well known to correlate with reduced glucose disposal and insulin resistance in some individuals (2–6), but this is not absolute. Intramyocellular TAG content in endurance-trained individuals, which can be higher than in obese insulin-resistant individuals (7), does not affect insulin sensitivity or oxidative capacity, a phenomenon described as the athlete's paradox (7–10). In addition, despite higher intramyocellular TAG levels, women are more insulin sensitive than are men (11). Therefore, new concepts have emerged to explain lipid-mediated muscular insulin resistance, which focus on abnormal lipid influx, storage, or build-up of lipid species arising from altered TAG lipolysis, rather than lipid content per se (12).

LDs in mammalian cells consist of an inner core of neutral lipids, such as TAGs, diacylglycerols (DAGs), or cholesteryl esters (CEs), surrounded by a single monolayer of phospholipids (PLs) with a protein coat (13, 14). The mechanisms for enzymatic degradation of the esterified neutral lipids in the LD core into FAs and glycerol in skeletal muscle are similar to those of many other tissues and involve active translocation of lipases to the LD surface. Thus, facilitated recruitment of proteins to the LD surface is the major mechanism regulating LD size and turnover. Adipose triglyceride lipase (ATGL) mediates the first step in TAG degradation (15), generating DAG, which is subsequently degraded by hormone-sensitive lipase (HSL) (16), followed by monoacylglycerol (MAG) cleavage by MAG lipase (17). Still, it is not understood mechanistically how lipases are actively recruited to the LD surface in muscle or how these enzymes can access the neutral lipids stored in the LD core through the protein and PL layer. Accumulating evidence suggests that perilipin (Plin) family proteins are involved [see reviews (8, 14, 18)]. As with other mammalian cell types, Plin proteins are among the most abundant LD coating proteins in skeletal muscle cells. The Plins derive from an ancient gene family that consists of five *Plin* genes in mammals, some with alternative splice variants (18–20). The *Plin* genes differ in their tissue expression and transcriptional regulation, and the encoded proteins differ in the number of residues, affinity to LDs, and stability when not bound to LDs. The fundamental understanding of Plin functions is based on the initial characterization of Plin1 in white adipose tissue. Plin1 interactions with lipases and their coactivators at the LD surface are differentially regulated by PKA phosphorylation (21) and serve as major regulatory steps controlling storage versus degradation of neutral lipids stored in the core of adipose LDs (22, 23). The other Plins are believed to regulate LD degradation in nonadipose tissues. This assumption is supported by the observations that removal of *Plin1* (22, 23), *Plin2* (24), *Plin4* (25), or *Plin5* (26) in mice results in reduced LD content in tissues where these proteins normally would be highly

expressed. Overexpression of certain Plins increases the relative LD accumulation of specific neutral lipid species as opposed to others, which suggests diversity of Plin function (27).

Plin2 is an abundant LD coating protein in skeletal muscle where the majority of the LDs are covered by Plin2 (28). Interventions that increase muscle insulin sensitivity might be accompanied with an increase in Plin2 protein expression (29), suggesting that Plin2 might play a role in decreasing intramuscular lipid toxicity by promoting lipid storage. On the other hand, comparable muscular Plin2 protein content has been observed when comparing obese nondiabetic and obese diabetic subjects (30). To clarify the functional role of Plin2 in skeletal muscle, we established myoblast cultures from *Plin2*^{+/+} and *Plin2*^{-/-} mice, differentiated these into myotubes, and compared myocellular lipid storage and energy metabolism. We observed enhanced lipolysis, reduced levels of TAG-containing LDs, and altered lipid and glucose oxidation rates in myotubes lacking Plin2 at the LD surface. *Plin2*^{-/-} myotubes show a shift in metabolic energy utilization toward FA oxidation, consistent with suppression of glucose oxidation within the parameters of the Randle cycle. Our results suggest that Plin2 balances energy utilization of glucose and FAs by stabilizing and packaging excess FAs in LD stores.

MATERIALS AND METHODS

Materials

DMEM (DMEM-GlutamaxTM, 5.5 mM glucose) with sodium pyruvate, DMEM without phenol red, Ham's F-10-GlutamaxTM nutrient mixture (5.5 mM glucose), horse serum, heat-inactivated FBS, basic fibroblast growth factor, collagenase II, penicillin-streptomycin, and amphotericin B, Bodipy 493/503, Hoechst 33258, Hoechst 33342, ABI 6100 Nucleic Acid Prep-Station solutions, and Superscript III RT were from Thermo Fisher Scientific (Waltham, MA). Matrigel was purchased from BD Biosciences (Bedford, MA). Insulin (Actrapid[®]) was obtained from Novo Nordisk (Bagsvaerd, Denmark). BSA (essentially FA free), L-carnitine, Dulbecco's PBS (DPBS, with Mg²⁺ and Ca²⁺), oleic acid (OA; 18:1, n-9), and glycogen were from Sigma-Aldrich (St. Louis, MO). [1-¹⁴C]oleic acid (58.2 mCi/mmol) and D-[¹⁴C-(U)]glucose (2.9 mCi/mmol) were from PerkinElmer NEN[®] (Boston, MA). Liberase Blendzyme 3 (0.038 WU/ml) and Complete Protease Inhibitor Cocktail were from Roche (Basel, Switzerland). Culture plates and flasks were from Corning (Corning, NY). Glass-bottom six-well plates were from MatTek (Ashland, MA). Ninety six-well Scintiplate[®], UniFilter[®] micro plate, Isoplate[®] scintillation plate, and OptiPhase Supermix were obtained from PerkinElmer (Shelton, CT). Ultracentrifugation tubes were from Beckman Coulter Inc. (#344062; Brea, CA). TLC plates (Silica gel 60) were from Merck Millipore (Billerica, MA). Atglistatin was from Xcess Biosciences (San Diego, CA). CAY10499 was from Cayman Chemical (Ann Arbor, MI). TG PAP 150-kit (#61236) was obtained from BioMerieux (Marcy l'Etoile, France). SYBR Master Mix was from Kapa Biosystems (Wilmington, MA). Criterion or Mini-Protean[®] TGXTM gels (4–20%), ClarityTM Western ECL Substrate, and the goat anti-rabbit HRP-conjugated (HRP) secondary antibody #1706515 were purchased from Bio-Rad (Copenhagen, Denmark). PierceTM BCA protein assay kit was from Thermo Fisher Scientific (Rockford, IL).

Antibodies against total thymoma viral proto-oncogene/AKT serine/threonine kinase (Akt) (#9272, rabbit polyclonal antibody), phosphorylated Akt (pSer473, #9271, rabbit polyclonal antibody), Slc2a1/Glut1 (#12938, rabbit monoclonal antibody), Pkm (#3106, rabbit monoclonal antibody), Pdha1 (#3205, rabbit monoclonal antibody), and β -actin (#4970, rabbit monoclonal antibody) were from Cell Signaling Technology (Beverly, MA). Antibody against Pdha1-p300 (#ABS194, rabbit polyclonal antibody) was from Millipore. Antibodies against muscle-associated glycogen phosphorylase (Pygm) (#ab81901, rabbit polyclonal antibody) and Pdk4 (#214938, rabbit monoclonal antibody) were from Abcam (Cambridge, UK). Antibody against Gapdh (#sc-25778, rabbit polyclonal antibody) was obtained from Santa Cruz Biotechnology (Dallas, TX). The goat anti-rabbit HRP-conjugated secondary antibody #111-035-144 was from Jackson ImmunoResearch (Suffolk, UK). All chemicals used were of standard commercial high-purity quality.

Generation of the *Plin2* null mice

A BAC clone containing the *Plin2* genetic locus (AB2.2 ES cells, strain 129S7/SvEvBrd-Hprt^b-m2, clone #bMQ-28H12) was modified with recombineering to generate a floxed *Plin2* targeting vector. Because the *Plin2* protein is rapidly degraded in the absence of LD targeting (31), *LoxP* sites were inserted in intron 3 and intron 6 of the *Plin2* gene to flank exon sequences that are essential for targeting of the *Plin2* protein to LD surfaces. With this design, any potential truncated *Plin2* protein sequence translated from the genetically modified gene would be expected to untarget from LDs and be rapidly degraded. The specific details for generation of the targeting vector will be published elsewhere (Y.K.L., K.T.D., and A.R.K., unpublished observations). Standard homologous recombination in 129/SvJEv embryonic stem (ES) cells was used to target the *Plin2* gene. Resulting chimeric mice were bred with C57BL/6J mice (Jackson Laboratory, Bar Harbor, ME) for germline transmission. The resulting *Plin2* floxed line on a mixed B6.129/Sv background was subsequently crossed with mice expressing MMTV-Cre recombinase (Jackson Laboratory) to generate *Plin2* null mice (*Plin2*^{-/-}). The floxed *Plin2* mice were generated in compliance with the guidelines given by the Animal Care and Use Committee of the National Institutes of Health under a Division of Intramural Research, National Institute of Diabetes and Digestive and Kidney Diseases, under approved animal study protocol K039-LCDB.

Animal experiments

Plin2^{+/+} and *Plin2*^{-/-} mice were housed in a temperature-controlled (22°C) facility with a strict 12-h light/dark cycle. Male mice backcrossed for 10 generations into C57BL/6N (Janvier Labs, Le Genest-Saint-Isle, France) were given standard chow (#RM3-801190, SDS diets, consisting of 12% calories from fat, 27% from protein, and 61% from carbohydrate) until 12 weeks of age. Mice were euthanized by cervical dislocation at 8:00 to 10:00 AM, and tissues were snap-frozen in liquid nitrogen and stored at -80°C until further analysis. All animal use was approved and registered by the Norwegian Animal Research Authority (NARA, under animal study protocols FOTS IDs: #6305 and #6922) and conformed to the guidelines from Directive 2010/63/EU of the European Parliament on the protection of animals used for scientific purposes.

Isolation of satellite cells

Female siblings (14 weeks) backcrossed into C57BL/6N for six generations were used for primary satellite cell isolation from the hind leg containing musculus gastrocnemius and musculus soleus. Primary muscle satellite cells (myoblasts) were isolated and purified, as has been previously described (32). Briefly, the muscle

tissue was incubated with 2% collagenase II at 37°C for 90 min to enzymatically dissociate the cells. Satellite cells were liberated by further digestion with Blendzyme at 37°C for 30 min. To enrich myoblasts, we split the cell population in DPBS with no trypsin or EDTA. Further enrichment of myoblasts was obtained by preplating for 15 min on collagen-coated flasks. This tends to leave behind cells that stick quickly, which are predominantly fibroblasts. Fibroblasts tend to be very flat when grown on collagen, whereas myoblasts are more compact and smaller in diameter. In addition, the F-10-based primary myoblast growth medium gives myoblasts a growth advantage over fibroblasts. *Plin2*^{+/+} and *Plin2*^{-/-} myotube cultures were considered established when fibroblasts were no longer visible in the cultures.

Cell culture and stimulation of myotubes

Purified myoblasts were proliferated on standard plasticware coated with collagen (0.01%). To enhance myotube formation, Matrigel (diluted 1:50 in DMEM) was used as coating when myoblasts were seeded to differentiate into myotubes. Mouse myoblasts were grown to subconfluence in DMEM/Ham's F-10 (1:1, 5.5 mM glucose) supplemented with 20% FBS, 5 ng/ml basic fibroblast growth factor, 25 IU penicillin, 25 μ g/ml streptomycin, and 1.25 μ g/ml amphotericin B at 37°C in 5% CO₂. At ~80% confluence, growth medium was replaced by DMEM supplemented with 2% horse serum and antibiotics to induce fusion of myoblasts into multinucleated myotubes. Unless otherwise stated, cells differentiated for 4 days were used in experiments.

OA was bound to FA-free BSA with an OA:BSA ratio of 2.5:1 in all experiments (further referred to as OA). Control myotubes and OA-stimulated myotubes received the same concentration of BSA. The lipase inhibitors (Atglistatin and CAY10499) were solved in DMSO and diluted in medium to a final concentration of 0.1% DMSO. Control myotubes and lipase inhibitor-stimulated myotubes received the same concentration of DMSO.

To measure insulin response, we incubated myotubes differentiated for 3 days in medium containing OA (100 μ M) for 24 h. Myotubes were subsequently incubated with glucose-free DMEM medium for 2 h in the presence of OA (100 μ M), followed by 15-min incubation in DMEM (5.5 mM glucose) in the presence or absence of insulin (100 nM). Myotubes from two wells (six-well plate) were pooled in RIPA buffer, supplemented with Complete Protease Inhibitor cocktail, and stored at -80°C until further analysis. Protein content in cell extracts was measured by PierceTM BCA protein assay kit.

Immunoblotting

Cell extracts were sonicated briefly, as has been described previously (33). Proteins (15 μ g) were mixed with Laemmli buffer and separated on a 4%–20% Criterion or Mini-Protean[®] TGXTM gels, followed by blotting to nitrocellulose or PVDF membranes. Membranes were immunoblotted with the following antibodies: rabbit anti-mouse *Plin2* [(31); #N510; 3 μ g/ml], rabbit anti-mouse *Plin3* [(34); 10 μ g/ml], rabbit anti-mouse *Plin4* and rabbit anti-mouse *Plin5* [(33); 10 μ g/ml], rabbit anti-human glucose transporter 1 (Slc2a1/Glut1, 1:1,000), rabbit anti-human pyruvate kinase (Pkm, 1:1,000), rabbit anti-human Pygm (1:1,000), rabbit anti-mouse pyruvate dehydrogenase kinase 4 (Pdk4, 1:1,000), rabbit anti-human muscle pyruvate dehydrogenase α 1 (Pdha1, 1:1,000), rabbit anti-human phosphorylated muscle pyruvate dehydrogenase α 1 (Pdha1-p300, 1:1,000), total Akt kinase (detects isoforms Akt1-3, 1:1,000), Ser473-phosphorylated Akt (1:1,000), GAPDH (Gapdh, 1:500), and β -actin (1:1,000), followed by HRP-labeled secondary antibodies (~1:10,000). Immunoreactive bands were detected with ClarityTM Western ECL Substrate, visualized with ECL using Chemidoc XRS (Bio-Rad), and quantified with

Image Lab software (version 4.0). The β -actin signal was used to normalize for protein loading.

Preparation and analysis of RNA

Cells were lysed in Nucleic Acid Purification Lysis Solution:PBS (1:1) and frozen at -80°C before isolation. Total RNA from cell extracts was isolated on a ABI 6100 Nucleic Acid Prep-Station with the preprogrammed "RNA-Cell method." RNA quality and quantity were determined with NanoDrop ND-1000 Spectrophotometer (Thermo Fisher Scientific, Waltham, MA). Reverse transcription quantitative real-time PCR (RT-qPCR) was performed in two steps. First, total RNA (20 ng/ μl) was reverse-transcribed into single-stranded complementary DNA with random hexamers and Superscript III RT (50°C for 60 min and 72°C for 15 min). Next, gene-specific regions (70–120 bp) were amplified from complementary DNA (10 ng) with assay primers (100 nM each) and KAPA SYBR Fast Master Mix (10- μl reaction, 95°C for 3 min, followed by 40 cycles; 95°C for 10 s and 60°C for 20 s) on the ABI 7900HT instrument (Applied Biosystems, Thermo Fisher Scientific, Waltham, MA). Assay primers ($T_m = 60$) were designed with Primer-BLAST software (35). All assay primer pairs were designed to bind to adjacent exons spanned by a large intron with amplicon sizes ranging from 70 to 110 nt. Primers used are listed in **Table 1**. Data were analyzed with relative quantification ($\Delta\Delta\text{C}_q$ method). Results are presented as gene expression in relation to endogenous control ($2^{-\Delta\Delta\text{C}_q}$). TATA-box binding protein (*Tbp*) mRNA was verified to not differ in expression among groups or treatments and was used as endogenous control in all experiments.

Microscopy

Myoblasts seeded on Matrigel-coated six-well glass-bottom dishes were differentiated into myotubes for 3 days before switching to media supplemented with OA (100 μM) for 24 h. For live imaging, LDs were stained by incubating myotubes with Bodipy 493/503 (2 $\mu\text{g}/\text{ml}$) for 10 min, followed by nuclei staining with Hoechst 33258 (2.5 $\mu\text{g}/\text{ml}$) for 15 min. Live images were randomly taken in 25 positions per well with a $\times 20$ objective on an

Olympus IX81 inverted fluorescence Scan[^]R platform (Olympus Corporation, Tokyo, Japan), as has been previously described (36). After gating out aggregates and dead cells, each parameter was determined from an average 150 images per donor group (average of 96 ± 25 nuclei per image). For confocal pictures, myotubes were fixated for 1 h with 4% PFA in 100 mM of phosphate buffer (pH 7.4), washed and stained with Bodipy 493/503 (1 μM) and Hoechst 33342 (5 μM) for 20 min. Pictures were taken with a $\times 40$ objective on a LSM 710 confocal microscope (Zeiss, Oberkochen, Germany).

FA accumulation and lipolysis assay

Accumulation (real-time uptake) and lipolysis (efflux) of FA were measured with scintillation proximity assay, as has been previously described (37). In this method, the radiolabeled substrates taken up will accumulate in the adherent cells and become concentrated close to the scintillator embedded in the plastic bottom of each well and provide a stronger radioactive signal than would the radiolabel dissolved in the medium alone. Cells were seeded and differentiated for 3 days in 96-well Scintiplate[®] coated with Matrigel. To determine OA uptake and accumulation, we gave myotubes fresh medium comprising DMEM without phenol red, supplemented with [^{14}C]OA (0.5 $\mu\text{Ci}/\text{ml}$) and unlabeled OA (final OA concentration 100 or 400 μM) in the presence of DMSO (0.1%) or the ATGL inhibitor Atglitatin [10 μM (38)]. Lipid accumulation was monitored regularly for the next 24 h on a 2450 MicroBeta² scintillation counter (PerkinElmer, Shelton, CT). Thereafter, to measure FA efflux (lipolysis), the labeled myotubes were washed twice with PBS containing 0.5% BSA before the myotubes were incubated in DPBS supplemented with 10 mM HEPES, 0.5% BSA, and 100 μM glucose. The decline in accumulated [^{14}C]OA was measured at 0, 2, 4, and 6 h.

Glucose and FA substrate oxidation assays

Cells were seeded and differentiated in 96-well plates coated with Matrigel solution and subjected to substrate oxidation assay, as has been described previously (37). To measure FA oxidation

TABLE 1. Primers used for RT-qPCR in this study

Gene	Forward Primer	Reverse Primer	Amplicon Size
<i>Acadl</i>	CGGAAGCTGCATAAGATGGGA	AGCTGGCAATCGGACATCTT	75
<i>Acadm</i>	TGGATTCATTGTGGAAAGCCGA	CCTCTGGTGTGAGAGCATCG	87
<i>Acadvl</i>	GCATTTGGCCTGCAAGTACC	AATCTCTGCCAAGCGAGCAT	78
<i>Acox1</i>	AATCTGGAGATCACGGGCACTT	GTCTTGGGGTCATATGTGGCAG	95
<i>Cd36</i>	AGGCATTCTCATGCCAGTCC	TGTACACAGTGGTGCCTGTT	119
<i>Cpt2</i>	TATGATGGCTGAGTGTCTCAA	CCGTAGAGCAAACAAGTGTCC	91
<i>Fabp3</i>	GGACAGCAAGAAATTTGATGACTAC	TTGGTCATGCTAGCCACCTG	78
<i>Gys1</i>	TTGGGGTCTTCCCCTCCTAC	GTGGAGATGCTGGGGATGC	82
<i>Hkl1</i>	GGACCACAGTTGGCGTAGA	CTCAGGGTCTGTGGAACCG	76
<i>Hkl2</i>	CTTCCCTTGGCCAGCAGAACA	TGACCACATCTTCAACCCTCG	95
<i>Pdha1</i>	CGTGGTTTCTGTCACCTTGTGTG	CGTAGGGTTTATGCCAGCCT	72
<i>Pdk4</i>	AAGATGCTCTGCGACCAAGTA	CAATGTGGATTGGTTGGCCTG	91
<i>Pkm</i>	GAAACAGCCAAAGGGGACTAC	CACAAGCTCTTCAAACAGCAGAC	108
<i>Plin2 (exon4-5)</i>	GGGCTAGACAGGATGGAGGA	CACATCCTTTCGCCCCAGTTA	99
<i>Plin2 (exon7-8)</i>	GTGGAAAGAGAAGCATCGGCT	GGCGATAGCCAGAGTACGTTG	82
<i>Plin3</i>	CGAAGCTCAAGCTGCTATGG	TCACCATCCCATACTGGAAC	98
<i>Plin4</i>	ACCAACTCACAGATGGCAGG	AGGCATCTTCACTGCTGGTC	109
<i>Plin5</i>	GGTGAAGACACCACCCTAGC	CCAGCACTGGATTACCACA	115
<i>Ppara</i>	ACTACGGAGTTCACGCATGT	GTCCGTACACCAGCTTCAGCC	74
<i>Pparg</i>	TTGCTGTGGGATGTCTCAC	AACAGCTTCTCCTTCTCGGC	70
<i>Ppard</i>	ACATGGAATGTCGGGTGTGC	CGAGCTTCATGCGGATTGTC	108
<i>Ppargc1a</i>	AGTCCCATACACAACCGCAG	CCCTTGGGGTCAITTTGGTGA	94
<i>Pygm</i>	GAGTGGAGGACGTGGAAAGG	CCGAAGCTCAGGAATTCCGCT	77
<i>Slc2a1</i>	CTCGGATCACTGCAGTTCGG	CGTAGCCGTGGTTCCATGTT	97
<i>Slc2a4</i>	CGACGGACACTGCATCTGTT	ACATAGCTCATGGCTGGAACC	104
<i>Tbp</i>	AGCCTTCCACCTTATGCTCAG	GCCGTAAAGGCATATTGGACT	90
<i>Ucp2</i>	TTGGCCTTACGACTCTGTCA	CAGGGCACCTGTGGTGTCA	98
<i>Ucp3</i>	CTACAGAACCATCGCCAGGGA	GTCCGTAGGTACCATCTCAGCA	109

from prelabeled intracellular lipid pools, we incubated myotubes with [^{14}C]OA (0.5 $\mu\text{Ci}/\text{ml}$) and unlabeled OA (final OA concentration, 100 or 400 μM) for 24 h, combined with various treatments (0.1% DMSO, 10 μM CAY10499 or 10 μM Atglistatin). Myotubes were then washed twice with PBS containing 0.5% BSA and given DPBS media supplemented with 10 mM HEPES, 10 μM BSA, and 1 mM L-carnitine to capture CO_2 . To measure glucose oxidation, we gave myotubes D- ^{14}C (U)glucose (0.58 $\mu\text{Ci}/\text{ml}$) and unlabeled glucose (final glucose concentration 200 μM) directly in the CO_2 -capturing media (DPBS supplemented with 10 mM HEPES, 10 μM BSA, and 1 mM L-carnitine). A 96-well UniFilter[®] microplate, activated for capture of CO_2 by the addition of 1 M NaOH, was subsequently mounted on top of the 96-well plate, and the sandwich was incubated at 37°C for 4 h. [^{14}C] CO_2 captured in the filter was counted by liquid scintillation on a 2450 MicroBeta² scintillation counter (PerkinElmer, Shelton, CT) as a measure of produced CO_2 . After CO_2 capturing, myotubes were washed with PBS and lysed with 0.1 M NaOH before cell-associated radioactivity (accumulated substrate) was determined by liquid scintillation. Acid-soluble metabolites (ASMs) in the media were measured, as has been previously described (36). ASMs consist of β -oxidation and tricarboxylic acid cycle metabolites and reflect incomplete FA or glucose oxidation in the mitochondria.

Lipid droplet isolation

Cells from six 10-cm petri dishes were stimulated with 200 μM of OA for 24 h, washed twice with cold PBS, harvested in suspension buffer (25 mM tricine pH 7.8, 8.6% sucrose, and Complete Protease Inhibitor cocktail), mixed gently, and frozen at -80°C . To disrupt cells, samples were thawed slowly in ice-water slurry for ~ 30 min and transferred to a precooled N_2 cell-disruption vessel (#4639, Parr Instrument Co., Moline, IL). Samples were exposed to 600 psi N_2 for 20 min, then released slowly (dropwise) into a 15-ml tube. The disrupted cell lysate was subsequently centrifuged for 10 min at 3,000 g at 4°C to remove nuclei and undisrupted cell debris. The suspension containing LDs was adjusted to 2 ml and transferred to the bottom of an ultracentrifugation tube, followed by a second layer consisting of 1.8 ml of wash buffer (20 mM HEPES pH 7.4, 100 mM KCl, 2 mM MgCl_2 , and 4% sucrose [w/v]), and a top layer of 0.4 ml of collection buffer (20 mM HEPES pH 7.4, 100 mM KCl, and 2 mM MgCl_2). Tubes were balanced and centrifuged for 60 min in a SW60Ti rotor at 200,000 g at 4°C in a XL-90 Ultracentrifuge (Beckman Coulter Inc.). The top layer (~ 0.4 ml) was isolated with a tube slicer prior to the collection of floating LDs.

Lipid composition of isolated LDs

Isolated LDs were mixed with $\times 2$ volume of chloroform:heptane:methanol (4:3:2, v/v/v) and lipids extracted by thoroughly mixing for 1–2 min prior to centrifugation for 5 min at 2,000 g. The lower organic phase was carefully transferred into a glass tube and evaporated under N_2 before lipids were dissolved in chloroform:methanol (2:1, v/v). TAG content in samples was determined with TG PAP 150 kit, adjusted to 250 ng TAG/ μl , and stored at -20°C under argon. The TLC plate was fully developed in methanol:ethyl acetate (6:4, v/v) to remove impurities, then dried for 6–8 min at 40°C. Lipid samples (1 μg TAG) and lipid standard mix (equal weights of TAG, DAG, MAG, PL, FFA, CE, and free cholesterol) were spotted on the plate and air-dried briefly, and the plate was developed in heptane:diethyl ether:acetic acid (55:45:1, v/v/v). The plate was subsequently dried for 10 min at 40°C and developed with copper sulfate staining (39) by exposing the plate to a developing reagent consisting of 10% $\text{CuSO}_4 \times 5\text{H}_2\text{O}$ (w/v) and 8% H_3PO_4 in H_2O (v/v) for ~ 40 s. Excess solution was removed by decanting, and the back of the plate was cleaned with tissue paper.

The plate was subsequently air-dried briefly, placed on a heating plate for 10 min at 60°C, and then for 10 min at 150°C. After being cooled down, the plate was scanned with an Epson Perfection V700 image scanner (Seiko Epson Corporation, Nagano, Japan).

Lipid distribution in cells

Myotubes were incubated with [^{14}C]OA (0.5 $\mu\text{Ci}/\text{ml}$) and unlabeled OA (final OA concentration 100 or 400 μM) for 24 h. The myotubes were washed twice with PBS and harvested with two additions of 125 μl dH_2O . Cellular lipid distribution was analyzed as has been previously described (40). Briefly, homogenized cell fractions were extracted, lipids were separated by TLC with hexane:diethyl ether:acetic acid (65:35:1, v/v/v) as developing solvent, and radioactivity in excised bands was quantified by liquid scintillation (Packard TriCarb 1600, PerkinElmer, Shelton, CT).

Triacylglycerol measurements

Myotubes were incubated with OA alone (100 μM) or in the presence of Atglistatin (10 μM) for 24 h. Thereafter, the myotubes were washed with PBS and harvested in PBS or RIPA buffer (50 mM Tris-HCl pH 7.4, 150 mM NaCl, 1% NP-40, 0.5% sodium deoxycholate, 0.1% SDS, and 2 mM EDTA). Measurement of cellular TAG was performed with the TG PAP 150 kit according to the supplier's protocol.

Glycogen synthesis

Myotubes were incubated in DMEM without glucose, supplemented with D- ^{14}C (U)glucose (0.5 $\mu\text{Ci}/\text{ml}$), unlabeled glucose (final glucose concentration 1 mM), pyruvate (1 mM), and BSA (10 μM) in the presence or absence of insulin (100 nM) for 3 h to measure glycogen synthesis. The myotubes were washed twice with PBS and harvested in KOH (1 M). After protein measurements, glycogen (final concentration 20 mg/ml) and more KOH (final concentration 4 M) were added to the samples. Thereafter, D- ^{14}C (U)glucose incorporated into glycogen was measured as has been previously described (36).

Statistical methods

Values are presented as means \pm SEM unless stated otherwise. The value n represents the number of experiments performed with at least duplicate samples. Two-tailed unpaired t tests were performed to determine the difference between groups ($Plin2^{+/+}$ and $Plin2^{-/-}$) with GraphPad Prism 5.0 Software (GraphPad Software Inc., San Diego, CA), whereas two-tailed paired t tests were performed to determine effects of treatments. Linear mixed-model analysis (SPSS 20.0.0.1, IBM SPSS Inc., Chicago, IL) was used to compare $Plin2^{+/+}$ and $Plin2^{-/-}$ myotubes in the time-course FA accumulation and lipolysis experiments (scintillation proximity assay). $P < 0.05$ was considered statistically significant.

RESULTS

Establishment of myotube cultures lacking Plin2

To investigate the functional role of Plin2 in myotubes, we first generated mice with homozygous disruption of the *Plin2* gene by deleting exons 4, 5, and 6 that are essential for functional targeting of Plin2 to LD surfaces. A thorough phenotypic characterization of $Plin2^{-/-}$ mice will be published elsewhere (Y.K.L., K.T.D., and A.R.K., unpublished observations). Hind legs from female $Plin2^{+/+}$ and $Plin2^{-/-}$ littermates, backcrossed into C57BL/6N for six generations, were used to isolate primary muscle satellite cells and establish $Plin2^{+/+}$ and $Plin2^{-/-}$ myoblast cultures. The $Plin2^{+/+}$

and *Plin2*^{-/-} myoblast populations differentiated equally well into myotubes on the basis of the presence of multinuclear fiber-like cells, observed by microscopic inspection (Fig. 1A) and by the comparable reduction in mRNA expression of the nonmyotube satellite cell marker paired box 7 (*Pax7*) (Fig. 1B). The structural *Plin2* gene differences in the *Plin2*^{+/+} and *Plin2*^{-/-} myotubes were validated by RT-qPCR. Primers that recognize sequences within deleted exons 4 to 5 failed to amplify mRNA target sequences from *Plin2*^{-/-} myotubes (Fig. 1C), confirming that these myotubes lack functional full-length *Plin2* mRNA. Primers amplifying across the retained exon 7 to 8 junction showed lower expression of the truncated *Plin2*^{-/-} mRNA (~15%) compared with wild-type *Plin2* mRNA (Fig. 1C). We next determined whether ablation of *Plin2* was compensated for by increased expression of other *Plin* genes in myotubes. *Plin3* mRNA expression was slightly (~40%) reduced, *Plin4*

mRNA was unchanged, whereas *Plin5* mRNA expression was increased (~5-fold) in *Plin2*^{-/-} compared with *Plin2*^{+/+} myotubes (Fig. 1D). Judged by mRNA levels in relation to *Tbp*, *Plin4* and *Plin5* mRNAs in the cultured myotubes were considerably lower (<1%) than *Plin2* and *Plin3* mRNAs in cultured wild-type myotubes.

Next, we analyzed Plin protein content. Plin2 immunosignals with an expected molecular mass of ~50 kDa were observed in *Plin2*^{+/+} myoblasts and myotubes (Fig. 1E), whereas the signal was absent in *Plin2*^{-/-} myotubes, which confirms correct genetic ablation of the *Plin2* gene. We observed a significant decline in Plin2 protein levels when *Plin2*^{+/+} myoblasts were differentiated into myotubes, whereas Plin3 protein content was essentially unchanged by differentiation, regardless of genotype (Fig. 1E). Less distinct protein bands were observed for the very weakly transcribed Plin4 and Plin5 (results not shown). Hence,

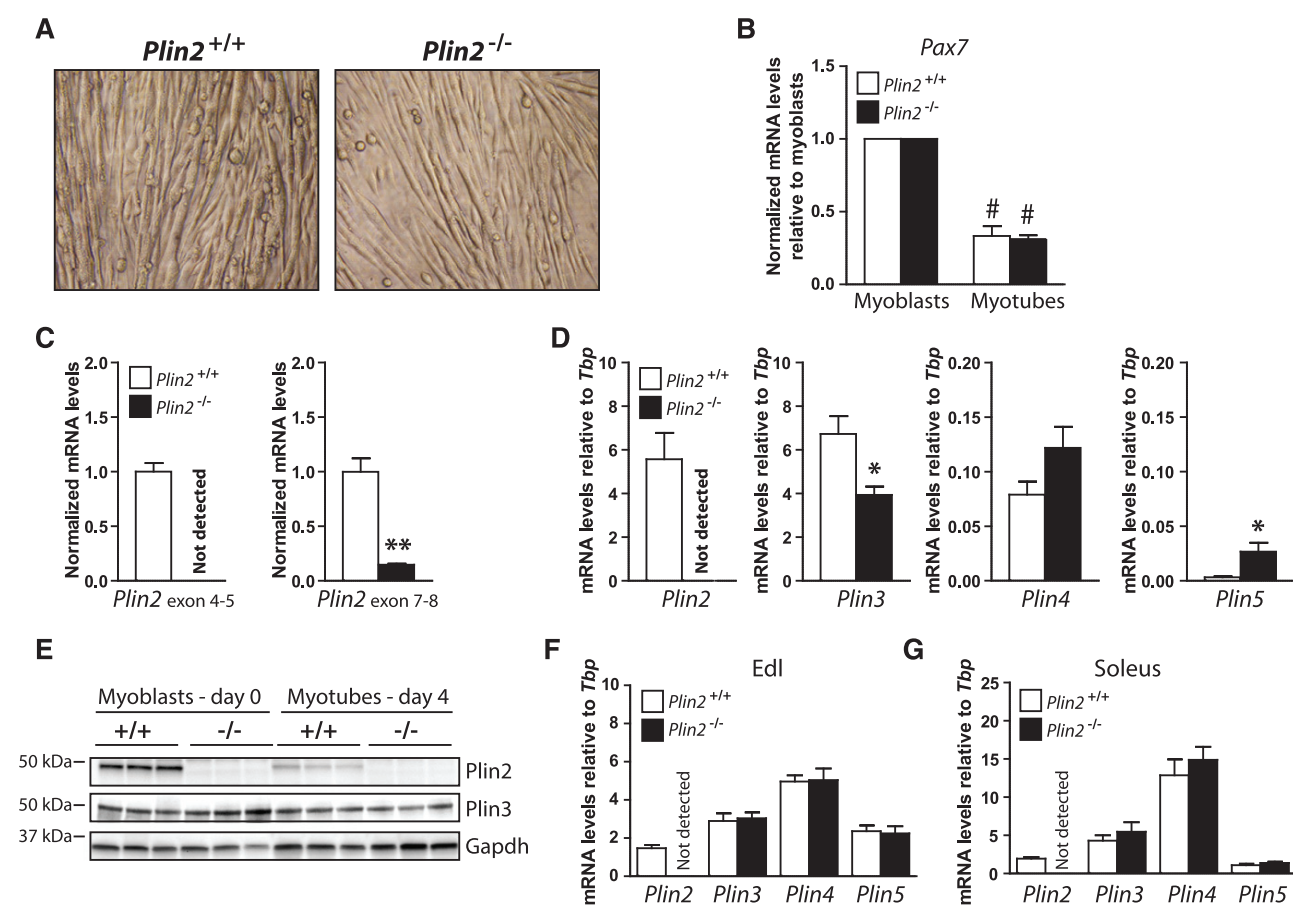


Fig. 1. Expression of Plins in muscle and established *Plin2*^{+/+} and *Plin2*^{-/-} myotubes and myoblasts. Primary muscle satellite cells (myoblasts) were isolated from the hind leg of *Plin2*^{+/+} and *Plin2*^{-/-} mice. A: Established *Plin2*^{+/+} and *Plin2*^{-/-} myoblast cultures differentiated equally well into multinucleated myotubes. B: Expression of *Pax7* mRNA in relation to the expression of TATA-box binding protein (*Tbp*) determined by RT-qPCR. The results are presented normalized to the expression levels in undifferentiated myoblasts. C: RT-qPCR with primers amplifying across the *Plin2* exon 4–5 junction and the *Plin2* exon 7–8 junction in relation to the expression of *Tbp* and normalized to the expression levels in *Plin2*^{+/+} myotubes, confirmed the absence of exon 4–6 *Plin2* mRNA sequences in *Plin2*^{-/-} myotubes. D: Expression of *Plin2*, *Plin3*, *Plin4*, and *Plin5* mRNAs determined by RT-qPCR in relation to the expression of *Tbp*. Results in B–D are presented as means ± SEM (n = 3–6, *P < 0.05 and **P < 0.01 vs. *Plin2*^{+/+} myotubes, #P < 0.05 vs. myoblasts). E: Expression of Plin2 and Plin3 proteins in myoblasts (day 0) and differentiated myotubes (day 4). The membrane contains samples from three independent experiments (n = 3). F: Relative mRNA expression of *Plin2*, *Plin3*, *Plin4*, and *Plin5* in extensor digitorum longus of chow-fed 12-week-old *Plin2*^{+/+} and *Plin2*^{-/-} male mice. G: Relative mRNA expression of *Plin2*, *Plin3*, *Plin4*, and *Plin5* in soleus. Gene expression levels in F and G were determined by RT-qPCR and are presented in relation to the expression of *Tbp* as means ± SEM (n = 9 in each group). Edl, extensor digitorum longus; Pax7, paired box 7.

the lack of Plin2 in cultured *Plin2*^{-/-} myotubes was not compensated for by elevated mRNA expression or accumulation of other Plin proteins.

We also examined mRNA levels of *Plins* in extensor digitorum longus and soleus muscle fibers dissected from chow-fed *Plin2*^{+/+} and *Plin2*^{-/-} mice. Disruption of *Plin2* did not alter expression of other *Plin* mRNAs (Fig. 1F, G). Furthermore, *Plin2* and *Plin3* mRNA levels were similar in myotubes and the two muscle fibers, whereas the expression of *Plin4* and *Plin5* mRNAs was more elevated in the muscle fibers than in the cultured myotubes. Thus, the *Plin2*^{+/+} and *Plin2*^{-/-} myotube cultures represent an important parallel model to analyze Plin2 function for muscle metabolism, allowing for defined biochemical benchmarkings that are not readily accessible in situ.

Reduced accumulation of lipids in the absence of Plin2

OA is easily taken up by cells and esterified into TAG that is incorporated into LDs, and thus, incubation with OA is an efficient strategy to promote LD formation and monitor relative intracellular lipid storage. *Plin2*^{+/+} myotubes cultured with 100 μ M OA for 24 h increased Plin2 mRNA and protein content considerably compared with cells cultured with BSA (Fig. 2A, B) but had no effect on mRNA (results not shown) and protein expression of Plin3 (Fig. 2B). To determine whether removal of a functional Plin2 in myotubes affected the ability to store lipids, we incubated

Plin2^{+/+} and *Plin2*^{-/-} myotubes with 100 μ M OA for 24 h before LDs were stained with Bodipy 493/503 (green) and nuclei stained with Hoechst 33258 (blue). A marked reduction in accumulated LDs was observed in *Plin2*^{-/-} compared with *Plin2*^{+/+} myotubes (Fig. 2C). There were fewer quantified LDs per nucleus, observed under a $\times 20$ objective, in *Plin2*^{-/-} than in *Plin2*^{+/+} myotubes (Fig. 2D). Because smaller LDs are not necessarily labeled and recognized with automatic quantification, we also determined lipid distribution after incubation with [¹⁴C]OA for 24 h. *Plin2*^{-/-} myotubes incorporated less OA into TAG (Fig. 2E) and DAG (Fig. 2F) and contained lower levels of FFAs (Fig. 2G) than did *Plin2*^{+/+} myotubes. Incorporation into phospholipids (Fig. 2H) and cholesteryl esters (results not shown) was unaffected by removal of *Plin2*. These observations demonstrate that *Plin2*^{-/-} myotubes exposed to FAs store reduced levels of LDs compared with *Plin2*^{+/+} myotubes.

Absence of Plin2 reduced accumulation of lipids by increasing lipolysis

To mechanistically determine why myotubes lacking Plin2 accumulated less TAG-containing LDs, we followed OA accumulation in the myotubes for 24 h. During the first ~ 4 h, *Plin2*^{+/+} and *Plin2*^{-/-} myotubes accumulated similar levels of [¹⁴C]OA, but total accumulation after 24 h was lower in *Plin2*^{-/-} myotubes incubated with 100 μ M OA (Fig. 3A, $P < 0.05$) or 400 μ M OA (Fig. 3B, $P = 0.06$) than in *Plin2*^{+/+}

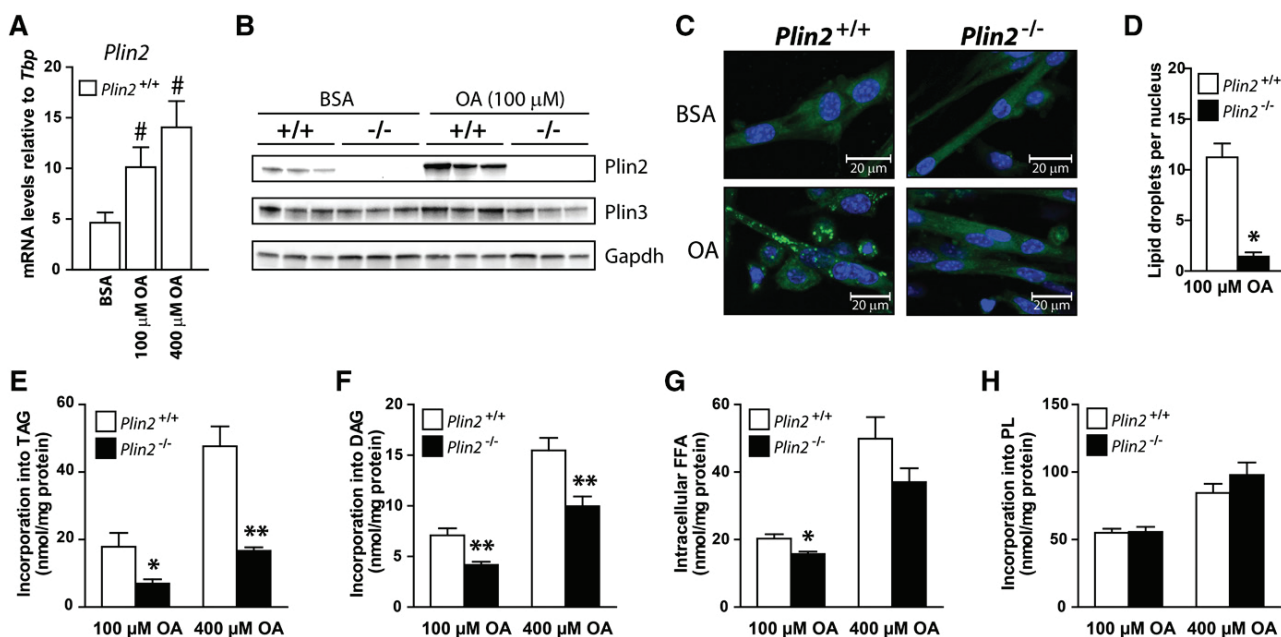


Fig. 2. Lipid storage and distribution in *Plin2*^{+/+} and *Plin2*^{-/-} myotubes. A–D: Myotubes were incubated for 24 h with BSA (40 μ M) or OA (100 or 400 μ M OA). A: Relative expression of *Plin2* mRNA determined by RT-qPCR normalized to the expression of TATA-box binding protein (*Tbp*). Results are presented as means \pm SEM ($n = 3$, # $P < 0.05$ vs. BSA). B: Expression of Plin2 and Plin3 proteins in myotubes. C: Lipid droplets (LDs) in *Plin2*^{+/+} and *Plin2*^{-/-} myotubes were labeled with fluorescent dyes sequestering in neutral LDs (Bodipy 493/503, green) or nuclei (Hoechst 33342, blue). Representative confocal images are presented ($\times 40$ objective; inserted bars are 20 μ m). D: Another set of images were acquired with a $\times 20$ objective with an Olympus IX81 fluorescence microscope. Images were analyzed by Scan^R analytical software by comparing the number of stained LDs in relation to the number of nuclei per image, with an average total of 150 images per parameter. Results are presented as means \pm SEM ($n = 3$, * $P < 0.05$ vs. *Plin2*^{+/+}). E–H: Myotubes were preincubated for 24 h with [¹⁴C]OA to label accumulated lipids. The content of radiolabeled TAG (E), DAG (F), FFA (G), and PL (H) in myotubes was determined by TLC and related to cellular protein content. The results are presented as means \pm SEM ($n = 6$, * $P < 0.05$, ** $P < 0.01$ vs. *Plin2*^{+/+}).

myotubes. In contrast, coincubation with Atglistatin (38), a reversible inhibitor of ATGL that catalyzes the first and rate-limiting step in lipolysis of TAG, increased accumulation of OA in *Plin2*^{-/-} myotubes, in a manner similar to that of *Plin2*^{+/+} myotubes (Fig. 3C, D). Coincubation with Atglistatin increased cell-associated [¹⁴C]OA in *Plin2*^{-/-} myotubes compared with DMSO with a more pronounced effect, with higher OA concentration (Fig. 3E). Myotubes cultured in 100 μM OA coincubated with the ATGL and HSL inhibitor CAY10499 (41, 42) alone or in combination with Atglistatin increased cell-associated [¹⁴C]OA only in *Plin2*^{-/-} myotubes (Fig. 3F). These results suggest that there were constantly higher ATGL and HSL lipolytic activities in *Plin2*^{-/-} myotubes than in *Plin2*^{+/+} myotubes.

Lipolytic rates are difficult to normalize between two cell populations with differences in LD content. To overcome this, we utilized our established culture conditions using Atglistatin to minimize TAG differences between the *Plin2*^{+/+} and *Plin2*^{-/-} myotubes. Whereas *Plin2*^{-/-} myotubes cultured with 100 μM OA alone accumulated less TAG than did *Plin2*^{+/+} myotubes (Fig. 4A), a combination of OA and Atglistatin resulted in TAG levels (Fig. 4A) and LD content (Fig. 4B) in *Plin2*^{-/-} myotubes that were similar to those in *Plin2*^{+/+} myotubes. These latter *Plin2*^{+/+} and *Plin2*^{-/-} myotubes were

then washed to remove the exogenous OA and Atglistatin before measurement of lipolysis. Lipolysis, measured as a loss of [¹⁴C]OA accumulated in the myotubes, was consistently overall higher in *Plin2*^{-/-} myotubes than in *Plin2*^{+/+} myotubes (Fig. 4C, D). To compare the lipid composition of the stored LDs, we stimulated *Plin2*^{+/+} and *Plin2*^{-/-} myotubes with 200 μM OA alone or coincubated with Atglistatin for 24 h prior to LD isolation. LD preparations containing the same amount of TAG (1 μg) were subsequently separated with TLC, and various lipid species were identified with copper sulfate staining. LDs isolated from OA-stimulated *Plin2*^{-/-} myotubes stained stronger for lipolytic degradation products such as DAG, MAG, and FFA than did those from *Plin2*^{+/+} myotubes (Fig. 4E, F), whereas inhibition of lipolysis by coincubation with Atglistatin lowered the relative staining (Fig. 4F). These differences further supported the notion that disruption of *Plin2* in cultured myotubes resulted in LDs prone to lipolytic attack.

Absence of *Plin2* increased FA oxidation

An important biological role for cytosolic LDs is to store energy-rich FAs that may be mobilized for energy production when needed. We were interested to determine whether the reduced LD stores in myotubes affected FA oxidation

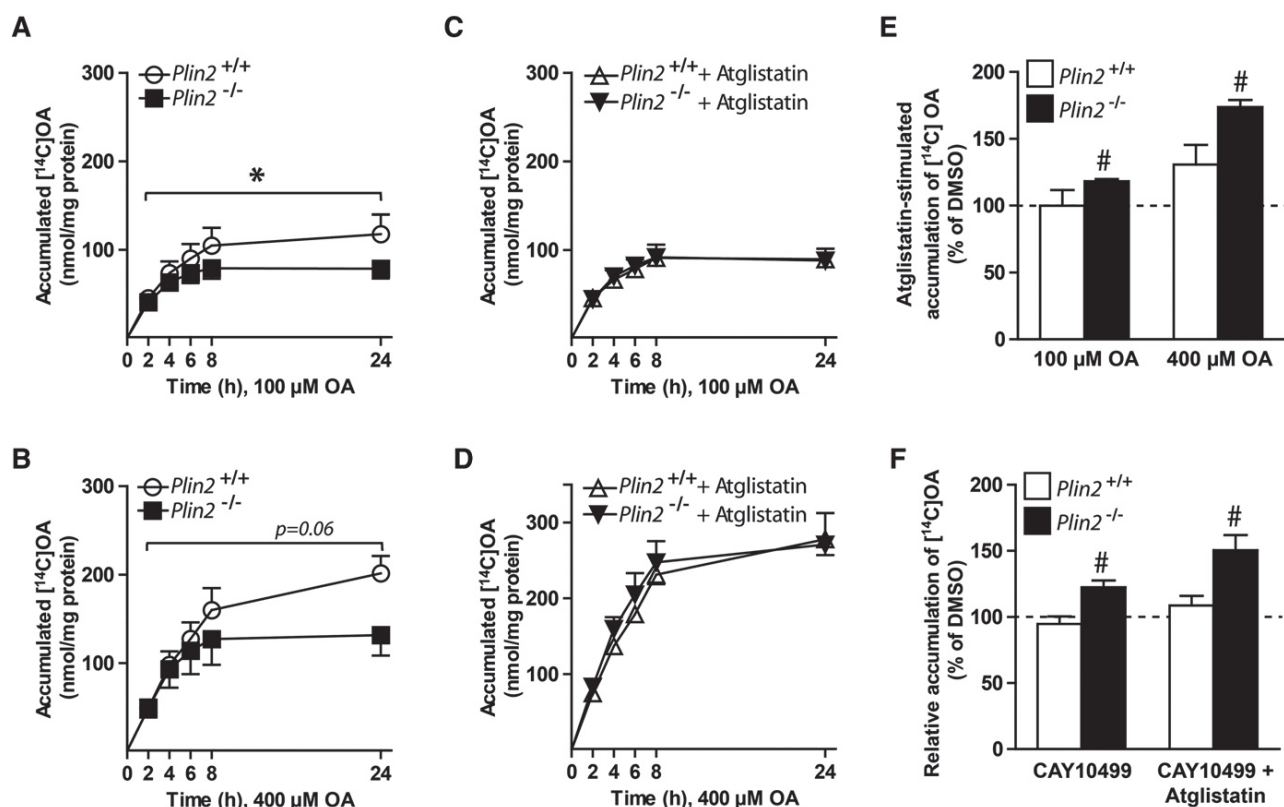


Fig. 3. Accumulation of oleic acid in *Plin2*^{+/+} and *Plin2*^{-/-} myotubes. Myotubes were incubated with [¹⁴C]OA (100 or 400 μM) and accumulation over 24 h was determined with scintillation proximity assay. Accumulation was determined in presence of DMSO (0.1%) (A, B) or in presence of the adipose triglyceride lipase inhibitor (Atglistatin, 10 μM) (C, D). The results are presented as means ± SEM (n = 3, *P < 0.05 vs. *Plin2*^{+/+} across all points in time). E: The effect of Atglistatin on accumulation of [¹⁴C]OA assessed as an average of all time points from A–D. F: Cell-associated [¹⁴C]OA after 24 h incubation with 100 μM OA in presence of the lipase inhibitor (CAY10499, 10 μM) or CAY10499 combined with Atglistatin (10 μM). For E and F, the results are presented as means ± SEM normalized to DMSO treated *Plin2*^{+/+} myotubes (n = 3, #P < 0.05 vs. DMSO).

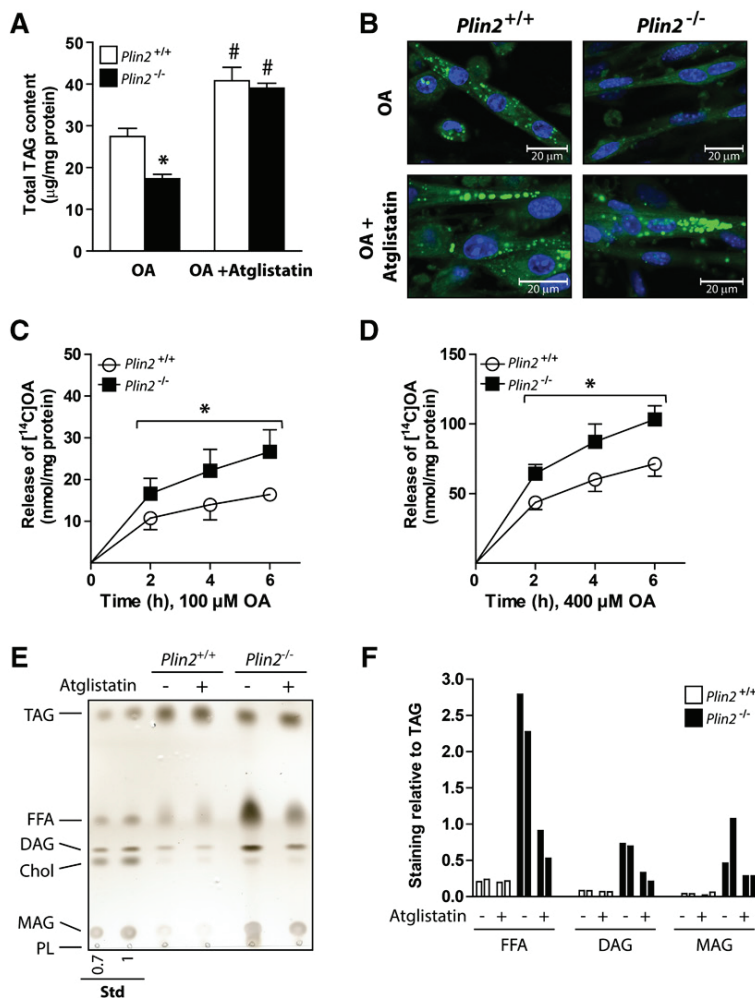


Fig. 4. Lipolysis in OA-loaded *Plin2*^{+/+} and *Plin2*^{-/-} myotubes. Myotubes were incubated for 24 h with OA (100 µM) alone (0.1% DMSO) or in the presence of the adipose triglyceride lipase inhibitor Atglistatin (10 µM). A: Total triacylglycerol (TAG) content in *Plin2*^{+/+} and *Plin2*^{-/-} myotubes. The results are presented as means ± SEM (n = 3, *P < 0.05 vs. *Plin2*^{+/+}, #P < 0.05 vs. OA). B: Confocal pictures of *Plin2*^{+/+} and *Plin2*^{-/-} myotubes. Fixed myotubes were labeled with fluorescent dyes sequestering in neutral lipid droplets (Bodipy 493/503, green) or in nuclei (Hoechst 33342, blue). C, D: Lipolysis (efflux) of OA after 24 h accumulation with [¹⁴C]OA (100 or 400 µM) in the presence of Atglistatin (10 µM). The results are presented as the release of accumulated [¹⁴C]OA to the medium at the various time points given as means ± SEM (n = 3–7, *P < 0.05 vs. *Plin2*^{+/+} across all time points). E: Cells were incubated with OA (200 µM) alone or in combination with Atglistatin (10 µM) for 24 h prior to isolation of lipid droplets and separation of lipid species with TLC. One representative of two independent experiments is shown. F: Staining intensities for the various bands in relation to the TAG signal (n = 2). Chol, cholesterol; Std, standard.

and thus incubated *Plin2*^{+/+} and *Plin2*^{-/-} myotubes with [¹⁴C]OA for 24 h before CO₂ production was captured over 4 h. Although cell-associated OA was lower in *Plin2*^{-/-} myotubes than in *Plin2*^{+/+} myotubes (Fig. 5A), CO₂ produced through oxidation of the stored intracellular lipids was higher in *Plin2*^{-/-} than in *Plin2*^{+/+} myotubes when preincubated with 100 µM OA alone or in combination with the lipolysis inhibitor CAY10499 (Fig. 5B). Clearly, a large fraction of the produced CO₂ originated from intracellular LDs in both *Plin2*^{+/+} and *Plin2*^{-/-} myotubes, because CO₂ production was drastically decreased in the presence of CAY10499. Similar results for increased CO₂ production (i.e., FA oxidation) in *Plin2*^{-/-} myotubes were obtained when cultures were preincubated with 400 µM OA (results not shown). Intermediary OA β-oxidation, measured as ASMs released from the myotubes into the cell media for 4 h, was also higher in *Plin2*^{-/-} than in *Plin2*^{+/+} myotubes, regardless of treatment (Fig. 5C). ASMs were similarly decreased in the two myotube populations in the presence of the lipase inhibitors CAY10499 and Atglistatin (Fig. 5C).

Absence of *Plin2* in myotubes decreased both cell-associated glucose and glucose oxidation

Muscle contraction derives energy from stored glucose as glycogen and FA as TAG. Therefore, elevated FA oxidation

in the absence of *Plin2*^{-/-} may be coordinated with altered glucose metabolism. To measure glucose oxidation, we preincubated *Plin2*^{+/+} and *Plin2*^{-/-} myotubes with BSA (40 µM) or OA (100 µM) for 24 h before CO₂ production from D-[¹⁴C(U)]glucose was captured over 4 h. Cell-associated glucose was lower in *Plin2*^{-/-} myotubes than in *Plin2*^{+/+} myotubes (Fig. 5D), as was the glucose oxidation (Fig. 5E). Furthermore, preincubation with OA for 24 h suppressed glucose oxidation approximately two-fold in *Plin2*^{-/-} myotubes in relation to *Plin2*^{+/+} myotubes (Fig. 5E), consistent with an inverse correlation between energy derived from FA or glucose oxidation in myotubes. Collectively, these substrate oxidative assays reveal a shift in energy metabolism from utilization of glucose toward that of FAs in *Plin2*^{-/-} myotubes.

Expression of genes involved in FA and glucose metabolism in the absence of *Plin2*

Prolonged changes in intracellular FA concentrations can directly affect the expression of several transcriptional factors and consequently the transcription of targeted gene families (43–45). First, we examined mRNA expression levels of *Ppar* members in *Plin2*^{+/+} and *Plin2*^{-/-} myotubes (Fig. 6A), because these transcription factors are known to be activated by various lipid moieties (46, 47). *Ppard*, the

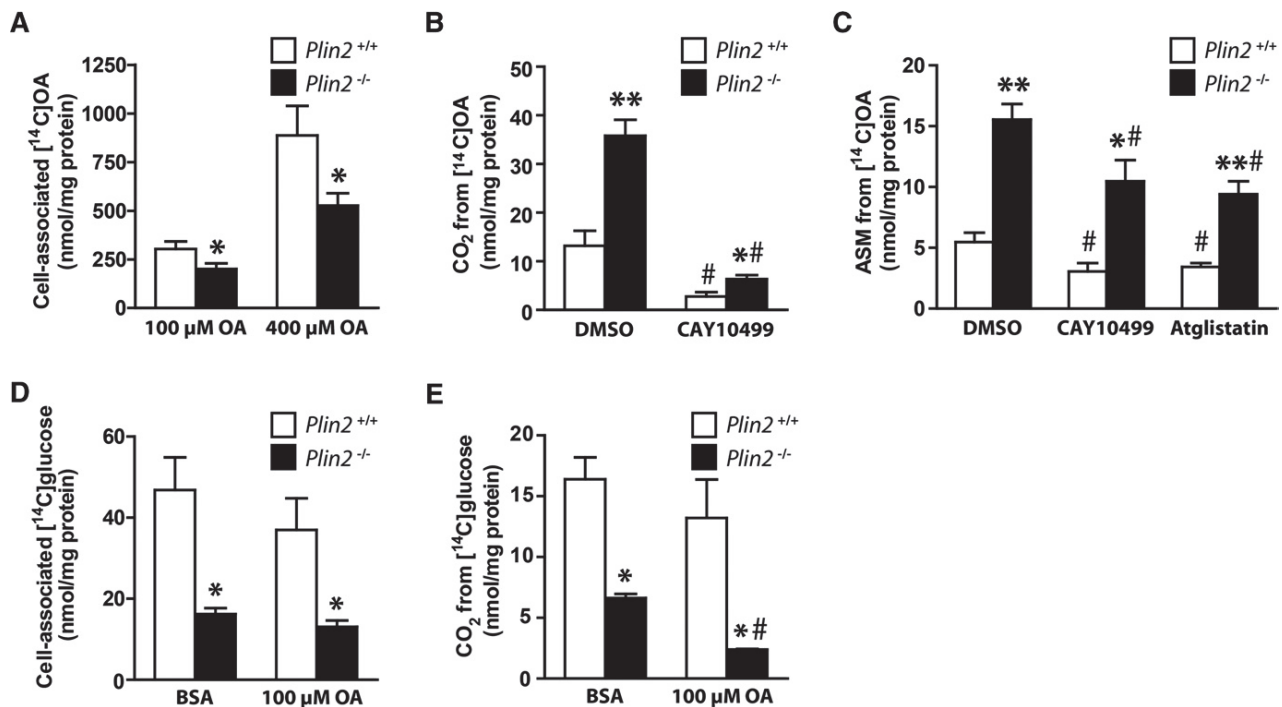


Fig. 5. Cell-associated radioactivity and oxidation of OA and glucose in *Plin2*^{+/+} and *Plin2*^{-/-} myotubes. For measurement of cell-associated radioactivity and oxidation of fatty acids (A–C), myotubes were preincubated with [¹⁴C]OA (100 or 400 μM) alone (0.1% DMSO) or in the presence of CAY10499 (10 μM) or Atglistatin (10 μM) for 24 h and then subjected to FA substrate oxidation assay for 4 h. A: Total cell-associated [¹⁴C]radioactivity remaining in *Plin2*^{+/+} and *Plin2*^{-/-} myotubes after 4 h. B: Released CO₂ arising from accumulated [¹⁴C]radioactivity after 4 h. C: FA intermediary oxidation products measured as [¹⁴C]radiolabeled ASMs released from the myotubes into the cell media during 24 h incubation with [¹⁴C]OA. The results are presented as means ± SEM (n = 3–7, *P < 0.05 and **P < 0.01 vs. *Plin2*^{+/+}, #P < 0.05 vs. DMSO). For measurement of cell-associated radioactivity and oxidation of glucose (D, E), myotubes were preincubated with BSA (40 μM, i.e., basal) or OA (100 μM) for 24 h, before myotubes were incubated with D-[¹⁴C(U)]glucose and subjected to glucose substrate oxidation assay for 4 h. D: Total cell-associated [¹⁴C]radioactivity accumulated in myotubes after 4 h. E: Released CO₂ from oxidation of D-[¹⁴C(U)]glucose. Results are presented as means ± SEM (n = 3–6, *P < 0.05 vs. *Plin2*^{+/+}, #P < 0.05 vs. BSA).

predominant subtype in skeletal muscle, was expressed to similar levels in *Plin2*^{+/+} and *Plin2*^{-/-} myotubes (Fig. 6A), whereas the subtypes *Ppara* and *Pparg* displayed completely opposite expression patterns (Fig. 6A). *Ppara* controls the expression of genes involved in FA oxidation (45) and was induced ~10-fold in the *Plin2*^{-/-} myotubes, with elevated FA levels compared with *Plin2*^{+/+} myotubes. Conversely, *Pparg* controls the expression of genes involved in FA storage and its expression was suppressed ~15-fold in *Plin2*^{-/-} myotubes compared with *Plin2*^{+/+} myotubes. Furthermore, the Ppar γ coactivator 1 α (*Pparg1a*), a master regulator of mitochondrial biogenesis (48), was elevated ~2-fold in *Plin2*^{-/-} compared with *Plin2*^{+/+} myotubes (Fig. 6A). Others have reported that mice with transgenic overexpression of *Ppara* in muscle have increased FA oxidation and reduced glucose oxidation (49) and that overexpression of *Pparg1a* in myotubes reduces glucose oxidation (50). The metabolic switches followed by overexpression of *Ppara* and *Pparg1a* resemble what we observed in the *Plin2*^{-/-} myotubes that also overexpress *Ppara* and *Pparg1a*. These results imply that a *Ppara/Pparg1a* component pathway is participatory in regulating FA versus glucose oxidative balance in myotubes lacking *Plin2*. Hence, we focused our continuing analyses on the expression of genes with linkage to FA and glucose oxidative pathways, which have been

shown previously to be transcriptionally regulated by this transcription factor pathway.

Among the genes important for FA oxidation, expression of plasma membrane FA transporter CD36 antigen (*Cd36*) and mitochondrial FA transporter carnitine palmitoyltransferase 2 (*Cpt2*) mRNAs were elevated in *Plin2*^{-/-} compared with *Plin2*^{+/+} myotubes (Fig. 6B). Although no changes were observed for FA-binding protein 3 (*Fabp3*), higher mRNA expressions of uncoupling proteins 2 and 3 (*Ucp2* and *Ucp3*), routinely associated with elevated FA oxidation, were also observed (Fig. 6B). Collectively, the expression of mRNAs for several enzymes oxidizing acyl-CoA to acetyl-CoA, such as the mitochondrial acyl-CoA dehydrogenases (*Acadm*, *Acadl*, *Acadvl*) and peroxisomal acyl-CoA oxidase 1 (*Acox1*), were unchanged in *Plin2*^{-/-} compared with *Plin2*^{+/+} myotubes (Fig. 6C).

We next analyzed expression of genes involved in glucose oxidative pathways (Fig. 6D–F). Expression of solute carrier family 2 member 1 (*Slc2a1*), encoding for the basal glucose transporter 1 (*Glut1*), was ~50% lower in *Plin2*^{-/-} myotubes than in *Plin2*^{+/+} myotubes (Fig. 6D), whereas expression of *Slc2a4*, encoding for the insulin-responsive *Glut4*, was unaltered (Fig. 6D). Hexokinase 1 and 2 (*Hk1* and *Hk2*), important for mobilization of glucose, and glycogen synthase 1 (*Gys1*) were also unaltered in expression (Fig. 6D).

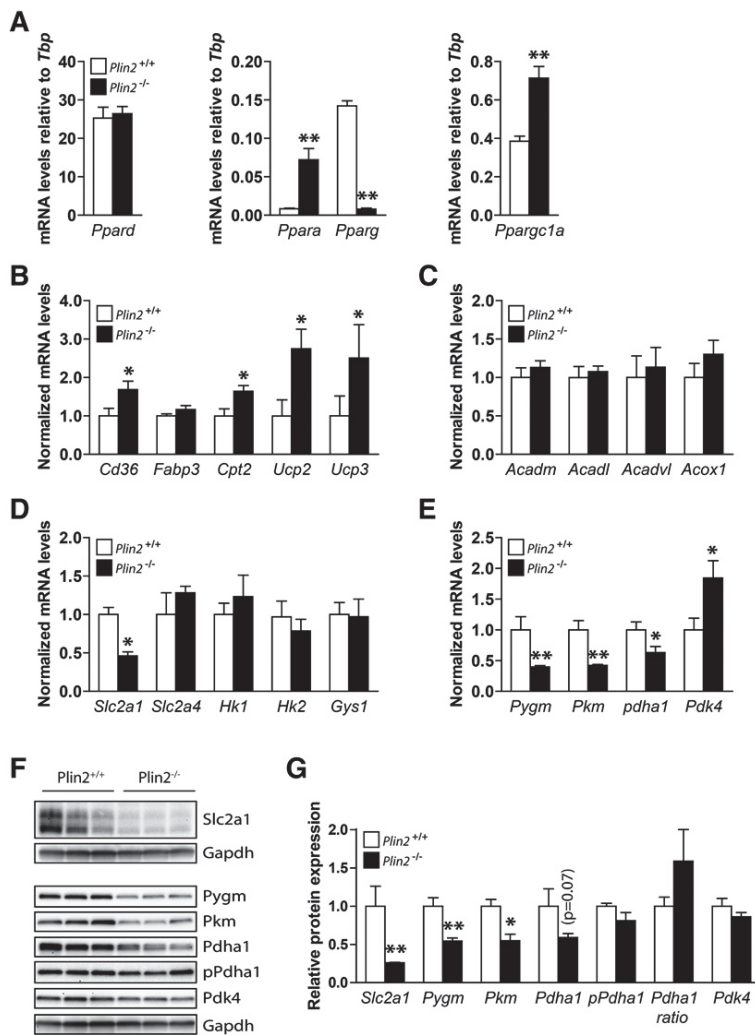


Fig. 6. Expression of genes involved in lipid metabolism in *Plin2*^{+/+} and *Plin2*^{-/-} myotubes. Gene expression of various mRNAs in differentiated *Plin2*^{+/+} and *Plin2*^{-/-} myotubes was analyzed by RT-qPCR and related to the expression of TATA-box binding protein (*Tbp*). A: Expression of transcription factors activated by FAs; *Ppar* α , γ and δ and *Ppar* γ coactivator 1 α (*Ppargc1a*). Results are presented as means \pm SEM (n = 4, **P* < 0.05 and ***P* < 0.01 vs. *Plin2*^{+/+}). B: Expression of genes involved in lipid uptake and mitochondrial function; FA transporter/CD36 antigen (*Cd36*), *Fabp3*, *Cpt2*, and uncoupling proteins 2 and 3 (*Ucp2* and *Ucp3*, respectively). C: Expression of genes catalyzing oxidation of FAs; mitochondrial *Acadm*, *Acadl*, *Acadvl*, and peroxisomal *Acox1*. D: Expression of genes involved in glucose uptake and storage; solute carrier family 2 member 1 and 4 (*Slc2a1* and *Slc2a4*, respectively), hexokinase 1 and 2 (*Hk1* and *Hk2*, respectively) and *Gys1*. E: Expression of genes involved in glycogen mobilization and glucose oxidation; muscle-associated glycogen phosphorylase (*Pygm*), muscle pyruvate kinase (*Pkm*), pyruvate dehydrogenase α 1 (*Pdha1*), and pyruvate dehydrogenase kinase 4 (*Pdk4*). Results in B–F are presented as means \pm SEM normalized to the expression in *Plin2*^{+/+} myotubes (n = 5, **P* < 0.05, ***P* < 0.01 vs. *Plin2*^{+/+}). F: Protein content of *Slc2a1*, *Pygm*, *Pkm*, *Pdha1*, *Pdha1* phosphorylated at Ser300 (pPdha1), and *Pdk4* (n = 3). G: Protein content, related to *Gapdh* normalized to the expression levels in *Plin2*^{+/+} myotubes, or the ratio of pPdha1 against total *Pdha1* (*Pdha1* ratio). The results are presented as means \pm SEM (n = 3, **P* < 0.05 vs. *Plin2*^{+/+}).

However, muscle-associated glycogen phosphorylase (*Pygm*), muscle pyruvate kinase (*Pkm*), and muscle pyruvate dehydrogenase α 1 (*Pdha1*), encoding for three enzymes that drive glucose oxidation via mobilization of pyruvate for the TCA cycle, were all less expressed in *Plin2*^{-/-} than in *Plin2*^{+/+} myotubes (Fig. 6E). Pyruvate dehydrogenase kinase 4 (*Pdk4*), which phosphorylates *Pdha1* at Ser300 and inhibits *Pdha1* enzymatic activity, was expressed at higher levels in *Plin2*^{-/-} than in *Plin2*^{+/+} myotubes (Fig. 6E).

We finally analyzed whether the altered gene transcript levels of the glucose transporter and the oxidative enzymes were reflected in protein level changes. Protein levels of *Glut1*, *Pygm*, *Pkm*, and to a lesser extent *Pdha1* (*P* = 0.7), were all lower in *Plin2*^{-/-} than in *Plin2*^{+/+} myotubes (Fig. 6F, G), and there was a further trended ratio for elevated levels of inactive phosphorylated *Pdha1* (Ser300) to total *Pdha1* (*P* = 0.1) in *Plin2*^{-/-} than in *Plin2*^{+/+} myotubes. Taken together, the altered gene expressions in pathways for FA (*Cd36*) and glucose (*Slc2a1*) transport, glycogen degradation (*Pygm*) and glycolysis (*Pkm*, *Pdha1*, and *Pdk4*) found in the *Plin2*^{-/-} myotubes follows similar trends as for mice with muscle overexpression of *Ppara* (49) or *Ppargc1a* (50). Interestingly, all these models exhibit

metabolic biases toward FA oxidation with a corresponding suppression of glucose oxidation. This change in oxidative balance may be further supported by the feedback inhibition of glucose oxidation by accumulated acyl-CoA substrates.

Absence of *Plin2* had no impact on insulin-stimulated phosphorylation of Akt

An important physiological role for skeletal muscle is whole-body glucose regulation by responding to insulin and thereby regulating active glucose transport into muscle cells. Mice with muscle-specific deletion of *Pparg* (51) or muscle-specific overexpression of *Ppara* (49) are both insulin resistant. Because *Plin2*^{-/-} myotubes oxidized less glucose, had suppressed levels of *Pparg*, and had elevated levels of *Ppara*, we analyzed insulin response in *Plin2*^{+/+} and *Plin2*^{-/-} myotubes. Compared with muscle tissue in vivo, cultured myotubes respond with only a modest increase in glucose uptake after insulin stimulation (52). Despite this reduced response, cultured myotubes provide a reliable model for testing factors affecting insulin signaling. First, we compared glycogen synthesis, which indirectly reflects cellular glucose uptake, after 24 h preincubation with

either BSA (40 μ M) or OA (100 μ M), followed by incorporation of D-[14 C(U)]glucose into glycogen for 3 h. The total amount of synthesized glycogen was lower in *Plin2*^{-/-} than in *Plin2*^{+/+} myotubes (Fig. 7A) but the fold induction of glycogen synthesis by insulin stimulation was essentially the same (Fig. 7A). To further determine whether the altered FA and glucose metabolism in *Plin2*^{-/-} myotubes affected insulin signaling, we determined insulin-stimulated mTORC2-mediated phosphorylation (Ser473) of the serine-threonine protein kinase Akt in the two cell populations. Akt phosphorylation in response to insulin was similar in *Plin2*^{+/+} and *Plin2*^{-/-} myotubes (Fig. 7B, C), despite total Akt (Akt1-3) being expressed at lower levels in *Plin2*^{-/-} myotubes than in *Plin2*^{+/+} myotubes (Fig. 7D). These findings suggest that although *Plin2*^{-/-} myotubes have reduced basal glucose uptake compared with *Plin2*^{+/+} myotubes, insulin signaling and insulin-stimulated glucose uptake are unaffected by removal of Plin2.

DISCUSSION

Plin2 was the second Plin-family member identified as a LD surface-coating protein (53), but its function in whole-body lipid metabolism is still poorly understood. Most cell types transcribe a high pool of *Plin2* mRNA but contain only a modest amount of the protein because of a rapid proteasomal degradation of the Plin2 pool that is not associated with LDs (31). Manipulation of *Plin2* mRNA with temporal gene silencing (54) or overexpression of Plin2 (55) may therefore result in only modest changes in Plin2 protein levels. This phenomenon and a likely partial functional redundancy among some Plins (54) complicate studies on Plin2 function. The expression of *Plin2* mRNA is induced and the produced Plin2 protein stabilized once LDs are formed in cells exposed to elevated levels of FAs. One example of this phenomenon is the large increase in *Plin2* mRNA, Plin2 protein, and TAG-containing LDs in

the liver of fasted mice (56). The significance of the fasting-induced hepatic Plin2 is unclear. Characterization of two separate *Plin2* null mouse models demonstrates that lack of *Plin2* protects against hepatosteatosis (24, 57, 58), emphasizing that Plin2 coating of LDs may not always be beneficial. The absence of *Plin2* also suppresses obesity in mice on certain high-caloric diets (58), despite that Plin2 protein is normally not present on adipose LDs (53), arguing that a lack of Plin2 in other tissues has an impact on energy storage and metabolism.

The consequences for muscle energy metabolism upon *Plin2* removal had not been fully investigated previously. To shed light on the function of Plin2 in skeletal muscle, we established myoblast cultures from *Plin2*^{+/+} and *Plin2*^{-/-} mice. Given the known discrepancies in *Plin2* mRNA and protein levels, our system with an absence of functional *Plin2* differs from earlier studies based on siRNA knockdown or ectopic expression of Plin2 (54, 55). In a manner similar to that in the earlier studies based on the partial depletion of Plin2 (54, 55), we show in this study that myotubes that lack *Plin2* have less accumulated TAG than wild-type myotubes. When *Plin2*^{-/-} myotubes were exposed to Atglistatin, an inhibitor of ATGL that reduces lipolysis of TAG in LDs, TAG content was comparable to *Plin2*^{+/+} myotubes, whereas removal of the inhibitor resulted in a faster release of FAs from the accumulated TAG pool in *Plin2*^{-/-} myotubes. The LDs retained in *Plin2*^{-/-} myotubes furthermore consist of reduced amount of TAG in relation to a higher amount of lipolytic degradation products such as DAG, MAG, and FFA compared with *Plin2*^{+/+} myotubes. These results suggest that a lack of Plin2 on LDs does not affect FA uptake or incorporation into LDs per se, but its absence increases degradation of the TAG deposited within LDs through enhanced lipolysis. Our observations complement other studies, suggesting that overexpression of Plin2 in embryonic kidney cells reduced the interaction of lipases with LDs (59) or that a combined *Plin2* and *Plin3* knockdown increased lipolysis in hepatocytes (54). Consistent with a model in which reduced TAG in

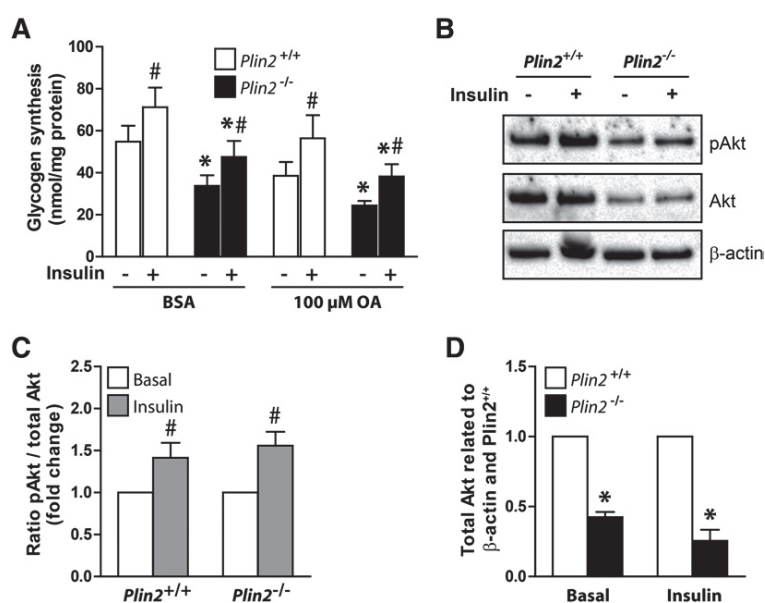


Fig. 7. Effect of insulin in *Plin2*^{+/+} and *Plin2*^{-/-} myotubes. A: Myotubes were preincubated with BSA (40 μ M) or OA (100 μ M) for 24 h. Glycogen synthesis was subsequently measured as incorporation of D-[14 C(U)]glucose into glycogen in the absence or presence of insulin (100 nM) for 3 h. B: Myotubes were preincubated with OA (100 μ M) for 24 h, then incubated in glucose-free medium supplemented with OA (100 μ M) for 2 h, and subsequently incubated in medium containing glucose (5.5 mM) with or without insulin (100 nM) for 15 min. Cell samples were subjected for immunoblotting analysis with antibodies against total Akt (Akt1-3), pAkt (Ser473), and β -actin (housekeeping protein). Immunoblots from one representative experiment are shown. C: Ratio of pAkt/total Akt related to myotubes receiving no insulin. D: The content of total Akt related to β -actin normalized to expression levels in *Plin2*^{+/+} myotubes. The results are presented as means \pm SEM (n = 4, **P* < 0.05 vs. *Plin2*^{+/+} with the same treatment, #*P* < 0.05 vs. without insulin). pAkt, phosphorylated Akt.

Plin2^{-/-} myotubes is caused by elevated lipolytic activity, skeletal muscles of ATGL null mice show increased TAG accumulation and reduced lipolysis (60). In our study, inhibitors of ATGL (i.e., Atglistatin) or ATGL and HSL (i.e. CAY10499) enhanced LD content and elevated total accumulated TAG with considerably higher potency in *Plin2*^{-/-} myotubes than in *Plin2*^{+/+} myotubes. These results support the notion that ATGL and HSL have limited access to LDs or have reduced activity in myotubes expressing Plin2 at the LD surface. Taken together, our results establish that one functional role for Plin2 in muscle is to protect TAG stored within LDs from lipases such as ATGL or HSL.

Metabolic consequences upon *Plin2* removal may at least partly be caused by increased efflux of FAs from LDs in *Plin2*^{-/-} myotubes. We observed a profound increase in OA oxidation and a reduction in glucose oxidation in *Plin2*^{-/-} myotubes. In line with a functional role of Plin2 as a protector of TAG stored within LDs, we observed that *Plin2*^{-/-} myotubes exposed to OA accumulated less DAG. Previous experiments in myotubes depleted of *Plin2* by siRNA showed a more modest increase in palmitic acid (PA) oxidation but also an increase in DAG (55). The incomplete removal of the Plin2 protein in *Plin2* siRNA knockdown myotubes compared with an absence of Plin2 in our *Plin2*^{-/-} myotubes likely contributes to these discrepancies. The different types of labeled FAs used may also be significant. PA is accumulated to a lower extent into LDs than is OA in myotubes (61). The strong repression of FA oxidation observed in myotubes exposed to the dual ATGL and HSL lipase inhibitor (CAY10499) demonstrates that OA converted into CO₂ derived mainly from LDs in our experiments. Consistent with LDs being an important source of substrate for FA oxidation, other investigators have reported that preservation of LDs by knockdown of the ATGL coactivator CGI-58 decreased lipolysis and FA oxidation while increasing glucose oxidation and incorporation into glycogen in cultured myotubes (62).

The enhanced release of FAs from the LDs observed in *Plin2*^{-/-} myotubes may support inhibition of glucose oxidation and stimulation of FA oxidation via mutual inhibition of substrate metabolism in the glucose-FA cycle (43). A similar enhanced FA oxidation is found in cultured hepatocytes isolated from *Plin2*^{-/-} mice (Y.K.L., K.T.D., and A.R.K., unpublished observations). Our data define a mechanistic function for Plin2 to regulate TAG stores and FA oxidation, in an antagonistic pathway that balances glucose oxidation. The observed alterations in expressions of genes facilitating glucose uptake and oxidation are consistent with the glucose-FA cycle described by Randle, which defines a metabolic competition between glucose and FAs, in which enhanced FA availability suppresses glucose oxidation. We observed decreased levels of proteins involved both in glucose uptake (Slc2a1/Glut1) and in glucose oxidation in *Plin2*^{-/-} myotubes, consistent with studies examining how elevated circulating FAs inhibit glucose oxidation in human skeletal muscle (63). To facilitate such an energy substrate switch, transcription factors known to stimulate expression of genes driving FA oxidation such as *Ppara* and *Ppargc1a* (64) were expressed at higher levels in *Plin2*^{-/-} myotubes, whereas *Pparg*, which stimulates expression of genes promoting lipid storage (65),

were suppressed. Elevated expression of *Ppara* has previously been noted in livers of *Plin2*^{-/-} mice (58), consistent with an opposite repression of *Ppara* expression in muscle overexpressing Plin2 (55). Interestingly, we found that our cultured *Plin2*^{-/-} myotubes resemble the FA oxidative phenotype and repressed expression of glucose oxidative genes characteristic of muscle cells that were engineered to overexpress either *Ppara* (49) or *Ppargc1a* (50). We also observed enhanced expression of uncoupling proteins, which disconnects energy production from oxidative flux when FA levels are too elevated. Taken together, our data suggest an increased acyl-CoA to acetyl-CoA flux in *Plin2*^{-/-} myotubes, as modeled in the Randle cycle, serving to metabolically inhibit and suppress expression of glycolytic enzymes and reduce glucose oxidation and favor FA oxidation.

With respect to insulin responsiveness, *Plin2* loss-of-function studies in liver or whole animals have shown contradictory results (54, 57, 66, 67). In our study, *Plin2*^{+/+} and *Plin2*^{-/-} myotubes had comparable insulin-stimulated responses judged by the increase in total Akt phosphorylation and glycogen synthesis, whereas glucose accumulation and oxidation were markedly decreased in *Plin2*^{-/-} myotubes. Normal insulin signaling was also reported after *Plin2* knockdown in C2C12 myotubes (55). It has been proposed that accumulation of lipotoxic intermediates in cells exposed to high levels of FAs may interfere with insulin signaling because of a mismatch among lipid storage, lipolysis, and oxidation (68). Enhanced FA oxidation in *Plin2*^{-/-} myotubes may therefore act as a compensatory mechanism to handle the increased availability of FAs released from the more rapidly degrading LDs. It remains to be investigated further whether the reduced expressions of Akt proteins, measured with a pan-Akt antibody, mechanistically contribute to reduced glucose metabolism in *Plin2*^{-/-} myotubes. The three different Akt isoforms (Akt1-3) have distinct roles, in which Akt2 is particularly involved in the maintenance of glucose homeostasis (69). Further studies are required to clarify whether a particular Akt protein is reduced in *Plin2*^{-/-} myotubes and signals to reduce glucose uptake.

In summary, by characterizing myotubes established from *Plin2*^{+/+} and *Plin2*^{-/-} mice, we demonstrate that loss of *Plin2* results in myotubes with reduced accumulation of neutral lipids in LDs due to elevated lipolysis. Similar to what has been shown previously for Plin1 and Plin5 (21, 70), this establishes a functional role of Plin2 as a protector against lipolytic degradation of LDs. The increased efflux of FAs from LDs in *Plin2*^{-/-} myotubes is likely to contribute to a metabolic shift in energy metabolism from utilization of glucose toward FAs. Such a shift may be facilitated by altered transcription of metabolic regulators in *Plin2*^{-/-} myotubes. Our results demonstrate that Plin2 is essential for balancing the pool of LDs in cultured myotubes to avoid an uncontrolled hydrolysis of intracellular TAG and altered energy metabolism caused by increased release of FAs from LDs. **FIG 6**

The authors thank Camilla Stensrud and Prabhat Khanal for technical assistance and members of the Rustan, Thoresen, and Dalen laboratories for scientific discussions. The authors thank the NORMIC-UiO imaging platform, Department of Biosciences,

University of Oslo, for support, use of equipment, and excellent technical assistance.

REFERENCES

- Hue, L., and H. Taegtmeier. 2009. The Randle cycle revisited: a new head for an old hat. *Am. J. Physiol. Endocrinol. Metab.* **297**: E578–E591.
- Eckardt, K., A. Taube, and J. Eckel. 2011. Obesity-associated insulin resistance in skeletal muscle: role of lipid accumulation and physical inactivity. *Rev. Endocr. Metab. Disord.* **12**: 163–172.
- Samuel, V. T., and G. I. Shulman. 2012. Mechanisms for insulin resistance: common threads and missing links. *Cell.* **148**: 852–871.
- Pan, D. A., S. Lillioja, A. D. Kriketos, M. R. Milner, L. A. Baur, C. Bogardus, A. B. Jenkins, and L. H. Storlien. 1997. Skeletal muscle triglyceride levels are inversely related to insulin action. *Diabetes.* **46**: 983–988.
- Jacob, S., J. Machann, K. Rett, K. Brechtel, A. Volk, W. Renn, E. Maerker, S. Matthaai, F. Schick, C. D. Claussen, et al. 1999. Association of increased intramyocellular lipid content with insulin resistance in lean nondiabetic offspring of type 2 diabetic subjects. *Diabetes.* **48**: 1113–1119.
- Goodpaster, B. H., R. Thieriault, S. C. Watkins, and D. E. Kelley. 2000. Intramuscular lipid content is increased in obesity and decreased by weight loss. *Metabolism.* **49**: 467–472.
- van Loon, L. J., R. Koopman, R. Manders, W. van der Weegen, G. P. van Kranenburg, and H. A. Keizer. 2004. Intramyocellular lipid content in type 2 diabetes patients compared with overweight sedentary men and highly trained endurance athletes. *Am. J. Physiol. Endocrinol. Metab.* **287**: E558–E565.
- Sztalryd, C., and A. R. Kimmel. 2014. Perilipins: lipid droplet coat proteins adapted for tissue-specific energy storage and utilization, and lipid cytoprotection. *Biochimie.* **96**: 96–101.
- Goodpaster, B. H., J. He, S. Watkins, and D. E. Kelley. 2001. Skeletal muscle lipid content and insulin resistance: evidence for a paradox in endurance-trained athletes. *J. Clin. Endocrinol. Metab.* **86**: 5755–5761.
- Amati, F., J. J. Dube, E. Alvarez-Carnero, M. M. Edreira, P. Chomentowski, P. M. Coen, G. E. Switzer, P. E. Bickel, M. Stefanovic-Racic, F. G. Toledo, et al. 2011. Skeletal muscle triglycerides, diacylglycerols, and ceramides in insulin resistance: another paradox in endurance-trained athletes? *Diabetes.* **60**: 2588–2597.
- Høeg, L., C. Roepstorff, M. Thiele, E. A. Richter, J. F. Wojtaszewski, and B. Kiens. 2009. Higher intramuscular triacylglycerol in women does not impair insulin sensitivity and proximal insulin signaling. *J. Appl. Physiol.* **107**: 824–831.
- Coen, P. M., and B. H. Goodpaster. 2012. Role of intramyocellular lipids in human health. *Trends Endocrinol. Metab.* **23**: 391–398.
- Brasaemle, D. L. 2007. Thematic review series: adipocyte biology. The perilipin family of structural lipid droplet proteins: stabilization of lipid droplets and control of lipolysis. *J. Lipid Res.* **48**: 2547–2559.
- Bickel, P. E., J. T. Tansey, and M. A. Welte. 2009. PAT proteins, an ancient family of lipid droplet proteins that regulate cellular lipid stores. *Biochim. Biophys. Acta.* **1791**: 419–440.
- Zimmermann, R., J. G. Strauss, G. Haemmerle, G. Schoiswohl, R. Birner-Gruenberger, M. Riederer, A. Lass, G. Neuberger, F. Eisenhaber, A. Hermetter, et al. 2004. Fat mobilization in adipose tissue is promoted by adipose triglyceride lipase. *Science.* **306**: 1383–1386.
- Haemmerle, G., R. Zimmermann, M. Hayn, C. Theussl, G. Waeg, E. Wagner, W. Sattler, T. M. Magin, E. F. Wagner, and R. Zechner. 2002. Hormone-sensitive lipase deficiency in mice causes diglyceride accumulation in adipose tissue, muscle, and testis. *J. Biol. Chem.* **277**: 4806–4815.
- Fredrikson, G., H. Tornqvist, and P. Belfrage. 1986. Hormone-sensitive lipase and monoacylglycerol lipase are both required for complete degradation of adipocyte triacylglycerol. *Biochim. Biophys. Acta.* **876**: 288–293.
- Kimmel, A. R., and C. Sztalryd. 2016. The perilipins: major cytosolic lipid droplet-associated proteins and their roles in cellular lipid storage, mobilization, and systemic homeostasis. *Annu. Rev. Nutr.* **36**: 471–509.
- Kimmel, A. R., D. L. Brasaemle, M. McAndrews-Hill, C. Sztalryd, and C. Londos. 2010. Adoption of PERILIPIN as a unifying nomenclature for the mammalian PAT-family of intracellular lipid storage droplet proteins. *J. Lipid Res.* **51**: 468–471.
- Dalen, K. T., T. Dahl, E. Holter, B. Arntsen, C. Londos, C. Sztalryd, and H. I. Nebb. 2007. LSDP5 is a PAT protein specifically expressed in fatty acid oxidizing tissues. *Biochim. Biophys. Acta.* **1771**: 210–227.
- Sztalryd, C., G. Xu, H. Dorward, J. T. Tansey, J. A. Contreras, A. R. Kimmel, and C. Londos. 2003. Perilipin A is essential for the translocation of hormone-sensitive lipase during lipolytic activation. *J. Cell Biol.* **161**: 1093–1103.
- Martinez-Botas, J., J. B. Anderson, D. Tessier, A. Lapillonne, B. H. Chang, M. J. Quast, D. Gorenstein, K. H. Chen, and L. Chan. 2000. Absence of perilipin results in leanness and reverses obesity in *Lepr*(db/db) mice. *Nat. Genet.* **26**: 474–479.
- Tansey, J. T., C. Sztalryd, J. Gruia-Gray, D. L. Roush, J. V. Zee, O. Gavrilova, M. L. Reitman, C. X. Deng, C. Li, A. R. Kimmel, et al. 2001. Perilipin ablation results in a lean mouse with aberrant adipocyte lipolysis, enhanced leptin production, and resistance to diet-induced obesity. *Proc. Natl. Acad. Sci. USA.* **98**: 6494–6499.
- Chang, B. H., L. Li, A. Paul, S. Taniguchi, V. Nannegari, W. C. Heird, and L. Chan. 2006. Protection against fatty liver but normal adipogenesis in mice lacking adipose differentiation-related protein. *Mol. Cell Biol.* **26**: 1063–1076.
- Chen, W., B. Chang, X. Wu, L. Li, M. Sleeman, and L. Chan. 2013. Inactivation of *Plin4* downregulates *Plin5* and reduces cardiac lipid accumulation in mice. *Am. J. Physiol. Endocrinol. Metab.* **304**: E770–E779.
- Kuramoto, K., T. Okamura, T. Yamaguchi, T. Y. Nakamura, S. Wakabayashi, H. Morinaga, M. Nomura, T. Yanase, K. Otsu, N. Usuda, et al. 2012. Perilipin 5, a lipid droplet-binding protein, protects heart from oxidative burden by sequestering fatty acid from excessive oxidation. *J. Biol. Chem.* **287**: 23852–23863.
- Hsieh, K., Y. K. Lee, C. Londos, B. M. Raaka, K. T. Dalen, and A. R. Kimmel. 2012. Perilipin family members preferentially sequester to either triacylglycerol-specific or cholesteryl-ester-specific intracellular lipid storage droplets. *J. Cell Sci.* **125**: 4067–4076.
- Shaw, C. S., M. Sherlock, P. M. Stewart, and A. J. Wagenmakers. 2009. Adipophilin distribution and colocalization with lipid droplets in skeletal muscle. *Histochem. Cell Biol.* **131**: 575–581.
- Phillips, S. A., C. C. Choe, T. P. Ciaraldi, A. S. Greenberg, A. P. Kong, S. C. Baxi, L. Christiansen, S. R. Mudaliar, and R. R. Henry. 2005. Adipocyte differentiation-related protein in human skeletal muscle: relationship to insulin sensitivity. *Obes. Res.* **13**: 1321–1329.
- Minnaard, R., P. Schrauwen, G. Schaart, J. A. Jorgensen, E. Lenaers, M. Mensink, and M. K. Hesselink. 2009. Adipocyte differentiation-related protein and OXPAT in rat and human skeletal muscle: involvement in lipid accumulation and type 2 diabetes mellitus. *J. Clin. Endocrinol. Metab.* **94**: 4077–4085.
- Xu, G., C. Sztalryd, X. Lu, J. T. Tansey, J. Gan, H. Dorward, A. R. Kimmel, and C. Londos. 2005. Post-translational regulation of adipose differentiation-related protein by the ubiquitin/proteasome pathway. *J. Biol. Chem.* **280**: 42841–42847.
- Hessvik, N. P., M. V. Boekschoten, M. A. Baltzersen, S. Kersten, X. Xu, H. Andersen, A. C. Rustan, and G. H. Thoresen. 2010. LXR β is the dominant LXR subtype in skeletal muscle regulating lipogenesis and cholesterol efflux. *Am. J. Physiol. Endocrinol. Metab.* **298**: E602–E613.
- Bindesbøll, C., O. Berg, B. Arntsen, H. I. Nebb, and K. T. Dalen. 2013. Fatty acids regulate perilipin5 in muscle by activating PPAR δ . *J. Lipid Res.* **54**: 1949–1963.
- Miura, S., J. W. Gan, J. Brzostowski, M. J. Parisi, C. J. Schultz, C. Londos, B. Oliver, and A. R. Kimmel. 2002. Functional conservation for lipid storage droplet association among Perilipin, ADRP, and TIP47 (PAT)-related proteins in mammals, *Drosophila*, and *Dictyostelium*. *J. Biol. Chem.* **277**: 32253–32257.
- Ye, J., G. Coulouris, I. Zaretskaya, I. Cutcutache, S. Rozen, and T. L. Madden. 2012. Primer-BLAST: a tool to design target-specific primers for polymerase chain reaction. *BMC Bioinformatics.* **13**: 134.
- Hessvik, N. P., S. S. Bakke, K. Fredriksson, M. V. Boekschoten, A. Fjorckenstad, G. Koster, M. K. Hesselink, S. Kersten, E. T. Kase, A. C. Rustan, et al. 2010. Metabolic switching of human myotubes is improved by n-3 fatty acids. *J. Lipid Res.* **51**: 2090–2104.
- Wensaas, A. J., A. C. Rustan, K. Lovstedt, B. Kull, S. Wikstrom, C. A. Devon, and S. Hallen. 2007. Cell-based multiwell assays for the detection of substrate accumulation and oxidation. *J. Lipid Res.* **48**: 961–967.
- Mayer, N., M. Schweiger, M. Romauch, G. F. Grabner, T. O. Eichmann, E. Fuchs, J. Ivkovic, C. Heier, I. Mrak, A. Lass, et al. 2013.

- Development of small-molecule inhibitors targeting adipose triglyceride lipase. *Nat. Chem. Biol.* **9**: 785–787.
39. Weerheim, A. M., A. M. Kolb, A. Sturk, and R. Nieuwland. 2002. Phospholipid composition of cell-derived microparticles determined by one-dimensional high-performance thin-layer chromatography. *Anal. Biochem.* **302**: 191–198.
 40. Gaster, M., A. C. Rustan, V. Aas, and H. Beck-Nielsen. 2004. Reduced lipid oxidation in skeletal muscle from type 2 diabetic subjects may be of genetic origin: evidence from cultured myotubes. *Diabetes.* **53**: 542–548.
 41. Grisouard, J., E. Bouillet, K. Timper, T. Radimerski, K. Dembinski, D. M. Frey, R. Peterli, H. Zulewski, U. Keller, B. Muller, et al. 2012. Both inflammatory and classical lipolytic pathways are involved in lipopolysaccharide-induced lipolysis in human adipocytes. *Innate Immun.* **18**: 25–34.
 42. Iglesias, J., J. Lamontagne, H. Erb, S. Gezzar, S. Zhao, E. Joly, V. L. Truong, K. Skorey, S. Crane, S. R. Madiraju, et al. 2016. Simplified assays of lipolysis enzymes for drug discovery and specificity assessment of known inhibitors. *J. Lipid Res.* **57**: 131–141.
 43. Randle, P. J., P. B. Garland, C. N. Hales, and E. A. Newsholme. 1963. The glucose fatty-acid cycle. Its role in insulin sensitivity and the metabolic disturbances of diabetes mellitus. *Lancet.* **1**: 785–789.
 44. Jump, D. B. 2004. Fatty acid regulation of gene transcription. *Crit. Rev. Clin. Lab. Sci.* **41**: 41–78.
 45. Georgiadi, A., and S. Kersten. 2012. Mechanisms of gene regulation by fatty acids. *Adv. Nutr.* **3**: 127–134.
 46. Poulsen, L., M. Siersbaek, and S. Mandrup. 2012. PPARs: fatty acid sensors controlling metabolism. *Semin. Cell Dev. Biol.* **23**: 631–639.
 47. Nakamura, M. T., B. E. Yudell, and J. J. Loor. 2014. Regulation of energy metabolism by long-chain fatty acids. *Prog. Lipid Res.* **53**: 124–144.
 48. Lin, J., H. Wu, P. T. Tarr, C. Y. Zhang, Z. Wu, O. Boss, L. F. Michael, P. Puigserver, E. Isotani, E. N. Olson, et al. 2002. Transcriptional co-activator PGC-1 alpha drives the formation of slow-twitch muscle fibres. *Nature.* **418**: 797–801.
 49. Finck, B. N., C. Bernal-Mizrachi, D. H. Han, T. Coleman, N. Sambandam, L. L. LaRiviere, J. O. Holloszy, C. F. Semenkovich, and D. P. Kelly. 2005. A potential link between muscle peroxisome proliferator-activated receptor-alpha signaling and obesity-related diabetes. *Cell Metab.* **1**: 133–144.
 50. Wende, A. R., J. M. Huss, P. J. Schaeffer, V. Giguere, and D. P. Kelly. 2005. PGC-1alpha coactivates PDK4 gene expression via the orphan nuclear receptor ERRalpha: a mechanism for transcriptional control of muscle glucose metabolism. *Mol. Cell. Biol.* **25**: 10684–10694.
 51. Hevener, A. L., W. He, Y. Barak, J. Le, G. Bandyopadhyay, P. Olson, J. Wilkes, R. M. Evans, and J. Olefsky. 2003. Muscle-specific Pparg deletion causes insulin resistance. *Nat. Med.* **9**: 1491–1497.
 52. Sarabia, V., L. Lam, E. Burdett, L. A. Leiter, and A. Klip. 1992. Glucose transport in human skeletal muscle cells in culture. Stimulation by insulin and metformin. *J. Clin. Invest.* **90**: 1386–1395.
 53. Brasaemle, D. L., T. Barber, N. E. Wolins, G. Serrero, E. J. Blanchette-Mackie, and C. Londos. 1997. Adipose differentiation-related protein is an ubiquitously expressed lipid storage droplet-associated protein. *J. Lipid Res.* **38**: 2249–2263.
 54. Bell, M., H. Wang, H. Chen, J. C. McLenthian, D. W. Gong, R. Z. Yang, D. Yu, S. K. Fried, M. J. Quon, C. Londos, et al. 2008. Consequences of lipid droplet coat protein downregulation in liver cells: abnormal lipid droplet metabolism and induction of insulin resistance. *Diabetes.* **57**: 2037–2045.
 55. Bosma, M., M. K. Hesselink, L. M. Sparks, S. Timmers, M. J. Ferraz, F. Mattijssen, D. van Beurden, G. Schaart, M. H. de Baets, F. K. Verheyen, et al. 2012. Perilipin 2 improves insulin sensitivity in skeletal muscle despite elevated intramuscular lipid levels. *Diabetes.* **61**: 2679–2690.
 56. Dalen, K. T., S. M. Ulven, B. M. Arntsen, K. Solaas, and H. I. Nebb. 2006. PPARalpha activators and fasting induce the expression of adipose differentiation-related protein in liver. *J. Lipid Res.* **47**: 931–943.
 57. Chang, B. H., L. Li, P. Saha, and L. Chan. 2010. Absence of adipose differentiation related protein upregulates hepatic VLDL secretion, relieves hepatosteatosis, and improves whole body insulin resistance in leptin-deficient mice. *J. Lipid Res.* **51**: 2132–2142.
 58. McManaman, J. L., E. S. Bales, D. J. Orlicky, M. Jackman, P. S. MacLean, S. Cain, A. E. Crunk, A. Mansur, C. E. Graham, T. A. Bowman, et al. 2013. Perilipin-2-null mice are protected against diet-induced obesity, adipose inflammation, and fatty liver disease. *J. Lipid Res.* **54**: 1346–1359.
 59. Listenberger, L. L., A. G. Ostermeyer-Fay, E. B. Goldberg, W. J. Brown, and D. A. Brown. 2007. Adipocyte differentiation-related protein reduces the lipid droplet association of adipose triglyceride lipase and slows triacylglycerol turnover. *J. Lipid Res.* **48**: 2751–2761.
 60. Haemmerle, G., A. Lass, R. Zimmermann, G. Gorkiewicz, C. Meyer, J. Rozman, G. Heldmaier, R. Maier, C. Theussl, S. Eder, et al. 2006. Defective lipolysis and altered energy metabolism in mice lacking adipose triglyceride lipase. *Science.* **312**: 734–737.
 61. Bakke, S. S., C. Moro, N. Nikolic, N. P. Hessvik, P. M. Badin, L. Lauvhaug, K. Fredriksson, M. K. Hesselink, M. V. Boekschoten, S. Kersten, et al. 2012. Palmitic acid follows a different metabolic pathway than oleic acid in human skeletal muscle cells; lower lipolysis rate despite an increased level of adipose triglyceride lipase. *Biochim. Biophys. Acta.* **1821**: 1323–1333.
 62. Badin, P. M., C. Loubiere, M. Coonen, K. Louche, G. Tavernier, V. Bourlier, A. Mairal, A. C. Rustan, S. R. Smith, D. Langin, et al. 2012. Regulation of skeletal muscle lipolysis and oxidative metabolism by the co-lipase CGI-58. *J. Lipid Res.* **53**: 839–848.
 63. Roden, M., T. B. Price, G. Perseghin, K. F. Petersen, D. L. Rothman, G. W. Cline, and G. I. Shulman. 1996. Mechanism of free fatty acid-induced insulin resistance in humans. *J. Clin. Invest.* **97**: 2859–2865.
 64. Nikolić, N., M. Rhedin, A. C. Rustan, L. Storlien, G. H. Thoresen, and M. Strömstedt. 2012. Overexpression of PGC-1α increases fatty acid oxidative capacity of human skeletal muscle cells. *Biochem. Res. Int.* **2012**: 714074.
 65. Azhar, S. 2010. Peroxisome proliferator-activated receptors, metabolic syndrome and cardiovascular disease. *Future Cardiol.* **6**: 657–691.
 66. Imai, Y., G. M. Varela, M. B. Jackson, M. J. Graham, R. M. Croke, and R. S. Ahima. 2007. Reduction of hepatosteatosis and lipid levels by an adipose differentiation-related protein antisense oligonucleotide. *Gastroenterology.* **132**: 1947–1954.
 67. Varela, G. M., D. A. Antwi, R. Dhir, X. Yin, N. S. Singhal, M. J. Graham, R. M. Croke, and R. S. Ahima. 2008. Inhibition of ADRP prevents diet-induced insulin resistance. *Am. J. Physiol. Gastrointest. Liver Physiol.* **295**: G621–G628.
 68. Moro, C., S. Bajpeyi, and S. R. Smith. 2008. Determinants of intramyocellular triglyceride turnover: implications for insulin sensitivity. *Am. J. Physiol. Endocrinol. Metab.* **294**: E203–E213.
 69. Cho, H., J. Mu, J. K. Kim, J. L. Thorvaldsen, Q. Chu, E. B. Crenshaw III, K. H. Kaestner, M. S. Bartolomei, G. I. Shulman, and M. J. Birnbaum. 2001. Insulin resistance and a diabetes mellitus-like syndrome in mice lacking the protein kinase Akt2 (PKB beta). *Science.* **292**: 1728–1731.
 70. Pollak, N. M., D. Jaeger, S. Kolleritsch, R. Zimmermann, R. Zechner, A. Lass, and G. Haemmerle. 2015. The interplay of protein kinase A and perilipin 5 regulates cardiac lipolysis. *J. Biol. Chem.* **290**: 1295–1306.

